The histone methyltransferase DOT1L is required for DNA damage recognition and repair

Doctoral Thesis

In partial fulfillment of the requirements for the degree
"Doctor rerum naturalium (Dr. rer. nat.)"
in the Molecular Medicine Study Program
at the Georg-August University Göttingen

submitted by

Sanjay Kumar Raul

born in **Baliapal, India**

Göttingen, 2016

Members of the Thesis Committee:

Prof. Dr. Steven A. Johnsen (Supervisor, First Referee)

Department of General, Visceral and Pediatric Surgery

University of Göttingen Medical School, Göttingen

Prof. Dr. mult. Thomas Meyer (Second Referee)

Department of Psychosomatic Medicine and Psychotherapy

University of Göttingen Medical School, Göttingen

Prof. Dr. Michael Zeisberg (Third member)

Department of Nephrology and Rheumatology

University of Göttingen Medical School, Göttingen

Date of Disputation: 20th of December 2016

AFFIDAVIT

Here I declare that my doctoral thesis entitled “The histone methyltransferase DOT1L is required for DNA damage recognition and repair” has been written independently and with no other sources and aids than quoted.

Sanjay Kumar Raul

Göttingen, 2016

List of Publications

Original articles

Kari, V., Mansour, W.Y., **Raul, S.K.,** Baumgart, S.J., Mund, A., Grade, M., Sirma, H., Simon, R., Will, H., Dobbelstein, M., Dikomey, E., and Johnsen, S.A. (2016). Loss of CHD1 causes DNA repair defects and enhances prostate cancer therapeutic responsiveness. EMBO Rep. *17*, 1609–1623.

Abstracts

Sanjay Kumar Raul, Vijaya Lakshmi Kari, Wael Yassin Mansour, Melanie Spitzner, Marian Grade, Jochen Gaedcke, Steven A. Johnsen (2015). The histone methyltransferase DOT1L required for DNA damage recognition and repair. 6th Molecular Medicine Retreat, Wernigerode, Germany, P-20

Sanjay Kumar Raul, Vijayalakshmi Kari, Melanie Spitzner, Wael Yassin Mansour, Steven A. Johnsen (2015). The histone methyltransferase DOT1L required for the DNA damage recognition and repair. The 2015 IMB Conference, Mainz, Germany, P98

Sanjay Kumar Raul, Vijaya Lakshmi Kari, Steven A. Johnsen (2014). The histone methyltransferase DOT1L required for DNA damage recognition and repair. 30th Ernst Klenk Symposium in Molecular Medicine, Center for Molecular Medicine Cologne, University of Cologne, D-15

V Kari, WY Mansour, **SK Raul**, S Baumgart, A Mund, R Simon, E Dikomey, H Will, SA Johnsen (2014). ATP-dependent chromatin remodeler CHD1 is required for homologous recombination repair pathway. 30th Ernst Klenk Symposium in Molecular Medicine, Center for Molecular Medicine Cologne, University of Cologne, D-9

Dedicated to my father

Late-Hara Prasad Raul

Who could not see me graduate with a doctorate but is always enlightening my life with his blessings and watching over me from the heaven.

Table of Contents

Acknowledgments

My path from Baliapal to Göttingen was not a straight line. During this, up and down phase and challenging journey of life I was passionate about it, worked hard and sincerely. And, I would like to express my sincere thanks to all those who have come across and inspired me to overcome the difficulties and made this thesis possible.

I would like to offer my humble gratitude to my supervisor Prof. Dr. Steven A. Johnsen for his incomparable guidance and constant support throughout my Ph.D. I thank him from the bottom of my heart for all the motivation, patience and all the discussions I had with him during this whole period. Without his help and supervision, I would never be able to continue and finish this project towards obtaining the degree.

Along with my supervisor, I would like to thank all the members of my thesis committee, Prof. Dr. mult. Thomas Meyer and Prof. Dr. Michael Zeisberg for their valuable comments and advice, which greatly helped me improve different aspects of the thesis and overcome many difficulties.

I would like to express my sincere gratitude to Dr. Vijaya Lakshmi Kari for her mentorship, guidance, priceless suggestions, advice, who trained me on several techniques during my Ph.D. career.

My thanks to our collaborator Wael Yassin Mansour, University Medical Center Hamburg-Eppendorf, Hamburg, Germany. I thank Jessica Eggert for assistance with immunohistochemistry, Dr. Melanie Spitzner for CFA assay and survival analyses with Dr. Frank Kramer.

I sincerely thank the beautiful and the intellectual research atmosphere of UMG, Göttingen and inside AGJ-Tumor Epigenetics laboratory for providing me with the necessary laboratory and research facilities along with a wonderful research-oriented atmosphere, without which this research would not have been possible.

I also want to thank my all lab-mates and colleagues for their steady support and help throughout my Ph.D. study. Not only the productive discussions I had with them, helped me in my research, but also all the fun and light moments I shared with them, made my stay in Hamburg and Göttingen very pleasant and memorable. I would also like to thank specially Robyn Laura Kosinsky and Feda Hamdan for their insightful revisions to this thesis. My heartfelt thanks to Julia Spotter from Hamburg, Honamann-Capito, Sabine Bolte and Nicole Molitor for technical support and Larissa Geier for administrative assistance.

I am grateful to Prof. Dr. Matthias Dobbelstein and all the members of our neighbor Department of Molecular Oncology for their kind co-operation and specially Priyanka and Yizu for their support during this study.

Acknowledgements

My study was supported by “National Overseas Scholarship” (from the Ministry of Social Justice and Empowerment, Government of India). I am highly grateful to Government of India for this scholarship and providing financial assistance to live in Germany.

I would like to thank Prof. Dr. Hans Will for his constant help, motivation and support from Hamburg to Göttingen journey of life.

I would like to thank my entire family, especially my mother, brothers Bijay and Ajay, and sister Madhusmita and my wife Mrs. Surajita Raul. My dear son Iswar Prasad Raul, and proof of my Ph.D. study here, newborn daughter Jahnavi is memorable gift and inspiration for the unending mental support and encouragement they have given me during the last four years including the period of research and thesis writing. I thank them for standing by me all along.

Last but not the least, I want to thank my father Late-Hara Prasad Raul who, by the most unfortunate turn in my life, could not live to see me graduate. He always motivated and inspired me to whatever it takes to achieve success. Wherever he might be, I wish he would see me succeed and fulfill his wish for me to earn a doctorate. Dear papa, you will always live in my heart and through your blessings and my hard work I will keep on climbing the stairs of success.

Abbreviations

A	Ampere
ac	Acetylation
APC	Adenomatous polyposis coli
APS	Ammonium persulfate
ATM	Ataxia telangiectasia mutated kinase
ATP	Adenosine triphosphate
ATR	Ataxia telangiectasia and Rad3 related
BER	Base-excision repair
BGP	β-Glycerophosphate
bp	Base pair
53BP1	p53 binding protein 1
BRAF	v-Raf murine sarcoma viral oncogene homolog B
BRCA1	Breast cancer 1
BRCA2	Breast cancer 2
BSA	Bovine serum albumin
°C	Degree Celsius
cDNA	Complementary DNA
CHD1	Chromo-domain helicase DNA-binding protein-1
Chk2	Checkpoint kinases
CIMP	CpG island methylator phenotype
CIN	Chromosomal instability
CO_2	Carbon dioxide
Con	Control
CpG	Cytosine phosphate guanine
CTD	Carboxy-terminal domain

CtIP	CtBP-interacting protein
DAPI	4',6-Diamidino-2-phenylindole
ddH_2O	Double distilled water
DDR	DNA-damage response
DEPC	Diethylpyrocarbonate
DMEM	Dulbecco/Vogt modified Eagle's minimal essential medium
DMSO	Dimethyl sulfoxide
DNA	Deoxyribonucleic acid
dNTP	Deoxyribonucleotide
DOT1L	Disruptor of telomeric silencing 1-like
DRB	5,6-dichloro-1-beta-D- ribofuranosylbenzimidazole
DSB	DNA double strand break
DTT	Dithiothreitol
EDTA	Ethylenediaminetetraacetic acid
EGTA	Ethylene glycol-bis (β-aminoethyl ether)
EtOH	Ethanol
F	Forward
FACS	Fluorescence-Activated Cell Sorting
FBS	Fetal bovine serum
g	Relative centrifugal force
GFP	Green-fluorescent protein
Gy	Gray
h	Hour
H2A	Histone 2A
γH2AX	Histone H2A.X variant at Ser139 by PI3K-like kinases

H2Aub1	Monoubiquitinated histone 2A
H2B	Histone 2B
H2Bub1	Monoubiquitinated histone 2B
H3	Histone 3
H3K79me3	Histone 3 trimethylated at position lysine 79
H&E	Hematoxylin and eosin
HMT	Histone methyltransferase
hnRNPK	Heterogeneous nuclear ribonucleoprotein K
HR	Homologous recombination
HRD	Homologous recombination deficiency
HRP	Horseradish peroxidise
HSC70	Heat shock 70kDa protein
IF	Immunofluorescence
IgG	Immunoglobulin G
IR	Ionizing radiation
IRI	Irinotecan
K	Lysine residue
KCl	Potassium chloride
kDa	Kilo Dalton
KRAS	V-Ki-ras2 Kirsten rat sarcoma viral oncogene homolog
L	Leucine residue
me	Methylation
MgCl2	Magnesium chloride
MLL	Myeloid/lymphoid or mixed-lineage leukemia
MRE11	Meiotic recombination 11
mRNA	Messenger RNA

MRN complex	Mre11-Rad50-Nbs1
NaCl	Sodium chloride
NAD+	Nicotinamide adenine dinucleotide
NBS1	Nijmegen-breakage syndrome
NCS	Neocarzinostatin
NEM	N-ethylmaleimide
NER	Nucleotide-excision repair
NHEJ	Non-homologous end joining
NP-40	Nonidet P40
p	Phospho
p300	E1A binding protein p300
p53	Tumor protein 53
PALB2	Partner and localizer of BRCA2
PAR	Polymers of ADP-ribose
PARP	Poly (adenosine diphosphate [ADP]) ribose polymerase
PARPi	PARP inhibitor
PBS	Phosphate-buffered saline
PBS-T	Phosphate-buffered saline with Tween-20
PCR	Polymerase chain reaction
PLA	Proximity ligation assay
Pol	Polymerase
P/S	Penicillin/streptomycin
PTMs	Post-translational modifications
qRT-PCR	Quantitative real-time PCR
R	Reverse
RAD	RecA homolog

Rad6	Radiation-sensitivity protein 6
RNA	Ribonucleic acid
RNAPII	RNA polymerase II
rRNAs	Ribosomal RNAs
RNF20	Ring-finger protein 20
RNF40	Ring-finger protein 40
RPA	Replication protein A
RPM	Revolutions per minute
RT	Room temperature
RT-PCR	Reverse transcription PCR
SAM	S-adenosyl-L-methionine
s.d.	Standard deviation
SDS	Sodium dodecylsulfate
SDS-PAGE	Sodium dodecylsulfate polyacrylamide gel electrophoresis
sec	Second
SET	(Su(var), Enhancer of zeste, Trithorax)
siRNA	Small interfering RNA
ssDNA	Single-stranded DNA
Taq	Thermus aquaticus
TEMED	Tetramethylethylenediamine
TMAs	Tissue microarrays
Top1	Topoisomerase I
Tris	Tris(hydroxymethyl)aminomethane
U	Unit (enzyme activity)
ub	Ubiquitination
UMG	University Medical Center Göttingen

UV	Ultra violet
V	Voltage
VEL	Veliparib
v/v	Volume per volume
XLF	Xrcc4 like factor
XRCC	X-ray cross-complementation group
WB	Western blot
wt	Wild type
w/v	Weight per volume

List of Figures

Abstract

New effective combinational therapeutic strategies are an alternative choice for a successful translational study. Disruptor of telomeric silencing 1-like (DOT1L) is a histone 3 lysine 79 (H3K79) methyltransferase enzyme and its inhibition is being tested in phase 1 clinical trials. DOT1L has been implicated in many biological functions ranging from cell cycle regulation, transcriptional regulation, and heterochromatin formation, however, the functions of DOT1L in DNA-damage response remains to be unraveled. DNA double-strand breaks (DSB) are one of the most lethal forms of DNA damage and can lead to several disease phenotypes, including cancer. In this study, we investigated the role of DOT1L in the DNA double-strand break repair-pathway. Our results indicate that DOT1L is required for proper DNA-damage response and repair of DNA DSBs via a homologous recombination (HR) pathway. DOT1L activity prevents the proliferation of cancer cells; therefore this is a potential future cancer therapeutic target. And more importantly, our results show the combination of small molecule inhibitor PARP with other available chemotherapeutics agents shows synergism in the colorectal cancer cells. The data further suggest DOT1L plays a role HR-mediated DNA double strand break and loss of DOT1L functions leads to increased sensitivity to PARP inhibition. Therefore, we hypothesize that DOT1L activity (i.e. H3K79me3) may serve as a marker for molecular stratification of colorectal cancer.

1 Introduction

1.1 Colorectal cancer (CRC)

Colorectal cancer (CRC) is the third most commonly occurring cancer and the fourth most common cause of cancer-related death (Favoriti et al., 2016). Different factors that influence the risk for colorectal cancer include several mutations, chronic intestinal inflammation, colorectal polyps, obesity, cigarette smoking, excessive alcohol use, increasing age and family history of colorectal cancer (Haggar and Boushey, 2009). The development and progression of normal cells to colon adenocarcinoma is a multistep process that involves mutations in genes such as Adenomatous Polyposis Coli (APC), v-Raf murine sarcoma viral oncogene homolog B (BRAF), and V-Ki-ras2 Kirsten rat sarcoma viral oncogene homolog (KRAS,) in addition to epigenetic alterations such as aberrant CpG island DNA methylation (Abdullah et al., 2012; Kocarnik et al., 2015; Okugawa et al., 2015). On the basis of molecular profiles, colorectal cancer is classified into specific sub-classes. These include microsatellite instability (MSI), CpG island methylator phenotype (CIMP), and chromosomal instability (CIN). CIMP and MSI are associated with mismatch repair deficiency (Issa, 2000; Toyota et al., 1999). DNA repair enzymes play a crucial role in driving the initiation and progression of CRC. Defects in DNA repair result in genomic instability which lead to the development of cancer (Bardhan and Liu, 2013; Ferguson et al., 2015). Therefore, DNA repair mechanisms should be further investigated to evaluate whether disturbed repair could represent a suitable therapy target.

1.1.1 Management of colorectal cancer

Over the last few decades due to early detection (via colonoscopy) treatment of colorectal cancer has been rapidly improving and became more effective. Generally,

the treatment of patients depends on upon the stage of the disease. The main options used for the treatment of colorectal cancer include surgery, radiation therapy, chemotherapy and targeted therapy (Cunningham et al., 2010). Combination treatment regimens have been shown to be better than standard drugs alone in improving overall survival, disease-free survival, progression rate, and quality of life. The most clinically effective specific combinations of chemotherapeutic agents currently used for CRC are FOLFOX (Folinic acid, 5- Fluorouracil (5-FU), and Oxaliplatin), FOLFOXIRI (Folinic acid, 5-FU, Oxaliplatin, and Irinotecan), and FOLFIRI (Folinic acid, 5-FU, and Irinotecan) (Braun and Seymour, 2011; Souglakos et al., 2006). Overall, several studies have shown that FOLFOXIRI regimen leads to better response and survival than FOLFIRI regimen (Akhtar et al., 2014; Souglakos et al., 2006). Additionally, several epigenetic inhibitors have been approved or are currently in preclinical trials for cancer treatment (Nebbioso et al., 2012).

1.2 Chromatin structure and organization

Epigenetic regulation of transcription involves the changes to gene expression without altering the underlying DNA sequence through three main mechanisms of covalent modifications to histones and DNA and through non-coding RNA pathways (Wu and Sun, 2006). Generally, in eukaryotic cells, chromatin is a highly compacted complex structure of DNA and histones. Chromatin plays a significant role in packing and protecting the genome. It also plays a key role in the regulation of many biological functions including transcription, DNA damage detection, signaling, and repair (Price and D'Andrea, 2013).

The basic unit of chromatin is the nucleosome. In eukaryotes, it contains 147 base pairs of DNA wound around an octamer of histone proteins which consist of two copies of each H2A, H2B, H3, and H4. Nucleosome assembly in the nucleus takes

place in two stages. First, hetero-tetramer H3/H4 integrates into the DNA and then, the heterodimer H2A/H2B is added. Nucleosomes are then compacted into 30 nm fibers through the fusion of linker histone H1, and further compression into 250-fold structural compaction associated in metaphase chromosomes (Woodcock and Ghosh, 2010) (Figure1). Therefore, the nucleosomes play an important role in the regulation of gene expression (Maze et al., 2014) and DNA repair (Peterson and Almouzni, 2013). The dynamic nature of the nucleosomes is due to covalent histone post-translational modifications and ATP-dependent chromatin remodeling (Hassa and Hottiger, 2005).

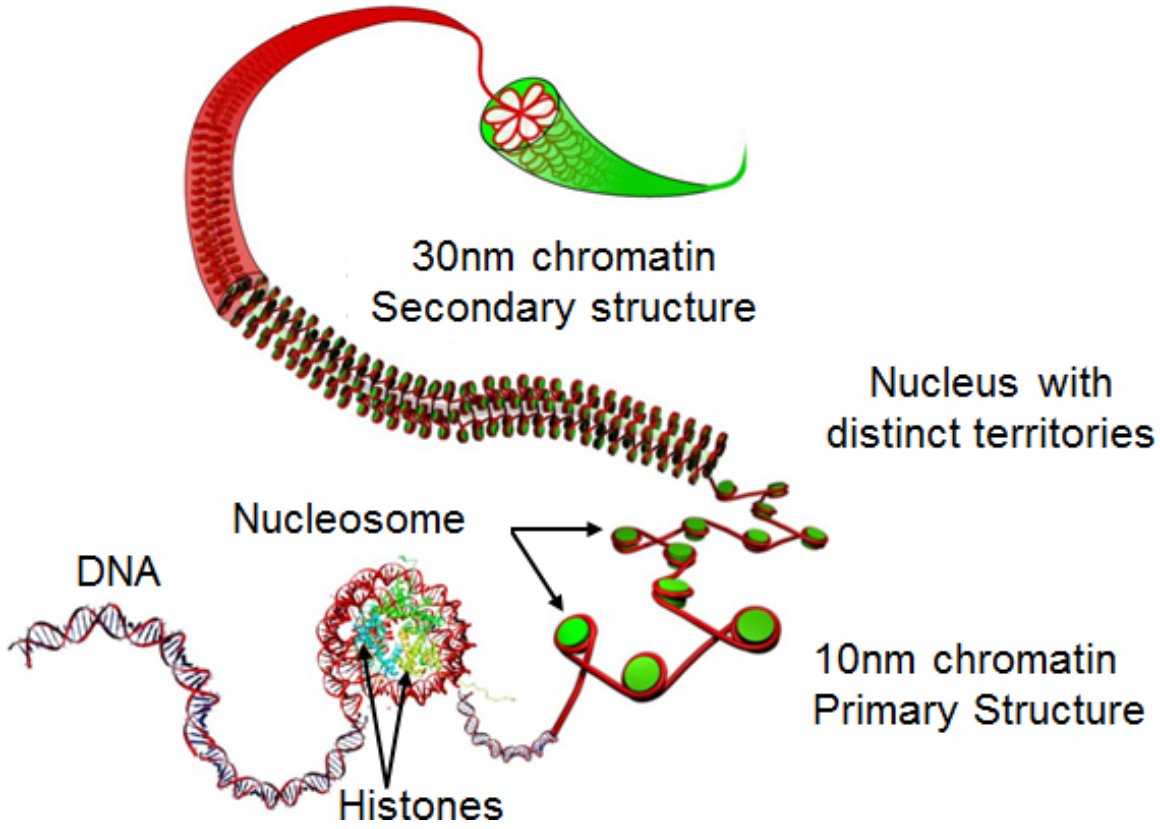

Figure 1: The structure of chromatin. DNA organization from decondensed (bottom) to higher condensed (top). DNA is wrapped around histone octamers to form nucleosomes. Further compression includes 10 nm and 30 nm chromatin structures which lead to the organization of the metaphase chromosome. Modified from (Iyer et al., 2011) and used with permission from the article.

1.2.1 Post-translational histone modifications

Posttranslational histone modifications regulate gene expression and are important for many biological processes to occur. Euchromatic regions, where DNA is accessible for transcription, are associated with active transcription while heterochromatic regions, where DNA is more compacted, is associated with gene repression. Different types of post-translational covalent modifications of histones such as phosphorylation, ubiquitination, methylation and acetylation (Figure 2) regulate different processes in the cell, such as DNA replication and repair (Strahl and Allis, 2000; Vardabasso et al., 2014). The crosstalk between multiple modifications of histones orchestrates the regulation of chromatin structure in different processes, such as replication, recombination, transcription, in addition to chromosome segregation and repair (Hunt et al., 2013).

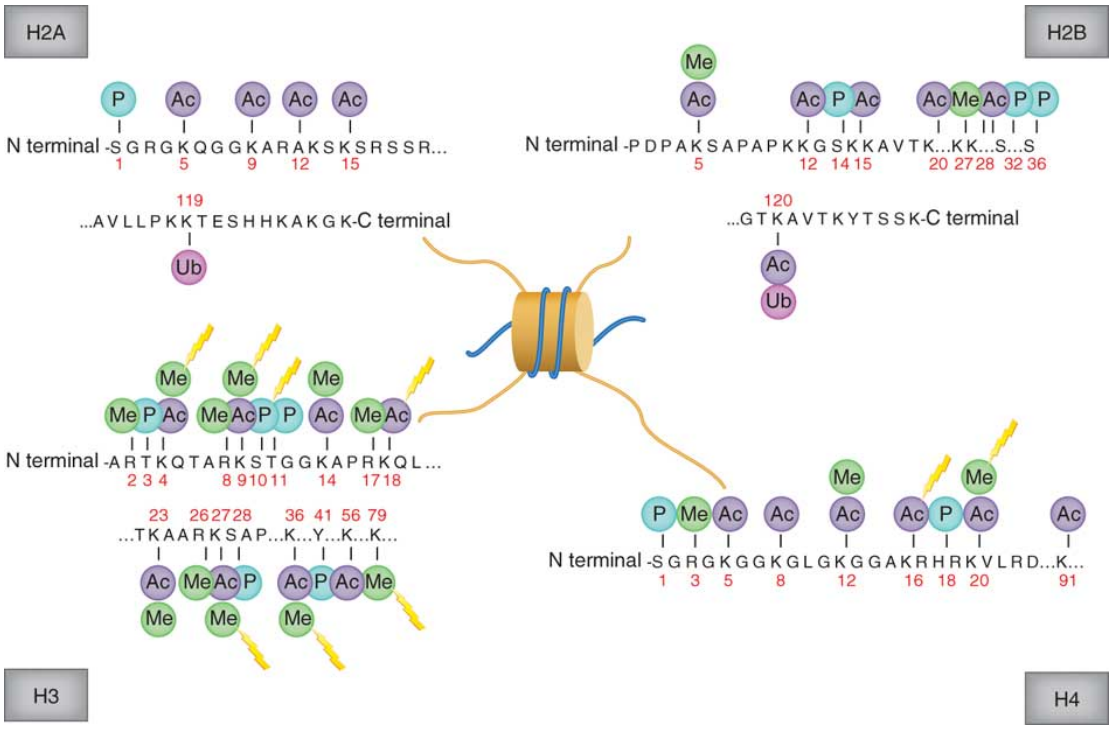

Figure 2: Post-translational histone modifications. A simplified view of H2A, H2B, H3, H4 post-translational histone modification at the marked amino acid positions of each histone. Ac, acetylation; Me, methylation; P, phosphorylation; Ub, ubiquitination. (Rodríguez-Paredes and Esteller, 2011). Used with permission of the Nature Publishing Group.

1.3 DNA damage and repair process

Genome integrity is always under attack from different agents. DNA lesions are caused by various endogenous and exogenous agents such as cytotoxic chemicals including reactive oxygen species (ROS) and ionizing radiation (IR), which either induce double strand breaks, single strand breaks, oxidative lesions or pyrimidine dimers. The majority of the DNA lesions induce the DNA damage response (DDR), which is mediated by cellular DNA mechanisms, which is further categorized into several distinct mechanisms such as nucleotide-excision repair, base-excision repair, mismatch repair and double-strand break repair based on the type of DNA breaks. Defects in DNA repair mechanisms can significantly increase genomic instability and lead to cancer progression (O'Connor, 2015). Therefore, preventing or repairing the DNA damage is crucial for the maintenance of genomic integrity (Polo and Jackson, 2011).

1.3.1 DNA damage sensors, mediators, and transducers

Upon DNA damage, various DNA damage sensors are recruited. In the case of DSBs, the MRN (Mre11–Rad50–Nbs1) complex recognizes DNA damage and recruits and activates ataxia-telangiectasia mutated (ATM), which is a member of the phosphoinositide 3-kinase (PI3K)-related protein kinase (PIKK) family, through interaction with protein Nbs1. ATM phosphorylates the histone H2A variant, H2AX, at serine position 139 known as γH2AX. Histone H2AX differs from the canonical H2A histone by its C-terminal tail. Moreover, ATM phosphorylates MRN complex which is involved in the initial processing of DSBs, checkpoint mediator MDC1 (Mediator of DNA Damage Checkpoint 1), checkpoint kinase CHK2 which are important signaling mediators during DSB repair. Phosphorylation of H2AX and the MRN complex leads to the recruitment of many repair factors which helps in the

homologous recombination (HR) repair process and signal transduction (Krajewska et al., 2015) (Figure 3).

In the DDR network, DNA damage sensors first detect the break sites, which further transduce the information, and activate cell cycle checkpoint control, apoptosis, transcription, and activation of DNA repair pathways. The signal transduction cascade includes protein kinases such as ATM, ATR, and DNA-PKcs. This signaling cascade modulates many downstream events (Harper and Elledge, 2007).

KAP1 is a scaffold protein which acts as a transcriptional repressor and associates with histone H3 lysine 9 methyltransferases, histone deacetylases and heterochromatin protein 1 (HP1). KAP1 plays a crucial role as a phosphorylation target by ATM Serine 824, during the DNA damage response and in DSB processing in heterochromatin (Lin et al., 2015).

1.4 Types of DNA damage and repair processes

In mammals, DNA lesions are repaired by four major repair pathways. Single-strand DNA breaks are repaired by nucleotide excision repair (NER), base excision repair (BER), while double-stranded breaks (DSBs) are mainly repaired by homologous recombination (HR) or non-homologous end joining (NHEJ) (Haber, 2000)

1.4.1 DNA double-strand breaks repair pathways

One of the most lethal forms of DNA damage is DNA double-strand breaks. The failure to repair DSBs can lead to severe genomic instability, cell death, chromosome translocation and mutation or cancer (Jackson and Bartek, 2009; Nambiar and Raghavan, 2011; Swift and Golsteyn, 2014). Therefore, the repair of DNA damage is pivotal for the treatment of cancer and carcinogenesis in the context of chromatin and its modification. Error-free homologous recombination (HR) and non-homologous end joining (NHEJ) are alternative pathways of double-strand DNA

break repair (Chapman et al., 2012). Additionally, the damage response is regulated by histone modifications and chromatin remodeling, for example, the ATP-dependent chromatin remodeler CHD1 alters chromatin landscape and repairs DSBs (Kari et al., 2016).

1.4.2 Non-homologous DNA end-joining (NHEJ)

The first mechanism to sense and respond to DNA damage is the Non-Homologous End-Joining pathway. Three important steps involved in this repair pathway are detection, processing, and ligation (Chiruvella et al., 2013).

In the NHEJ pathway, the KU70/80 heterodimer acts as an early sensor of a double strand break and leads to the binding of the broken ends followed by the recruitment of DNA-dependent protein kinase (DNA-PK) which brings these ends into proximity and activates the downstream substrates by phosphorylation. Finally, ligation occurs by the XRCC4-DNA Ligase IV-XLF complex, which is the most critical factor in rejoining separated DNA ends (Figure 3). Mainly G0-G1 and S phases of the cell cycle are involved in this repair pathway. This is an error-prone mechanism as opposed to HR (Rodgers and McVey, 2016).

1.4.3 Homologous recombination (HR) pathway

DNA repair pathways are based on various phases of the cell cycle (Kim et al., 2014). The most commonly known pathway is Homologous Recombination (HR), which is mainly predominant in the late S and G2 phases of the cell cycle. HR is a template-based repair process which requires a sister chromatid or a homologous chromosome. Therefore, this is considered to be an error-free repair mechanism. During HR-mediated repair, DNA end-resection is the first step, which takes place during this phases of cell cycle and generates single-stranded DNA, which is covered with replication protein A (RPA). The repair is supported by recruitment of

DNA-binding proteins such as BRCA1, BRCA2, and Rad51. MRN (MRE11-RAD50-NSB1) contributes to DNA resection, which is followed by recruitment of replication protein A (RPA) (Figure 3). This ssDNA-binding factor removes secondary structures of ssDNA and is subsequently replaced by Rad51. Besides this, a number of proteins, are required and recruited for maintaining chromosome structure and for efficient HR. The most frequently HR-mutated genes, BRCA1 and BRCA2 associated with hereditary breast and ovarian cancer (Fackenthal and Olopade, 2007; Hall et al., 2009), are targets for homologous recombination repair of DNA.

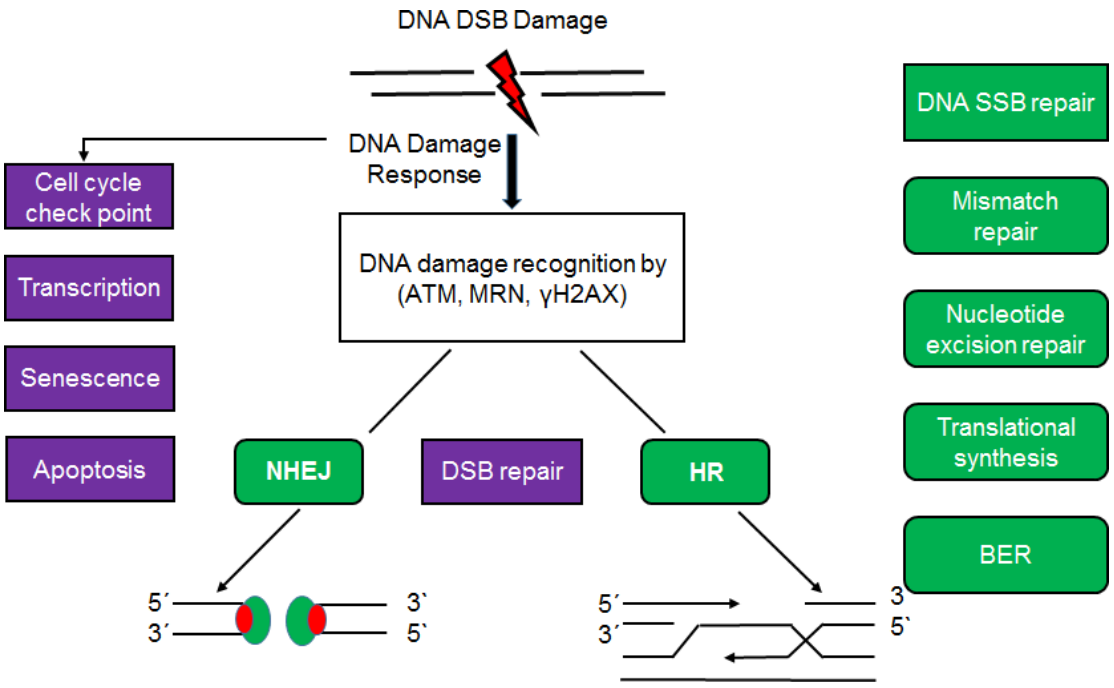

Figure 3: DNA damage and repair pathway. The two major DSB repair pathways in mammals: Upon DSB damage MRN complex recognizes and ATM activates and phosphorylates H2AX. DSB repair can occur through non-homologous end joining (NHEJ) or homologous recombination (HR). Based on (Shrivastav et al., 2008)

1.5 PARP in DNA repair process

Poly (ADP-ribose) polymerases (PARPs) are a family of enzymes, which plays different biological processes through the covalent transfer of ADP-ribose from NAD^+ onto substrate proteins. PARP-1 and PARP-2 enzymes are involved in DNA repair, chromosome maintenance, chromatin regulation, and gene expression (Michels et al., 2014). In general, PARP1 enzyme plays a key role in repairing single-strand breaks (SSBs), by the base excision repair pathway. The inhibition of PARP1 leads to the accumulation of DNA SSBs, which gives rise to DSBs at replication forks during DNA replication. PARP inhibitors (PARPi) have been used against tumors that are deficient in BRCA1 or BRCA2 (Leung et al., 2011). The deficiency in homologous recombination repair is thus specific to the tumor and can be exploited by employing PARP inhibitors. Therefore, PARP inhibition in tumor cells with deficient homologous recombination repair (absence of BRCA1 or BRCA2) generates unrepaired SSBs that cause an overwhelming accumulation of DSBs leading to tumor cell death (Figure 4). In contrast, cells that are heterozygous for BRCA1 or BRCA2 retain homologous recombination repair function and have a low sensitivity to PARP inhibitors similar to that of wild-type cells. PARP inhibition induces selective tumor cell death while sparing normal cells and thus is considered as a therapeutic target for the treatments of various types of cancers displaying defects in the HR pathway (Dobbelstein and Sørensen, 2015).

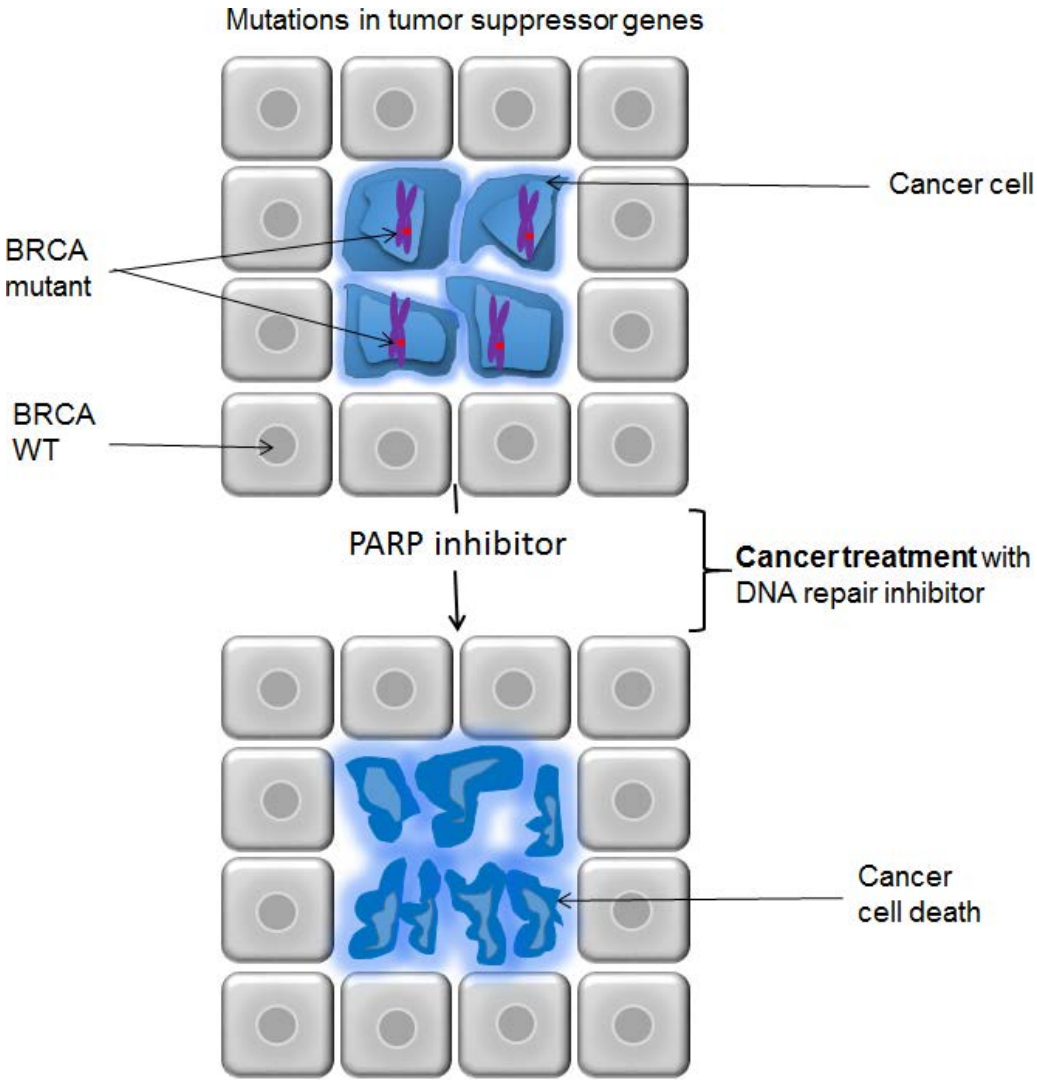

Figure 4: PARP inhibitor in DNA repair cancer treatment. Mutations (red dots) on chromosomes make cancer cells susceptible to DNA repair with PARP inhibitors. Based on (Jackson and Helleday, 2016).

1.5.1 PARP inhibitors in combination therapy of colorectal cancer

Standard treatments for colorectal patients include oxaliplatin, the topoisomerase I (Top1) inhibitor irinotecan, and 5-fluorouracil (5-FU) (Davies and Goldberg, 2011). PARP inhibitors play a key role in DNA repair (Schreiber et al., 2006). Presently, there are different PARP inhibitors are in clinical trials. Among them, olaparib is the first PARP inhibitor approved by the European Medicines Agency, and also by the US Food and Drug Administration (FDA) for platinum-based chemotherapy in BRCA1/2 mutant ovarian cancer (Bixel and Hays, 2015). This also tested along with topoisomerase I (Top1) inhibitors (irinotecan hydrochloride) in patients with locally

advanced or metastatic colorectal cancer (NCT00535353) (Chen et al., 2016; Genther Williams et al., 2015). Combining PARP inhibitors with different cytotoxic DNA damaging agents is a promising therapeutic approach that is currently under study (Benafif and Hall, 2015). Olaparib (AZD2281) demonstrated an anti-tumor activity in phase 1 clinical trials in castration-resistant prostate cancers characterized by mutations in different HR biomarkers BRCA1/2, ATM, PALB2, CHEK2, FA NCA and HDAC2 (Mateo et al., 2015). Olaparib was tested in phase I trials in ovarian cancer (Fong et al., 2009) and phase II trial in breast cancer, endometrial cancer, prostate cancer and pancreatic cancer. Olaparib has recently been approved for treating ovarian, fallopian tube and primary peritoneal cancer with BRCA1 or BRCA2 mutations (Ledermann et al., 2014). Rucaparib (AG014699) is in phase 3 clinical trials (NCT02855944) tested in ovarian cancer, epithelial ovarian cancer, fallopian tube cancer and peritoneal cancer with BRCA mutation (Kristeleit et al., 2015). Niraparib (MK4827) is in phase 1/2 clinical study (NCT02657889, NCT02354131) in combination with Pembrolizumab/Bevacizumab with advanced or metastatic triple-negative breast cancer and with recurrent/HRD platinum-sensitive ovarian cancer (Mirza et al., 2016). Talazoparib (BMN-673) in an ongoing phase 3 clinical trial (NCT01945775) with BRCA mutant breast cancer (Roche et al., 2015).

Veliparib (ABT-888) is an orally active small molecule inhibitor of PARP-1 and PARP-2 enzymes, is an attractive candidate and is already in phase 3 clinical development (NCT02163694) among women with early-stage triple-negative breast cancer. Mutations in the BRCA1 or BRCA2 genes cause defects in homologous recombination (HR) and studies suggest that microsatellite instability (MSI) and microsatellite stable (MSS) colorectal cancers which are defective in HR are sensitive to PARP inhibition (Genther Williams et al., 2015). Overall, ongoing trials in

patients with and without BRCA mutation imply a promising role of PARP inhibitors need for biomarkers for patient stratification in colorectal cancer management.

1.6 Histone modifications in DNA damage response (DDR) and repair

Histone modifications affect chromatin structure and dynamically change nucleosome positions which affect transcription. Upon induction of DDR, post-translational modifications of histone and repair proteins are activated (Rossetto et al., 2010). The four well-known histone modifications are acetylation, methylation, phosphorylation, and ubiquitination.

1.6.1 Phosphorylation

Histone phosphorylation plays an important role during cell division, transcriptional regulation, chromatin remodeling (Rossetto et al., 2012). Additionally, it plays a role in DNA damage response by recruiting different repair proteins to DNA breaks. The best-known earliest marker for DSB epigenetic modification in mammalian cells is phosphorylation of histone variant H2AX (γH2AX) at ser139, which is mediated by members of the PI3K kinase superfamily (ATM, ATR, DNA-PK) (Rogakou et al., 1998). H2AX is phosphorylated in the region of DSBs up to $2x10^6$ bp around the break (Lowndes and Toh, 2005; Rogakou et al., 1999). In yeast, the phosphorylation occurs on S129 of H2A (Downs et al., 2000). Besides histones are phosphorylated at the other sides of breaks such as H3 at T11 and H4 at Ser1 (Rossetto et al., 2012) in response to DNA damage and repair.

1.6.2 Acetylation

Acetylation is mainly associated with transcriptional activation. Histone acetylation is associated with open chromatin structure and helps to make chromatin accessible to transcription factors and enable gene expression. Acetylation is controlled by the

writers histone acetyltransferases (HATs), which determine transcriptionally active states. Whereas deacetylation mediated by the erasers, histone deacetylases (HDACs), lead to transcriptional repression (Davie, 2003). Histone acetylation facilitates DNA repair by enabling DNA repair proteins to access the sites of damage or serving as a platform for the interaction and recruitment of the DNA repair proteins by means of bromodomains. The HAT complex Tip60, which binds to neighboring chromatin, is involved in DSB repair and induces histone H4 acetylation (Ikura et al., 2000; Murr et al., 2006).

1.6.3 Ubiquitination

Histone ubiquitination is important for the regulation of chromatin structure. Ubiquitin is a 76-amino acid polypeptide that is attached to lysine residues of target proteins via the sequential action of three enzymes, (E1) ubiquitin-activating, (E2) ubiquitin-conjugating and (E3) ubiquitin-ligating enzymes. Histone H2A and H2B are the most abundant ubiquitinated proteins in the nucleus (Vissers et al., 2008). H2A monoubiquitination is catalyzed by polycomb group proteins, which is mainly associated with gene silencing. RNF8 (RING finger-containing nuclear factor 8) is an E3 ubiquitin ligase enzyme which catalyzes regulatory ubiquitylation at sites of DSBs (Panier and Durocher, 2009), which help in the recruitment of downstream factors, such as 53BP1 and BRCA1 (Huen et al., 2007; Mailand et al., 2007). Monoubiquitination of H2B by RNF20 facilitates HR repair (Moyal et al., 2011; Nakamura et al., 2011). DNA repair factors such as BRCA1 and 53BP1 determine the DNA DSB repair pathway choice of either NHEJ or HR (Daley and Sung, 2014). It was first identified in yeast that histone H2B monoubiquitination on Lys123 by the Rad6/Bre1 complex is required for proper H3K79 trimethylation by Dot1L (Ng et al., 2002). Recent studies (McGinty et al., 2008; Oh et al., 2010) demonstrated that recombinant human DOT1L protein was capable of increasing mono- and

dimethylated H3K79; however, no trimethylation was detected in correlation with H2B ubiquitination. It is reported that human Dot1-containing complex (DotCom) dimethylates and trimethylates H3K79 when nucleosomal substrates are monoubiquitinated on H2B (Mohan et al., 2014).

1.6.4 Methylation

Histone methylation is a type of covalent histone modification, which is carried out by a group of enzymes called histone methyltransferases (HMTs). Methylation occurs at lysine (K), arginine (R) residues (Greer and Shi, 2012). In general, to lysine (K) and arginine (R) residues, methyl groups can be transferred, i.e. to the ε-amino group of lysine residues or to the guanidino group of arginine residues. Methylation mainly occurs on the side chains of lysines, arginines and also N-terminals of many proteins. Depending on the positions and degree of methylation, the lysine residues can be mono (me1), di (me2) or trimethylated (me3). It can either be a mark for transcriptionally active or inactive chromatin. Histone lysine methylation plays a dynamic role in development and disease (Black et al., 2012). There are many lysine residues in histones targeted for methylation: H3K4, H3K9, H3K27, H3K36, H3K79, and H4K20, which are the substrates of different histone methyltransferases in humans (Copeland et al., 2009). Methylation of H3 lysine (H3K4 and H3K36) is associated with transcription activation, whereas methylation of H3K9, H3K27 and H4K20 appears to correlate with transcriptional repression (Vakoc et al., 2006). In response to UV irradiation, H3K79 and H4K20 are methylated and found to play a role in efficient repair of UV-induced damage (Bostelman et al., 2007; Sanders et al., 2004). Human DOT1L binds to methylated H3K79. Dot1/DOT1L enzyme methylates H3K79 within the histone globular core and leads to 53BP1 recruitment (Huyen et al., 2004a).

1.6.5 The trimethylation of histone H3 at lysine 79 (H3K79me3)

Histone methylation occurs using S-adenosylmethionine (SAM) as a methyl group donor. The 3 families of enzymes that catalyze histone methylation are the PRMT (protein arginine N-methyltransferase) family, the SET (Su[var]3–9, Enhancer of Zeste, Trithorax)-domain-containing family, and the non-SET domain proteins (Greer and Shi, 2012). Lysine methylation of H3K4, H3K9, H3K27, H3K36, and H4K20 is mediated by lysine methyltransferases (KMTs) that contain a SET domain whereas, H3K79 is methylated by the non-SET domain-containing protein DOT1L (Nguyen and Zhang, 2011a; Singer et al., 1998).

1.7 DOT1L (Disruptor of telomeric silencing 1-like)

Dot1 (KMT4) is the lysine methyltransferase responsible for H3K79 methylation and was initially discovered in budding yeast and homologs have been found in a range of species like *Drosophila*, protozoa and mammals (Janzen et al., 2006; Jones et al., 2008a; List et al., 2009). The mouse DOT1L gene shares 88% similarity with human DOT1L (Wong et al., 2015). This is a non-SET histone modifying enzyme and the only characterized lysine HMTase responsible for catalyzing mono-, di- and tri-methylation. H3K79 mono-and di-methylation leads to active gene transcription (Nguyen and Zhang, 2011b; Wong et al., 2015). DOT1L methylates K79 only when histone H3 is incorporated in the nucleosomal histone H3, not in free/soluble form (Lacoste et al., 2002). There are no identified non-histone substrates of the DOT1L enzyme, which may help in understanding DOT1L-mediated cellular functions. The unique crystal structure of the catalytic domain of DOT1L reveals an AdoMet-binding pocket in proximity to a potential lysine-binding channel and a positively charged, flexible region at the C-terminus of the catalytic domain which is required for nucleosome binding and enzymatic activity (Barry et al., 2010) (Figure 5).

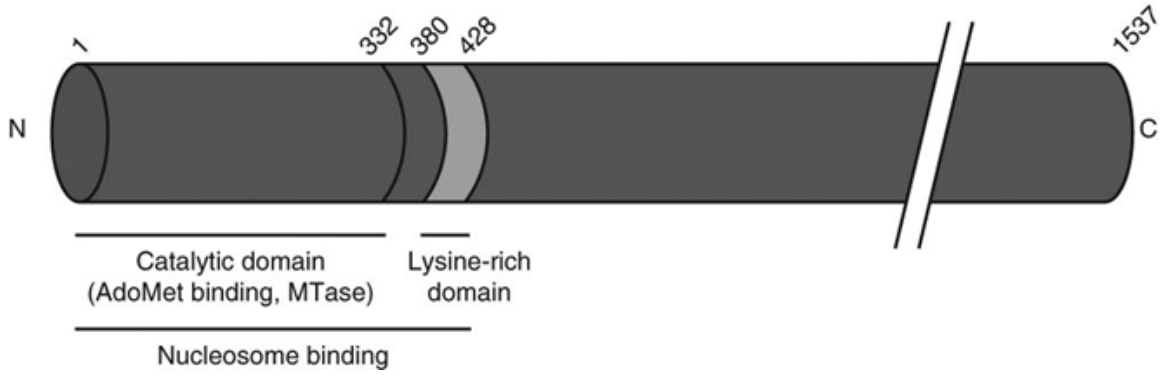

Figure 5: Structure of the DOT1L protein. The amino-terminal 332 amino acids of DOT1L comprises the catalytic domain, including the methyltransferase (MTase) and *S*-adenosyl –L-methionine (AdoMet)-binding activities. The catalytic region, together with a short, lysine-rich domain located between amino acids 380 and 428, functions as a nucleosome-binding domain (Barry et al., 2010). Used with permission of the Taylor & Francis Group.

DOT1L/KMT4 is involved in many biological functions (Figure 6) like transcriptional regulation, cell cycle regulation, hematopoiesis, cardiac function, (Kim et al., 2014; Nguyen and Zhang, 2011a, 2011b), heterochromatin formation, and embryonic development (Jones et al., 2008a; Okada et al., 2005). The loss of DOT1L results in complete loss of H3K79 methylation in yeast (van Leeuwen et al., 2002), flies (Shanower et al., 2005), and mice (Jones et al., 2008b). In addition, DOT1L dis-regulation has been linked to poor patient prognosis in breast, lung, and colorectal cancer (Huyen et al., 2004b; Wakeman et al., 2012; Wong et al., 2015).

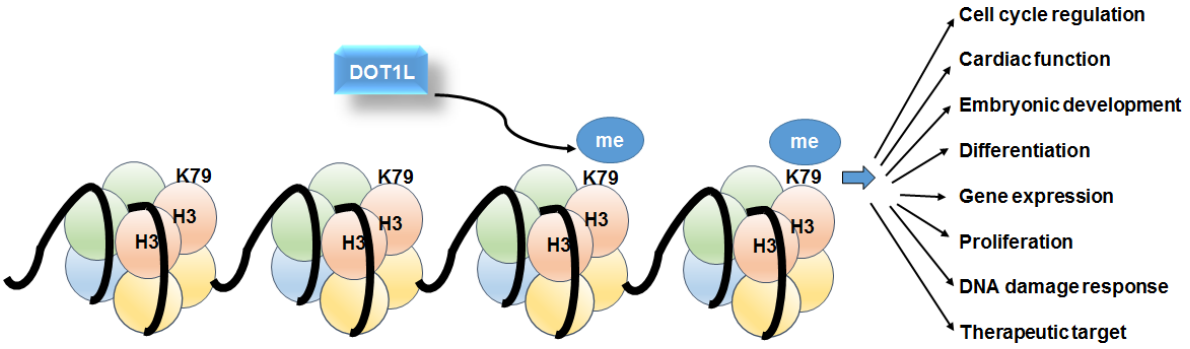

Figure 6: General functions of DOT1L-dependent H3K79 methylation. Based on (Kim et al., 2014). The H3K79 methyltransferase involved in diverse cellular processes ranging from gene expression, cell cycle regulation, DNA damage response and in therapeutic targeting.

1.7.1 Role of DOT1L in cancer

In addition to its role in gene regulation, DOT1L plays a critical role in diseases. Interaction of DOT1L and Mixed Lineage Leukemia (MLL) fusion proteins, leads to increased H3K79 methylation and maintenance of open chromatin leading to leukemogenesis (Bernt et al., 2011; Daigle et al., 2013a; Deshpande et al., 2013; Okada et al., 2005). The AF10 co-factor regulates DOT1L-mediated H3K79 in MLL fusion leukemia (Chen et al., 2015). Recent studies suggest that DOT1L cooperates with a c-Myc/p300 complex to promote breast cancer progression and enhance epithelial–mesenchymal transition (EMT) and breast cancer stem cell (CSC)-like properties (Cho et al., 2015). Deregulation of DOT1L function leads to mitotic misregulation, loss of cell cycle control, apoptotic failure (Nguyen and Zhang, 2011a) and osteoarthritis (Castaño et al., 2012). Depletion or deletion of DOT1L cause a complete disappearance of H3K79 methylation (Jones et al., 2008b). A loss of DOT1L-dependent H3K79 methyltransferase activity inhibits cell proliferation and leads to senescence in lung cancer cells, indicating that DOT1L is required for proliferation of lung cancer cells (Kim et al., 2011). H3K79me2 is required to maintain chromosomal stability (Guppy and McManus, 2015). Genome-wide profiling studies indicate that DOT1L, as well as H3K79 methylation, is enriched in actively transcribed regions of genes, thus identifying DOT1L as an active chromatin modifier (Nguyen and Zhang, 2011a; Steger et al., 2008). Moreover, human DOT1L functionally interacts with actively transcribing RNAPII, which targets the methyltransferase to active genes at the transcription start sites (TSS) (Kim et al., 2012a). DOT1L and AF10 are found and required within β-catenin-dependent TCF4 complexes in mouse crypt and human colon cancer cells (Ho et al., 2013) and are important in governing Wnt-dependent transcription in CRC cells. Histone H3 lysine 79 (H3K79) contributes to the stimulation of the G1/S checkpoint (Humpal et al.,

2009). It has been suggested that DOT1L may serve as a prognostic marker for colorectal cancer (Kryczek et al., 2014). The epigenetic mark DNA methylation (CpG island microarray) is identified as a marker for pre-therapeutic options in advanced rectal cancers molecular stratification, primarily in combination with 5-FU response to preoperative radiochemotherapy (Gaedcke et al., 2014).

1.7.2 DOT1L-mediated H3K79 methylation in DNA damage signaling

DOT1L was shown to be required for the recruitment of the double-stranded DNA break repair protein 53BP1 to the DNA damage sites during different cell cycle phases (Huyen et al., 2004a; Wakeman et al., 2012). Overall, DOT1L is required to maintain chromosomal stability (Kim et al., 2014) and may play a critical role in DNA damage signaling. DOT1L was shown to be important for meiotic checkpoint control and is also involved in double-strand break repair via sister chromatid recombination (Conde et al., 2009a).

1.7.3 Role of DOT1L inhibitors in cancer therapy

Several small molecule inhibitors/drugs which block DDR kinases such as Ataxia Telangiectasia Mutated (ATM), Rad3-related (ATR), checkpoint kinase 1 (CHK1) and the cell-cycle–related kinase WEE1 have been examined for their potential use in anti-tumor therapy (Dobbelstein and Sørensen, 2015). DNA repair inhibitors are currently in different phases of clinical trials along with radio- and chemotherapy regimens. Currently, one of the most advanced and promising drugs targeting DNA repair are PARP inhibitors (Samol et al., 2012). The PARP inhibitor olaparib was FDA-approved for use in BRCA deficient ovarian cancer patients (Meehan and Chen, 2016). Loss of the HR pathway genes such as RAD51, RPA, NBS1 and CHK1 also conferred sensitivity to PARPi, expanding the range of potential targets for PARPi therapy (McCabe et al., 2006)

DOT1L-mediated H3K79me evaluated as the potential therapeutic target (Anglin et al., 2012; Daigle et al., 2011). So far, three small molecule inhibitors are available for DOT1L (EPZ004777, EPZ-5676, and SGC0946) and they display high specificity to DOT1L compared to other HMTs (Daigle et al., 2013b; Yu et al., 2012). These compounds function by competing with S-adenosyl methionine, a cofactor needed for the methyltransferase activity of DOT1L.

EPZ-5676, which was shown to be a potent and selective inhibitor of the DOT1L histone methyltransferase (HMT), is currently undergoing phase 1 trials in children and adult patients with MLL translocated leukemias and shows initially promising results in adult patients with acute leukemias (Song et al., 2016). DOT1L inhibitors suppress proliferation and migration of breast cancer cells (Zhang et al., 2014). It was reported that the small molecule inhibition of DOT1L represents a potential therapeutic option in DNMT3A-mutant human leukemia, and could be used for the treatment of multiple refractory patients (Rau et al., 2016). Therefore, it is important to understand DOT1L's role in DNA repair in relation to identifying potential therapeutical options and evaluate its role in cancer treatment.

Many studies are investigating DOT1L as it plays an important role in a variety of biological processes in different organisms from yeast to mammals. However, much less is known regarding the involvement of this protein in DNA-DSB-break repair functions. Previous reports suggest that efficient methylation of H3K79 requires the presence of H2B ubiquitination in the same nucleosome. We hypothesize that a specific portion of the effects observed upon loss of H2Bub1 may be mediated through downstream effects on H3K79 methylation. Consistent with this hypothesis, one report described a correlative decrease in the expression of the H2B ubiquitin ligase RNF40 and H3K79me2 in seminoma (Chernikova et al., 2012). Therefore, we propose that the histone methyltransferase DOT1L may have a role during

epigenetic processes involving the DNA damage response in human colorectal cancer cells in response to DNA double-strand breaks.

In this study, we aimed to investigate the role of the histone modifying enzyme DOT1L in DNA double-strand break repair processes in colorectal cancer cells. Therefore, we investigated the mechanisms underlying the regulation of chromatin modification and the intermediate factors responsible for repair. Importantly we identified H3K79me3 as a potential marker for CRC cancer patient stratification for the utilization of personalized therapies such as a combination of PARP inhibitors and irinotecan, which in combination preferentially target tumors with HR defects.

2 Materials

2.1 Devices/ Technical equipment

-20°C Freezer	Liebherr GmbH, Biberach, Germany
-80°C Freezer “Hera freeze”	Thermo Fisher Scientific, Waltham, USA
-150°C Freezer (MDF-C2156VAN)	Panasonic, Kadoma, Japan
Axioscop microscope	Carl Zeiss, Jena, Germany
Balance	Sartorius AG, Göttingen, Germany
Bandelin Sonoplus Sonicator	Bandelin electr. GmbH & Co. KG, Berlin
Biological Safety Cabinet (Safe 2020)	Thermo Fisher Scientific
Bioruptor® Plus sonication device	Diagenode SA, Liège, Belgium
Celigo^{TM} Cytometer	Cyntellect Inc., USA
CO_2-Incubator (HERAcell 150i)	Thermo Fisher Scientific
Confocal Microscope Zeiss LSM 510 Meta	Carl Zeiss
Counting chamber (Neubauer)	Brand GmbH & Co. KG, Wertheim, Germany
DS-11+ Spectrophotometer	Wilmington, United States
Electrophoresis & Electrotransfer Unit (Western blotting)	Bio-Rad Laboratories, Hercules, USA
FACScan	BD Bioscience, Germany
Inverted Microscopes Eclipse TS100	Nikon, Tokyo, Japan
Irradiation device (200kv, 15Ma) RS225 research system	GLUMAY MEDICAL, UK
Isotemp® water bath	Thermo Fisher Scientific
Magnet stirrer “MR3001”	Heidolph GmbH & Co. KG, Schwabach, Germany
Manual hand cell counter	Tamaco LTD., Taiwan

Microwave	Clatronic International GmbH, Kempen, Germany
Mini-PROTEAN Tetra Cell	Bio-Rad Laboratories
Mini Trans-BlotTM Cell	Bio-Rad Laboratories
Nano Drop® ND-1000	Peqlab Biotechnology GmbH, Erlangen, Germany
Optical Reaction Module CFX96TM	Bio-Rad Laboratories
pH-meter inoLab®	WTW GmbH, Weilheim, Germany
Pipettes (0.1-2.5, 0.5-10, 2-20, 10-100, 20-200, 100-1000 µL)	Eppendorf AG, Hamburg, Germany
Pipette Aid® portable XP	Drummond Scientific Co., Broomall, USA
Pipettes “Research” Series	Eppendorf AG
PowerPacTM Basic Power Supply	Bio-Rad Laboratories
PowerPacTM HC Power Supply	Bio-Rad Laboratories
Power supply Power Pack P25T	Biometra GmbH, Göttingen, Germany
Pressure cooker	Pascal (Dako, Hamburg), Germany
Refrigerator	Liebherr GmbH, Biberach, Germany
Repeat Pipette	Gilson Inc., Middleton, USA
Scanner Epson V700 Photo	Seiko Epson, Suwa, Japan
Schuttler Duomax 1030	Heidolph Instruments GmbH
Schuttler Minishaker	MS2 IKA GmbH, Staufen, Germany
Shaker “Rocky”	Schütt Labortechnik GmbH, Göttingen, Germany
Test tube rotator	Schütt Labortechnik GmbH
Thermal Cycler T100TM	Bio-Rad Laboratories
Thermomixer Comfort	Eppendorf AG
Vortex-Genie 2	Electro Scientific Industry. Inc., Portland, USA

Western Blot Imager	Bio-Rad Laboratories
X- Ray Cassettes	Rego X-ray GmbH, Augsburg, Germany

2.2 Centrifuges

Centrifuge 4°C (5417R)	Eppendorf AG
Centrifuge 4°C (Fesco 21)	Thermo Fisher Scientific
Centrifuge (Megafuge 1.OR)	Thermo Fisher Scientific
Microcentrifuge C1413-VWR230	VWR, Radnor, USA
Table centrifuge (GMC-060)	LMS Co., Ltd., Tokyo, Japan

2.3 Consumable materials

96-Well Flat Clear Bottom Black	Corning GmbH, Germany
96-well Multiplate® PCR plate white	Bio-Rad Laboratories
Cell scraper (16 cm)	Sarstedt AG & Co., Nümbrecht, Germany
Cellstar 6, 12, and 24- well culture plate	Greiner Bio-One GmbH
Cellstar PP-tube 15 and 50 mL	Greiner Bio-One GmbH
Cellstar tissue culture dish 100×20 mm	Greiner Bio-One GmbH
Cellstar tissue culture dish 145×20 mm	Greiner Bio-One GmbH
Cellstar cell culture flasks 50 mL (T25)	Greiner Bio-One GmbH
Cellstar cell culture flasks 250 mL (T75)	Greiner Bio-One GmbH
Cover Slides (12 mm)	Thermo Fisher Scientific
CryoTube Vial (1.8 mL)	Thermo Fisher Scientific
Cuvettes	Heinemann Labortechnik GmbH, Germany
Gel blotting paper (Whatman paper)	Sartorius AG
Microtube 1.5 mL	Sarstedt AG & Co.
Microtube 2 mL	Sarstedt AG & Co.
Millex-HV Filer (0.45µM) PVDF	Merck Millipore KGaA, Darmstadt, Germany
Mr. Frosty® Cryo Freezing Container	Thermo Fisher Scientific

Nitrocellulose (NC) Transfer Membrane (Amersham Protran 0.45 NC)	GE Healthcare Europe GmbH, München
Parafilm® “M”	Pechiney Plastic Packaging, Chicago, USA
Pipette filter tips	Sarstedt AG & Co.
Pipette tips non-sterile (10, 20-200, 1000 µL)	Eppendorf AG
Serological pipettes, sterile	Corning GmbH
Sterile filter (0.2 µm, 0.45 µm) (1, 2, 5, 10, 25 mL)	Millipore, Molsheim, France
X-ray films “Super RX”	Fujifilm Corp., Tokyo, Japan
UV-Cuvettes (micro)	Brand GmbH

2.4 Chemicals

Acetic acid	Carl Roth GmbH & Co. KG, Karlsruhe, Germany
Albumin fraction V	Carl Roth GmbH & Co. KG
Ammonium persulfate	Carl Roth GmbH & Co. KG
Ammonium sulfate	Carl Roth GmbH & Co. KG
Ampicillin	AppliChem GmbH, Darmstadt, Germany
Anti-Anti	LifeTechnology, Carlsbad, USA
Aprotinin	Carl Roth GmbH & Co. KG
Bromophenol blue	Sigma-Aldrich Co., St. Louis, USA
Calcitriol	Biomol GmbH, Hamburg, Germany
Calcium chloride	Carl Roth GmbH & Co. KG
Chloroform	Carl Roth GmbH & Co. KG
Diaminobenzidine (DAB) substrate	Dako, Hamburg, Germany
Diethylpyrocarbonate (DEPC)	Carl Roth GmbH & Co. KG
Dimethyl sulfoxide (DMSO)	AppliChem GmbH
Dithiothreitol	Carl Roth GmbH & Co. KG
DNA Loading Dye 6x	Fermentas GMBH, St. Leon, Germany

Ethanol absolute	Th. Geyer GmbH & Co. KG, Renningen, Germany
Ethylenediaminetetraacetic acid	Carl Roth GmbH & Co. KG
Fetal bovine serum (FBS)	Thermo Scientific HyClone, Logan, USA
Formaldehyde	Sigma-Aldrich Co.
Fluorescence mounting medium	Dako
FuGENE® HD Transfection Reagent	Promega GmbH, Mannheim, Germany
Glycine	Carl Roth GmbH & Co. KG
Glycerol	Carl Roth GmbH & Co. KG
β-Glycerolphosphate	Sigma-Aldrich Co.
Hoechst 33342 solution	Thermo Scientific HyClone
Hydrochloric acid	Carl Roth GmbH & Co. KG
Hydrogen peroxide	Carl Roth GmbH & Co. KG
Iodoacetamide	Sigma-Aldrich Co.
Isopropanol	Carl Roth GmbH & Co. KG
L-Ascorbic acid	Sigma-Aldrich Co.
Leupeptin	Carl Roth GmbH & Co. KG
Magnesium chloride	Carl Roth GmbH & Co. KG
Mayer's hemalaun	Merck
β-Mercaptoethanol	Sigma-Aldrich Chemie GmbH, Munchen, Germany
Methanol	Carl Roth GmbH & Co. KG
N,N-Dimethylformamide	Sigma-Aldrich Co.
Monopotassium phosphate	Carl Roth GmbH & Co. KG
Opti-MEM	LifeTechnology
PageRuler^{TM} Plus Prestained Protein Ladder	Thermo Fisher Scientific
Paraformaldehyde, EM grade	Merck
PBS Tablets	LifeTechnology
Pefabloc	SC Carl Roth GmbH & Co. KG
Penicillin-Streptomycin solution	Sigma-Aldrich Co.

Penicillin-Streptomycin solution (PenStrep 100 units/mL Penicillin, 100 µg/mL Streptomycin)	Sigma-Aldrich Co.
Ponceau-S	SERVA Electrophoresis GmbH, Heidelberg
Potassium acetate	Carl Roth GmbH & Co. KG
Potassium chloride	AppliChem GmbH
Potassium dihydrogen phosphate	Carl Roth GmbH & Co. KG
Propidium iodide solution	Sigma-Aldrich Co.
Puromycin	Invitrogen GmbH, Karlsruhe, Germany
RNAiMAX LifeTechnology,	Carlsbad, USA
RNase inhibitor	New England Biolabs, Frankfurt am Main, Germany
Roti®-Phenol	Carl Roth GmbH & Co. KG
Rotiphorese® Gel 30	Carl Roth GmbH & Co. KG
Rotipuran® Chloroform	Carl Roth GmbH & Co. KG
Rotipuran® Isoamylalcohol	Carl Roth GmbH & Co. KG
SEA BLOCK Blocking Buffer	Thermo Fisher Scientific
Skim milk powder	Carl Roth GmbH & Co. KG
Sodium acetate	Carl Roth GmbH & Co. KG
Sodium chloride	Carl Roth GmbH & Co. KG
Sodium deoxycholate	AppliChem GmbH
Sodium dodecyl sulfate	Carl Roth GmbH & Co. KG
di-Sodium hydrogen phosphate	Carl Roth GmbH & Co. KG
Sodium hydroxide	Carl Roth GmbH & Co. KG
Sodium pyruvate	Invitrogen GmbH
SYBR Green	Roche Diagnostics GmbH, Mannheim, Germany
Tetramethylethylenediamine (TEMED)	Carl Roth GmbH & Co. KG
α,α-Trehalose Dihydrate	AppliChem GmbH
Tris	Carl Roth GmbH & Co. KG
Triton X-100	AppliChem GmbH
TRIzol® Reagent	Invitrogen GmbH

Trypsin-EDTA (0.05%)	LifeTechnology
Tween-20	AppliChem GmbH

2.5 Ready to use kits and solutions

Duolink® In Situ Red Starter Kit Mouse/Rabbit (DUO92101)	Sigma-Aldrich Co.
Immobilon™ Western HRP substrate	Merck
Lipofectamine™ RNAiMAX	LifeTechnology
NuPAGE MOPS SDS Running Buffer (20x)	Invitrogen GmbH
Pierce™ BCA Protein Assay Kit	Thermo Fisher Scientific

2.6 Cell culture media

DMEM/F12 GIBCO®	LifeTechnology
DMEM GIBCO®	LifeTechnology
RPMI 1640, GlutaMAX™ GIBCO®	LifeTechnology

2.7 Inhibitors/drugs

DOT1L inhibitor (EPZ-5676)	Selleckchem, Germany
5-Flurouracil (5-FU)	Sigma-Aldrich, Steinheim, Germany
Irinotecan hydrochloride	Sigma-Aldrich Co.
NCS	Sigma-Aldrich Co.
Veliparib (ABT-888)	Selleckchem

2.8 Nucleic acids

2.8.1 siRNA oligonucleotides

Name	Target Gene	siRNA sequence 5'-3' direction	Source
siDOT1L-01	DOT1L	CGAAGUGGAUGAAAUGGUA	Dharmacon Inc
siDOT1L-02	DOT1L	CCGAGAAGCUCAACAACUA	Dharmacon Inc
siDOT1L-03	DOT1L	GAAGCCGUCUCCCUCCAAA	Dharmacon Inc
siDOT1L-04	DOT1L	GCAGAAUCGUGUCCUCGAA	Dharmacon Inc
Luciferase GL2 duplex	-	CGUACGCGGAAUACUUCGA	Dharmacon Inc
siGENOME Nontargeting siRNA pool # 1	-	-	Dharmacon Inc

2.8.2 RT-PCR primers

Primers are shown in a 5' to 3' orientation.

Name	Sequence	Source
h DOT1L F	CCACCAACTGCAAACATCAC	This study
h DOT1L R	AGAGGAAATCGCCTCTCTCC	This study
HNRNPK F	ATCCGCCCCTGAACGCCCAT	(Karpiuk et al., 2012)
HNRNPK R	ACATACCGCTCGGGGCCACT	(Karpiuk et al., 2012)
18S rRNA F	AACTGAGGCCATGATTAA	(Nagarajan et al., 2015)
18S rRNA R	GGAACTACGACGGTATCTGA	(Nagarajan et al., 2015)

2.9 Enzymes

Proteinase K Invitrogen GmbH

Restriction enzymes	New England Biolabs
Reverse transcriptase (M-MuLV)	New England Biolabs
RNase A	Qiagen GmbH, Hilden
RNase inhibitor	New England Biolabs
Taq DNA polymerase	Prime Tech, Mink, Belarus
T4 DNA ligase	New England Biolabs

2.10 Antibodies

2.10.1 Primary antibodies

The following antibodies were used for Western blot, immunofluorescence, and immunohistochemistry analyses.

Name	Clone	Cat. No.	WB	IF	IHC	Source
53BP1	H-300	sc-22760	1:1000	1:500		Santa Cruz
ATM	B-12	sc-8434	1:500			Santa Cruz
Chk1	2G1D5	2360	1:1000			Cell Signaling Technology
Chk2	A-12	sc-5278	1:10,000			Santa Cruz
CtIP	14-1	61141	1:1000			Active Motif
DOT1L	OTI1D8	CF802482	1:500			ORIGENE
DOT1L		A310-953A	1:500			Bethyl Laboratories
DOT1L		A300-954A	1:500			Bethyl Laboratories
H2B		ab52484	1:40,000			Abcam
H3		ab10799	1:1000			Abcam
H3K79me3		C15410068 (pAb-068-	1:500	1:500	1.250	Diagenode

		050)				
HSC70	B-6	sc-7298	1:40,000			Santa Cruz
Phospho-ATM (Ser1981)	10H11.E12	4526	1:500			Cell Signaling Technology
Phospho-(Ser/Thr) ATM/ATR Substrate Antibody		2851	1:1000			Cell Signaling Technology
Phospho-Chk1 (Ser317)		2344	1:500			Cell Signaling Technology
Phospho-Chk1 (S317)		A300-163A	1:1000			Bethyl Laboratories
Phospho-Chk2 (Thr68)		2661	1:500			Cell Signaling Technology
Phospho-Histone H2AX (Ser139)	JBW301	05-636	1:1000	1:1000		Millipore
Phospho-Mre11 (Ser676)		4859	1:500			Cell Signaling Technology
Phospho-p95/NBS1 (Ser343)		3001	1:500			Cell Signaling Technology
Phospho KAP-1 (S824)		A300-767A	1:10,000			Bethyl Laboratories

KAP1		A300-274A	1:10,000			Bethyl Laboratories
Mre11	31H4	4847	1:500			Cell Signaling Technology
Rad50		3427	1:1000			Cell Signaling Technology
Rad51	H-92	sc-8349	1:10,000			Santa Cruz
RPA 70	EPR3472	2589-1	1:500			Epitomics

2.10.2 Secondary antibodies

Name	Cat. No.	WB Dilution	IF Dilution	IHC Dilution	SOURCE
Alexa-fluor488 goat anti-rabbit	A11008	-	1:500	-	LifeTechnology
Alexa-fluor594 goat anti-mouse	A11005	-	1:500	-	LifeTechnology
Envision Goat-anti-rabbit				1:200	Dako
Goat anti-mouse IgG-HRP	Sc-2005	1:20,000	-	-	Santa Cruz
Goat anti-rabbit IgG-HRP	Sc-2004	1:5,000	-	-	Santa Cruz

2.11 Cell lines

Cell Line	Species	Tissue Origin	Disease	Source
HeLa	Human	cervix	cervical carcinoma	ATCC® CCL-2™
SW480	Human	colon	Dukes' type B, colorectal adenocarcinoma	ATCC (Manassas, VA)

SW837	Human	rectum	grade IV, adenocarcinoma	ATCC (Manassas, VA)
U2OS	Human	bone	osteosarcoma	Sigma-Aldrich (St. Louis, MO)

2.12 Buffers and solutions

Blocking solution:
1 x TBS-T, 5% (w/v) milk

Cell culture freezing medium:
42% (v/v) DMEM, 50% (v/v) FBS, 8% DMSO

Cell culture PBS sterile:
1 PBS tablet per 500 mL distilled H_2O

4'-6-Diamidino-2-phenylindole (DAPI, 10ng/mL):
10ng/mL (w/v) DAPI in deionized water (dH_2O)

Laemmli buffer (6x):
0.35 M Tris (pH 6.8), 30% glycerol, 10% SDS,
9.3% DTT, 0.02% Bromophenol blue

Lysis Buffer (Buffer A) for (CF):
10mM HEPES (pH 7.9), 10 mM KCL,
1.5mM $MgCl_2$, 0.34 M sucrose, 10% glycerol,
0.1% Triton X-100, 1mM DDT and protease inhibitors

Nuclear lysis buffer for (CF):
3mM EDTA, 0.2 mM EGTA, 1 mM DTT and protease inhibitors

PBS:
137 mM NaCl, 2.68 mM KCl,
4.29 mM $Na_2HPO_4 \times 2H2O$,
1.47 mM KH_2PO_4, (pH 7.4)

PBS-T:
PBS including 0.1% (w/v) Tween-20

PCI:
Phenol: Chloroform: Isoamylalcohol (25:24:1)

Proteinase inhibitor cocktail:
1 ng/µL Aprotinin/Leupeptin,
10 mM Glycerol 2-phosphate disodium salt hydrate,
1 mM NEM, 1 mM Pefabloc

qPCR buffer:
75 mM Tris-HCl (pH 8.8), 20 mM $(NH_4)2SO_4$,
0.01% Tween-20, 3 mM $MgCl_2$, 200 µM dNTPs,
0.5 U/reaction Taq DNA Polymerase, 0.25% Triton X-100,
1: 80,000 SYBR Green I, 300 mM Trehalose

RIPA buffer:
1x PBS, 1% (v/v) NP-40, 0.5% (v/v) sodium deoxycholate,
0.1% (w/v) SDS

SDS separating gel (6%):
6% (v/v) acrylamide, 375 mM Tris-HCl (pH 8.8),
0.1% (w/v) SDS, 0.1% (w/v) APS, 0.04% (v/v) TEMED

SDS separating gel (15%):
15% (v/v) acrylamide, 375 mM Tris-HCl (pH 8.8),
0.1% (w/v) SDS, 0.1% (w/v) APS, 0.04% (v/v) TEMED

SDS stacking gel (5%):
5% (v/v) acrylamide, 125.5 mM Tris-HCl (pH 6.8),
0.1% (w/v) SDS, 0.1% (w/v) APS, 0.1% (v/v) TEMED

Stripping Buffer (harsh)
10% SDS, 1M Tris pH 6.8,
Water-volume adjusted, 0.08 % β-Mercaptoethanol

TAE buffer (50×):
2 M Tris, 1 M Acetic acid, 0.1 M EDTA

TBS:
150 mM NaCl, 2.68 mM KCl, 4.29 mM $Na_2HPO_4 \times 2H_2O$,
1.47 mM KH_2PO_4, (pH 7.4)

TBS-T:
TBS including 0.1% (w/v) Tween-20

TE buffer:
10 mM Tris-HCl, 1 mM EDTA, (pH 8.0)

Tris-glycine electrophoresis buffer:
25 mM Tris, 200 mM Glycine, 0.1% (w/v) SDS

Transfer buffer:
10% 10x Western salts, 20% Methanol

Triton X-100 (0.5%):
PBS including 0.5% Triton X-100

Unmasking buffer:
Citrate buffer pH 6.0, 05% Tween 20

Western salts (10×):
1.92 M Glycine, 250 mM Tris-HCl (pH 8.3),
0.02% (w/v) SDS

2.13 Software and databases

Adobe Photoshop 7.0	Adobe Systems Inc., San Jose, USA
Bio-Rad CFX Manager 3.1	Bio-Rad Laboratories
ImageJ 1.41	NIH, USA
Microsoft Office 2007	Microsoft Cooperation, 2008
Image Lab Version 5.2 build 14	Bio-Rad Laboratories
National Center for Biotechnology Information (NCBI)	http://www.ncbi.nlm.nih.gov
Primer designing tool NCBI/Primer-BLAST (www.ncbi.nlm.nih.gov/tools/primer-blast/)	Ye et al., 2012
Reference ZOTERO	https://www.zotero.org

3 Methods

3.1 Description of cell lines, cultivation and cryopreservation

The human rectum adenocarcinoma cell line SW837, human colon adenocarcinoma cell line SW480, human osteosarcoma cell line U2OS and human cervix cancer cell line HeLa were cultivated in the respective growth media (SW837: DMEM/F12, SW480: RPMI 1640, U2OS: high glucose, phenol red-free DMEM and extra 1x sodium pyruvate, HeLa: DMEM) supplemented with 10% FBS (fetal bovine serum), 100U/mL P/S (Penicillin/Streptomycin) at 37°C in 5% CO_2 humidified incubator. The cells were further sub-cultivated every 48-72 hours and the media was removed from the cells, followed by washing with PBS. Cells were then subjected to 1 mL trypsin/EDTA solution for five minutes at 37° C. The trypsinized cells were collected in a 15 mL falcon tube and to inhibit tryptic activity, 5 mL of media was added to the suspension. Cells were counted with a hemocytometer and seeded in cell culture plates. For cryopreservation cells were centrifuged, followed by washing with PBS. Cells were finally suspended and frozen in 42 % respective cell line media with 50 % FBS and 8 % DMSO at a density of $2\text{-}3.10^6$ cells/ml.

3.1.1 Determination of cell viability

The viability of the cells was analyzed by adding trypan blue to the cell suspension. Living cells do not show staining, while dead cells with a destabilized plasma membrane layer take up the dye and turn blue. The viability of cells was analyzed manually utilizing a cell counter hemocytometer.

3.2 RNA interference

3.2.1 Optimization of transfection conditions

To obtain efficient transfection with negligible effects on cell viability, the transfection conditions were optimized. Cells were plated at five distinctive densities and four concentrations of Lipofectamine™ RNAiMAX transfection reagent as suggested by the manufacturer's instructional manual. For siDOT1L transfections, the Dharmacon siRNAs (#1, #2, #3, and #4) were pooled in a 1:1:1:1 ratio. Non-targeting, Scramble, and mock siRNA were utilized as negative controls to discover conditions that show target mRNA knockdown efficiency at > 80 % cell viability.

3.2.2 Reverse transfection

Small interfering RNA (siRNA) was transfected with Lipofectamine® RNAiMAX. For a six-well plate format, 30 pmol of siRNA were mixed together with 5 µL RNAiMAX reagent in 500 µL of optiMEM and incubated for 20 minutes at room temperature. In the meantime, cells were trypsinized and suspended in the respective cell line growth medium without antibiotics or antifungal reagents. Then 250,000-300,000 cells, counted in the hemocytometer, were seeded in 1.5 mL of transfection medium. After 20 minutes of incubation time, the 500 µL transfection mix was added directly to the medium and incubated overnight. Next day, the medium was changed to the normal growth medium.

3.3 Irradiation of the cells

To study the effect of ionizing radiation on the molecular aspects of the DNA repair machinery, the cells were irradiated at a dose rate of 2 Gy/minute (1, 2, 4, 6, and 8 Gy of X-rays (200 kV, 15 mA, 0.5 mm Cu filter, Gulmay Medical, Camberley, United Kingdom). The facility and co-operation were provided by the department of

radiation therapy. These cells were collected to study the change in morphology as well as translational profiles of the cells.

3.4 Cell treatment and proliferation assays using Celigo

For evaluating the sensitivity towards multiple small molecule inhibitors, 1,000-2,000 cells/100 µL of media were seeded into 96-well plates (Flat Clear Bottom Black, Corning GmbH) and allowed to incubate overnight to adhere. On the next day, cells were observed under a microscope and measured confluency using the Celigo™ Cytometer every 24 hours before treatment with Neocarzinostatin (NCS) 100 ng/mL, DOT1L inhibitor (EPZ-5676), PARP inhibitor veliparib, chemoradiotherapy drugs 5-FU and irinotecan as indicated in various concentration in the study. Chronic drug treatment was followed by a medium exchange every alternate day and was followed up by 7 days. In addition to chemoradiotherapy, we also tested the sensitivity of two cell lines to alone drugs and combined modality treatment.

3.5 Colony formation assays (CFA)

The colony formation assay (CFA) was performed to determine the surviving fractions (SF) of cells after transfection with DOT1L siRNA and radiation. Briefly, cells were transfected in duplicates either with mock and targeted siRNA and seeded with 300,000 cells/well as described earlier into six-well plates. After 48 hours of attachment, the cells were trypsinized and seeded in dilutions 750 cells/well for 1 Gy and 2 Gy, 1,500 cells/well for 4 Gy, 2,250 cells for 6Gy and 3,000 cells for 8Gy in six-well plates for CFA assay and seeded 750 cells/well for plating efficiency in duplicates for both mock and siRNA knockdown, and simultaneously the rest cells were plated for whole cell lysates for checking knockdown efficiency. 72 hours after transfection, cells were irradiated at a dose rate of 2 Gy/minutes (1, 2, 4, 6, and 8 Gy of X-rays (200 kV, 15 mA, 0.5 mm Cu filter, Gulmay Medical, Camberley, United

Kingdom)). Experiments were performed in technical triplicates and placed in an incubator (37°C, 5% CO_2). CFA growth period was up to 19 days. The medium was removed carefully and wells were fixed with 70% ethanol for 20 minutes. After complete removal of ethanol, the plates were kept for drying around 2-3 hours at RT. Then, samples were stained with Mayer's hemalaun for 5 minutes. The staining solution was removed and each plate was rinsed first with ionized tap water and subsequently with normal tap water. The plates were completely dried at room temperature. The colonies were counted using a stereomicroscope manually. Colonies are considered to represent survivors if they contain more than 50 cells. Firstly, the number of colonies in control cells, which were not exposed to IR, was determined to calculate the plating efficiency. Survival fractions were calculated. The mean values of three independent experiments were evaluated and normalized to the plating efficiency.

3.6 Immunofluorescence microscopy

Cells with 70-80 % confluence were harvested by trypsinization and counted with a hemocytometer. Prior to seeding cells in six-well plates, the cells were transfected with either target siRNA or control siRNA and incubated for 48 hours as described previously. After 48 hours, they were trypsinized and diluted into to a seeding concentration of 10,000-50,000 cells/mL and seeded 24-well cell culture plates containing coverslips. The cells were incubated overnight (37°C, 5% CO_2). After attachment of the cells to the slides overnight some plates were treated with NCS or mock for the indicated time point and followed by fixation with 4% PFA/PBS for 10 minutes at RT. The coverslips were washed carefully 3 times for 5 minutes with PBS and permeabilization was carried out with 0.5% Triton X-100 for 10 minutes at room temperature. Following two washing steps, cells were blocked with 3% BSA for 30 minutes and incubated with primary antibodies overnight at 4° C. On the next day,

the coverslips were washed thrice for each 5 minutes incubation with 0.1% Triton X-100/PBS. Then cell was incubated at RT for 60 minutes in the dark with fluorescently conjugated secondary antibodies. The nuclei were counterstained with DAPI (10 ng/mL) or Hoechst blue-33342 (Benzamide-tris-hydrochloride) for 1 minute. Finally, coverslips were mounted onto slides using the mounting medium. After complete drying, we stored the coverslips at 4°C in dark until analysis. Images were acquired with a Zeiss LSM 510 Meta Confocal Microscope using 25x or 63x oil immersion lens.

3.7 Proximity ligase assays (PLA)

We used proximity ligase assays (PLA) to study the interaction or the close proximity between γH2AX and H3K79me3 by DOT1L siRNA knockdown in NCS-treated SW837 cells. In general, the interaction of two different proteins is examined in cell samples utilizing two secondary antibodies from different species which are conjugated to DNA oligonucleotides (PLA probes). When two antibodies are in close proximity to one another, they can be bridged by two additional circle forming oligonucleotides, joined via ligation, amplified by rolling circle amplification, and the signal from each pair of PLA probe is visualized as a focus.

We performed this assay using the Duolink® In Situ Red Starter Kit Mouse/Rabbit (DUO92101) kit according to the manufacturer's instructions. Briefly, the cells were seeded on coverslips and treated with primary antibodies as previously described (Kari et al., 2016). After incubation with primary antibodies, all incubations steps were performed in a humidity chamber. With washing steps in PBS, added PLA probe solutions were freshly prepared in the 3% BSA blocking solution and the coverslips were incubated in a humidity chamber for 1 h at +37 ° C. Then, PLA probe solution was washed using 1x wash buffer under very gentle agitation. After

which added ligase solution and incubated for 30 minutes at 37°C for ligation. Following two washing steps with 1x wash buffer, and carefully after tapping off all wash solution, an amplification-polymerase solution which is light sensitive was added in each sample and further incubated for 100 minutes at 37°C. After final washing steps, staining with DAPI, mounting and drying at room temperature in the dark coverslips were analyzed in the confocal microscope.

3.8 Immunohistochemistry (IHC)

Immunohistochemistry was performed using rectum tissue microarrays. For immunostaining, initially, paraffin-embedded sections (2 µm) were de-paraffinized and rehydrated. Sections were incubated in 100% xylene for 20 minutes, followed by rehydration in descending dilutions of EtOH series (100%, 90%, and 70 %) before washing with PBS. Proteins were then unmasked by cooking slides in the pressure cooker (Pascal, Dako, Hamburg) for 3 minutes with unmasking buffer (citrate buffer pH 6, 0.05% Tween 20). Tissue sections were allowed to cool to room temperature and washed with PBS three times, quenched for endogenous peroxidase activity with 3% hydrogen peroxide (H_2O_2) treatment for 10 minutes at RT and then washed three times with PBS. Afterward, sections were blocked using SEA BLOCK Blocking Buffer for 20 minutes at RT. The primary antibody H3K79me3 was diluted in PBS (1:250) containing 5% FBS, applied and incubated overnight at 4°C in a humid chamber. Sections were washed three times using PBS before adding the biotinylated secondary antibody (Envision Goat-anti-rabbit, Dako, Hamburg) 1:200 diluted in PBS and incubated for 1 hour at RT. Sections were washed three times with PBS followed by Avidin-Peroxidase incubation diluted 1:1,000 in PBS for 45 minutes. Staining signals were detected using diaminobenzidine (DAB) substrate (Dako, Hamburg) for 8 minutes at RT. Slides were washed and hematoxyline (Mayer’s hemalaun solution) was used for counterstaining for 5 minutes. Histological

slides were imaged using an Axioscop microscope and ZEN software (Carl Zeiss, Jena, Germany).

3.9 Double-strand break (DSB) repair reporter assay

DSB reporter assay was used to measure the double strand break repair efficiency. To induce DSBs, HeLa cells harboring stably an integrated reporter construct for HR (pGC) or for NHEJ (pEJ) were transfected with control or DOT1L siRNA (1,4). After 24 hours of siRNA transfection, the cells were transfected with the I-SceI expression vector pCMV3xnls-I-SceI (1µg) using Fugene HD (Promega) as a transfection reagent to induce DSBs. 48 hours after transfection, cells were assessed for green fluorescence-positive cells by flow cytometry (FACScan, BD Bioscience) for HR and NHEJ efficiency normalized to the transfection efficiency (Kari et al., 2016).

3.10 Molecular Biology

3.10.1 RNA isolation and analysis

RNA isolation was performed according to the manufacturers' instructions. Briefly, 500 µL of QIAzol reagent was added to cells grown in a 6-well plate and incubated for 3 minutes at room temperature. Afterward, the cells were carefully scraped and transferred into a reaction tube containing 100 µL Chloroform and vortexed for 15 seconds. The mix was centrifuged for 15 minutes at 12,000 g and subsequently, the aqueous supernatant was transferred to a fresh tube containing 99% isopropanol in a 1:1 ratio. The solution was stored overnight at -20 °C. The next day the solution was spun down for 30 minutes at 15,000 g and subsequently washed two times with 70% ethanol at 12,000 g. After removing the ethanol, pellets were allowed to dry for 5-10 minutes and finally RNA was dissolved in 30 µL H_2O.

3.10.2 Quantification of the isolated RNA

The quality, as well as concentration of the isolated RNA, was verified using the Nanodrop ND 1000 Spectrophotometer.

3.10.3 First-strand cDNA synthesis

One µg of RNA was diluted in 10 µL of nuclease-free water and supplemented with 2 µL of 15 µM random 9mer primer and 4 µL of 2.5 mM dNTPs to a total volume of 16 µL. The mixture was incubated for 5 minutes at 70°C and then placed immediately on ice. After the samples cooled down 0.125 µL of 25 U MMLV-reverse transcription enzyme and 0.25 µL of 10 U Murine RNase-Inhibitor were added together with the reverse-transcription buffer to a final volume of 20 µL. The mix was incubated for 1 h at 42°C and subsequently heat inactivated at 90°C for 10 minutes. The complementary DNA (cDNA) was diluted to 50 µL with nuclease-free water and used for real-time quantitative PCR (qPCR).

3.10.4 Quantitative real-time PCR

Quantitative real-time PCR was performed according to the below qPCR reaction composition for each reaction volume of 25 µl. Samples were pipetted in technical duplicates for each qPCR measurement.

3.10.5 qPCR reaction composition

Component	Volume/reaction [µl]
qRT-PCR buffer mix	14
Primer mix forward+reverse (10 µM)	1.5
Distilled water	8.5
Template DNA	1
Total volume	**25**

For amplification and readout the below qRT-PCR program was performed:

Step	Temperature	Time	Number of cycles
Step 1 **Initial denaturation**	95°	2 minutes	1
Step 2 Denaturation	95°	15 seconds	40
Step 3 Annealing	60° C	1 minute	

After initial denaturation for PCR amplification step 2 and 3 are repeated for 40 cycles for the cDNA. The PCR reaction was followed by a melting curve analysis from 60°C to 95°C with one read every 0.5°C. For the quantification of the mRNA levels of the candidate gene, the reference gene HNRNPK or 18S ribosomal RNA was used to normalize the values and for further statistical analysis.

3.11 Chromatin fractionation

After appropriate treatment and experimental conditions, cells were washed with 1x PBS and were resuspended in lysis buffer added with freshly prepared protease inhibitor mixture. After 5 minutes incubation time, cells were scraped and centrifuged at 1,300 g for 5 minutes. After washing with lysis buffer, the nuclear pellet was lysed in nuclear lysis buffer for 30 minutes on ice. Soluble chromatin fractions were separated by centrifuging at 1,700 g for 5 minutes. Insoluble chromatin fractions were further sonicated and analyzed by SDS–PAGE electrophoresis. Western blotting was performed according to the standard protocol.

3.12 Protein biochemistry

3.12.1 SDS polyacrylamide gel electrophoresis

3.12.2 Protein analysis

For whole cell lysate protein preparation, the culture medium completely aspired and cells were washed twice with PBS followed by addition of RIPA buffer containing a freshly prepared proteinase inhibitor cocktail at 4°C for 10 minutes. The suspension was then collected in a 1.5 mL Eppendorf tube and stored immediately at -20°C until further use. Just prior to first use genomic DNA was sheared by sonication for 15 seconds pulse at 80% power amplitude on/off using a tip sonicator. Then, protein concentration was determined according to the manufacturer's protocol in the BCA Protein Assay kit and reading taken using DS-11+ Spectrophotometer. Before loading samples in the previously mentioned stacking and resolving gel, protein samples were boiled in 6x Laemmli Buffer at 95°C for 10 minutes and then loaded onto an SDS-Polyacrylamide gel and electrophoresed in SDS running buffer at 20 mA/gel or 60-110 V/gel.

3.12.3 Western blot

The separated proteins in the gel were transferred to a nitrocellulose membrane. The transfer of the proteins was performed at a constant voltage of 100 V for 1.5 hours at 4° C in transfer buffer. After transferring the proteins onto the nitrocellulose membrane, the membrane was blocked with 5% non-fat dry milk in TBS-T at room temperature for minimum 20 minutes or at 4° C overnight and then incubated with the primary antibody for 2 hours at RT or at 4° C overnight. After three washes with TBS-T for 10 minutes, the membranes were incubated for 60 minutes with a secondary antibody coupled to horseradish peroxidase. After incubation, the membranes were washed three times with TBS-T and the blots were developed

using enhanced chemiluminescence procedure and exposed to X-ray films or by using the Bio-Rad gel documentation system. Normalizations were performed with the loading control H2B, H3 or HSC70 throughout the study. The working antibody dilutions for the immunoblot analysis were supplemented with 0.01% sodium azide as preservative in 5% skimmed milk in 1x TBS-T and stored at 4°C for short term and for long term 5% BSA of 1x TBS-T and stored at -20°C.

3.13 Membrane stripping

For investigating several proteins on the same membrane, the primary and secondary antibodies were removed from the membrane before further protein detection. For this, the membrane was treated twice with stripping buffer for 10 minutes at RT inside a fume hood followed by two washes with PBS for 10 minutes and further three washes with TBS-T for 5 minutes. Then, blocking with 5% non-fat dry milk was followed by primary and secondary antibody incubation as described above.

4 Results

4.1 H3K79me3 levels in DOT1L-depleted cells

DOT1L posses histone methyltransferase activity towards histone H3 at lysine 79 (H3K79). One of the aims of this study was to determine the effects of DOT1L loss in CRC cells. Thus, initially, we examined the efficiency of DOT1L knockdown with individual and Smart Pool siRNAs after transfecting SW837 cells for 72 hours. DOT1L expression was detected by quantitative reverse transcription PCR/RT-PCR by measuring the relative mRNA expression levels in control and DOT1L siRNA-transfected cells (Figure 7A). To determine, if an individual or Smart Pool siRNA of DOT1L is efficient to decrease H3K79me3, the efficacy of knockdown was accessed in multiple colorectal cancers cell lines. As shown here, Immunoblotting using anti-DOT1L antibody (Figure 7B) demonstrate that individual siRNA-1, 4 and Smart Pool are more efficient in knockdown of DOT1L in our model system. The level of H3K79 trimethylation (H3K79me3) was determined using an antibody directed against H3K79me3 and was decreased upon DOT1L loss. These findings indicate that siRNAs targeting DOT1L can reduce DOT1L levels sufficiently at the mRNA and protein levels and are therefore suitable for studying the consequences of DOT1L loss in CRC cells. Moreover, this reduction of DOT1L is able to induce the decrease of H3K79me3 levels, especially when using the Smart Pool.

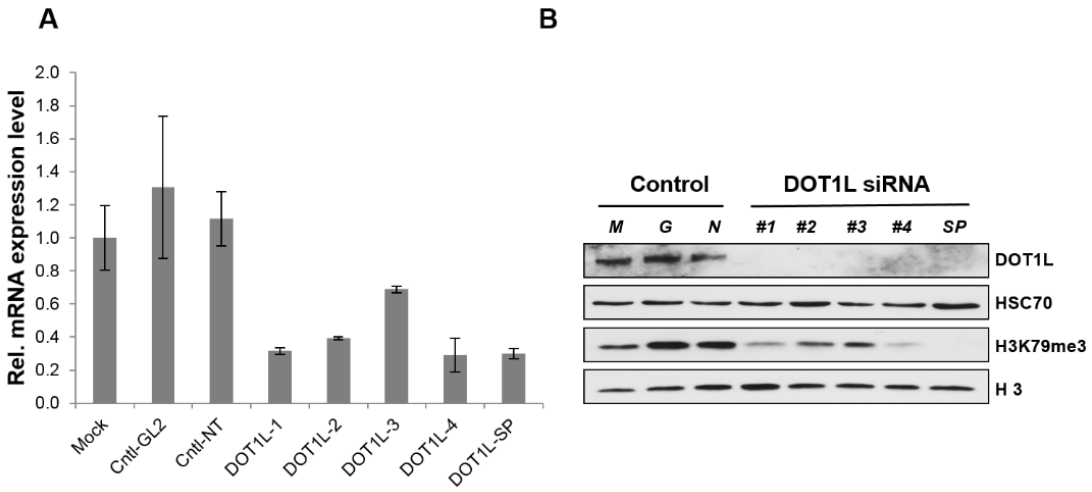

Figure 7: Depletion of DOT1L leads to decreased H3K79 trimethylation. SW837 cells were transfected with individual siRNAs (#1, #2, #3, #4,) or Smart Pool (SP) targeting DOT1L and after 72h knockdown efficiency was evaluated. (A) Relative DOT1L mRNA expression in control or DOT1L siRNA transfected cells. (B) SW837 whole cell lysates were analyzed by western blotting with DOT1L and H3K79me3 antibodies. H3 and HSC70 were used as loading controls. M, G, and N were used as 3 independent controls (M – mock, G – GL2 Duplex non-targeting siRNA, N – siGENOME Non-targeting siRNA).

4.2 Depletion of DOT1L affects γH2AX response

Evidence from previous studies suggests that the DOT1L-mediated H3K79 methylation plays a role in the DNA damage response (Nguyen and Zhang, 2011b). DNA double-strand breaks (DSBs) are a most toxic form of DNA damage, which causes genetic changes and/or cell death. Upon DNA DSB induction, H2AX is phosphorylated by PI3 family kinases including ATM and ATR. In response to DNA DSB, γH2AX (H2AX-S139) is the most well-documented histone modification and an important marker for DNA damage. This is a critical step in the activation of the DNA damage response and DNA repair. Hence, we first investigated the impact of DOT1L knockdown on DNA damage response and repair pathway. To address this question, we induced DNA to double strand breaks by NCS (Neocarzinostatin) treatment in both control and DOT1L siRNA (Smart Pool) transfected cells. The whole cell lysates were harvested at different time points of NCS treatment and analyzed by immunoblotting. We observed an increased level in γH2AX upon treating control cells with NCS for 15 minutes. Interestingly, the siRNA-mediated

knockdown of DOT1L led to decreased γH2AX induction compared to control cells (Figure 8A), thereby supporting a role of DOT1L in DNA damage recognition. To further confirm the role of DOT1L in γH2AX induction upon DSB, immunofluorescence studies were performed. We induced the DSB by NCS, in both mock and DOT1L siRNA-transfected cells which cause γH2AX recruitment to foci by immunofluorescence study. Immunofluorescence analyses confirmed this observation (Figure 8B) that with initial NCS treatment for 15 minutes, there is γH2AX induction in control cells whereas there is less γH2AX induction in DOT1L depleted cells. The disappearance of foci with increasing treatment time indicates that the breaks are repaired.

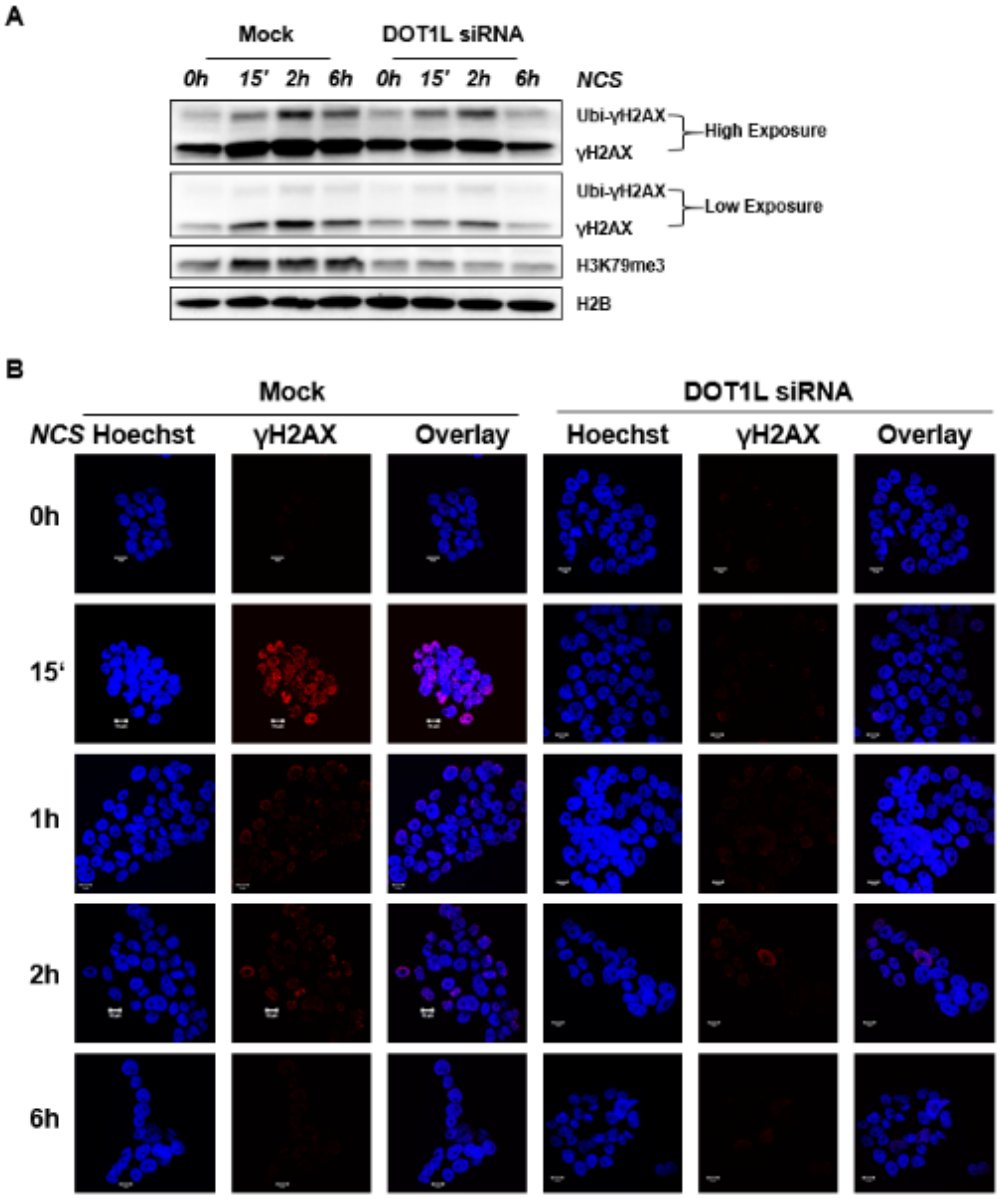

Figure 8: Knockdown of DOT1L affects γH2AX and DNA damage recognition (A) SW837 cells were either transfected with mock or DOT1L siRNA (SP). After 72 hours of transfection cells were treated with NCS (100 ng/ml) for the indicated time points. Whole cell protein lysates were harvested and immunoblotted with indicated antibodies using H2B as a loading control. (B) Immunofluorescence studies to check the induction of γH2AX after indicated time point treatments with NCS (100 ng/ml) in mock or DOT1L siRNA transfected SW837 cells.

4.3 DOT1L is involved in the DNA damage response pathway

Since we observed that DOT1L is required for γH2AX inductions we hypothesized that DOT1L might play an important role in DNA damage response. For this, DOT1L was transiently depleted using siRNA in SW837cells which were treated for different time points (15 minutes to 6 hours) with NCS to induce DSB. Whole cell lysates were analyzed by Western blotting to check the DNA damage response. As expected,

increased effects of γH2AX were seen in control cells. In addition, we observed increased levels of pCHK2 (checkpoint kinase 2), pKAP1 (KRAB-interacting protein 1), pNBS1 (gene mutated in Nijmegen breakage syndrome), and pATM (gene mutated in the ataxia telangiectasia syndrome) in DOT1L-depleted cells compared to control cells (Figure 9).

DOT1L-depleted cells show increased KAP1 phosphorylation (pKAP1), indicating that heterochromatin-associated DNA damage response may be particularly affected by altering chromatin structure. KAP1 phosphorylation is increased by DOT1L depletion indicating that DSB repair in heterochromatin may require DOT1L. However, we did not observe any change in the heterochromatin markers H3K9me2 and H3K9me3 levels upon DOT1L depletion. Upstream phosphorylation of CHK2 leads to check point-activation and cell-cycle arrest so may be less time require for DNA repair. The ATM protein is responsible for the cellular response to DNA damage by regulating the G1, S, and G2/M cell cycle checkpoints and by the phosphorylation of a number of protein substrates. Upregulation of pATM, pCHK2 confers the DOT1L-mediated regulation of CHK2- and ATM-dependent phosphorylation. These data suggest that DOT1L is involved in repair of DNA DSBs.

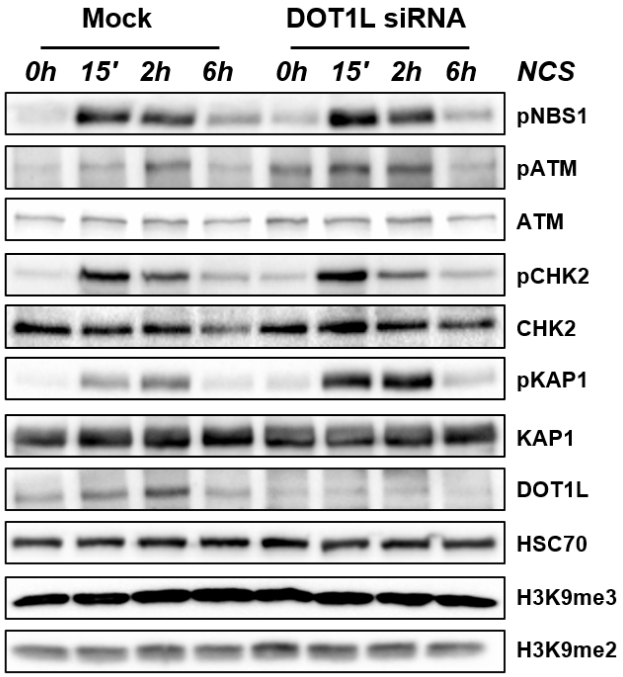

Figure 9: DOT1L is required for proper DNA damage response. SW837 cells were either transfected with mock or DOT1L siRNA (SP). After 72 hours of transfection cells were treated with NCS (100 ng/ml) for indicated time points. Whole cell protein lysates were harvested and immunoblotted with indicated antibodies.HSC70 was used as a loading control.

4.4 Inhibition of DOT1L leads to an altered DNA damage response

Small molecule epigenetic inhibitors are emerging as a new direction for cancer therapy. Among them, an inhibitor, SGC094a, targeting DOT1L methyltransferase activity showed promising findings in MLL-rearranged leukemia cells. To validate the role of DOT1L methyltransferase activity in DNA DSB repair process, we compared the H3K79me3 levels in DOT1L wild-type and knockdown cells. Moreover, we have investigated the effect of an incubation with the DOT1L Inhibitor (SGC094a) or siRNA transfection for 48 hours. The efficiency of inhibition and siRNA transfection was further determined by measuring relative DOT1L mRNA expression levels. We observed decreased H3K79me3 levels with either knockdown or inhibition of DOT1L. As expected, there is a significant decrease in mRNA expression levels only with DOT1L knockdown but not with inhibition (Figure 10 A-B). Further, we wanted to know beyond chronic treatment of 48 hours if a short acute treatment time will block new methylation (H3K79me3) with DOT1L inhibition, therefore we further checked

long and short treatment periods (48 and 3 hours). In addition, we induced DSB breaks with NCS from 15 minutes to 2 hours and found there is no change of DOT1L levels. Interestingly, we observed less γH2AX both in short and long treatment with the DOT1L inhibitor with 15 minutes to 2 hours of break induction and also less phosphorylation of ATM compared to control cells suggesting new H3K79 methylation by DOT1L is required for proper DNA damage response. This further confirms the requirement of DOT1L in DNA DSB repair (Figure 10 C). Furthermore, SW837 cells were treated with increasing concentrations of another DOT1L inhibitor EPZ-5676, which is being tested clinically. The effectiveness of DOT1L inhibition was shown with chronic treatment of 4 days and observed to be sufficient for cellular depletion of H3K79me3 levels (Figure 10D).

Due to these findings, we inhibited DOT1L by cell treatment with the DOT1L inhibitor EPZ-5676 for 3 hours and subsequently induced DSB by NCS from 15 minutes to 6 hours in SW837 cells. Surprisingly, after 15 minutes of NCS treatment, DOT1L-depleted SW837 cells showed significantly lower γH2AX levels compared to control cells (Figure 10E). Inhibiting DOT1L also led to increased phosphorylation of ATM, KAP1 and NBS1 and CHK2 after 15 minutes of NCS treatment (Figure 10E). These effects are consistent with the effects observed following DOT1L siRNA-mediated depletion. Based on these findings, we aimed to explore whether H3K79me3 co-localizes with γH2AX at the break sites.

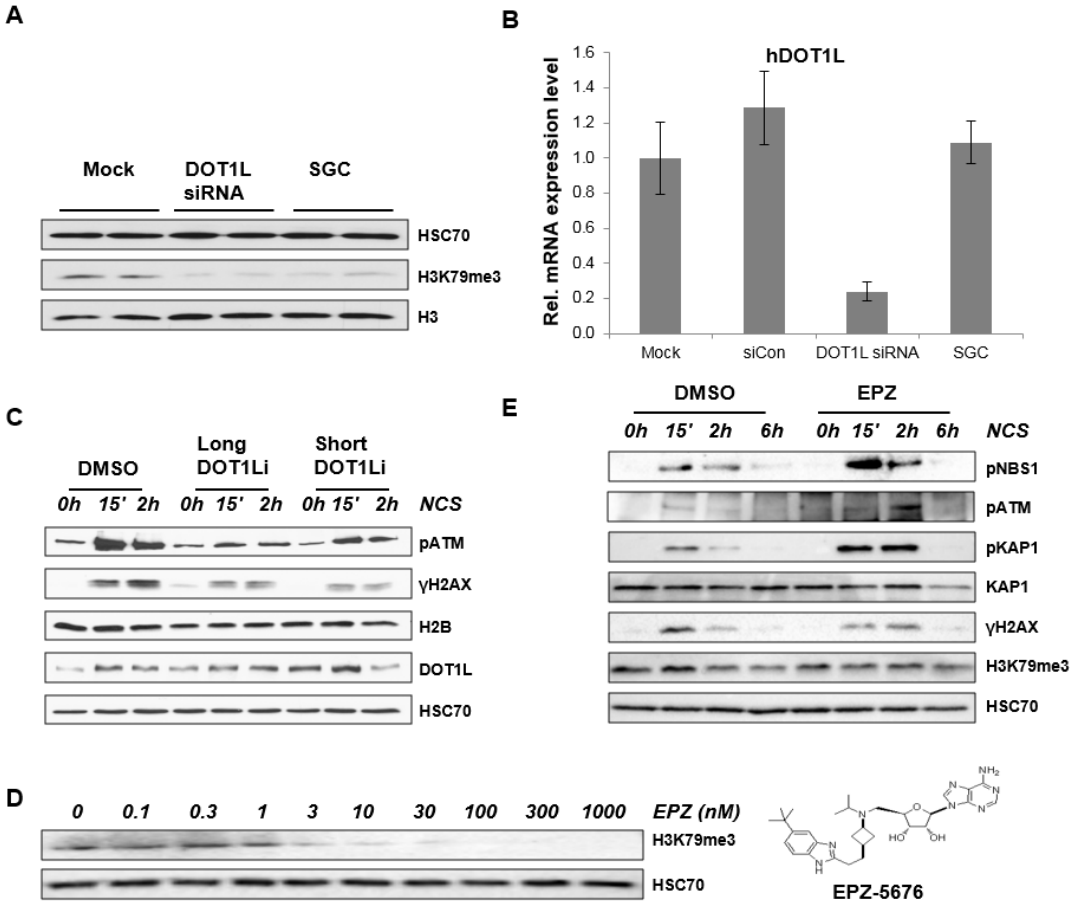

Figure 10: Inhibition of DOT1L leads to decreased H3K79 methylation and altered DNA damage response (A) Immunoblot analysis of total protein lysates from SW837 cells after 72 hours of DOT1L siRNA transfection and 48 hours of DOT1L inhibitor (SGC094a) treatment (100 nM) (duplicates) for indicated proteins. Both resulted in the decrease of H3K79me3. (B) Relative DOT1L mRNA expression in control, DOT1L siRNA-transfected cells and SGC094a-treated samples. (C) SW837 cells were treated with 100 nM SGC094a for 48 hours as long treatment and 3 hours as short treatment and followed by NCS treatment (100 ng/ml). (D) Immunoblot analysis of total protein lysates revealed clear effects on four days of chronic kinetic treatment with EPZ-5676 with increasing doses H3K79me3 levels were found to be reduced. (E) SW837 cells were pretreated with DOT1L inhibitor EPZ-5676 (1 µM) for 3 hours followed by NCS (100 ng/ml) for indicated time points. Whole cell lysates were immunoblotted and outcomes were similar to results obtained using siRNA targeting DOT1L.

4.5 γH2AX and H3K79me3 are co-localized at the DSB sites

H3K79 methylation has been implicated in the DNA damage response (Huyen et al., 2004a). Next, we tried to determine whether H3K79me3 and histone variant γH2AX colocalize at the break region. To determine the co-localization of γH2AX and H3K79me3 at the DNA damage site; we performed PLA (Proximity ligation assay) following NCS treatment and checked signals by immunofluorescence microscopy. This method is used to study the interaction between two proteins in fixed cells based on the utilization of two secondary antibodies against primary antibodies from

different species, which are conjugated to DNA oligonucleotides. When the two antibodies are in close proximity to one another, they can be bridged by two additional circle-forming oligonucleotides, joined via ligation, amplified by rolling circle amplification and visualized as foci using a complementary fluorescently labeled oligonucleotide probe. First, we confirmed the specificity of the test using a positive control (γH2AX and 53BP1) and confirmed the colocalization with a focus, which compared with the negative control (BSA). In addition, we tested the specificity of the interaction between H3K79me3 and γH2AX in NCS-treated samples after depletion of DOT1L by siRNA. Using the PLA approach, we confirmed the co-localization of γH2AX and H3K79me3 upon DNA damage induction and the interaction is abolished in the DOT1L depleted cells. Importantly, the absence of DOT1L did not enhance the number of γH2AX foci (Figure 11). Taken together, PLA demonstrated that γH2AX and H3K79me3 are co-localizing at the DSB sites.

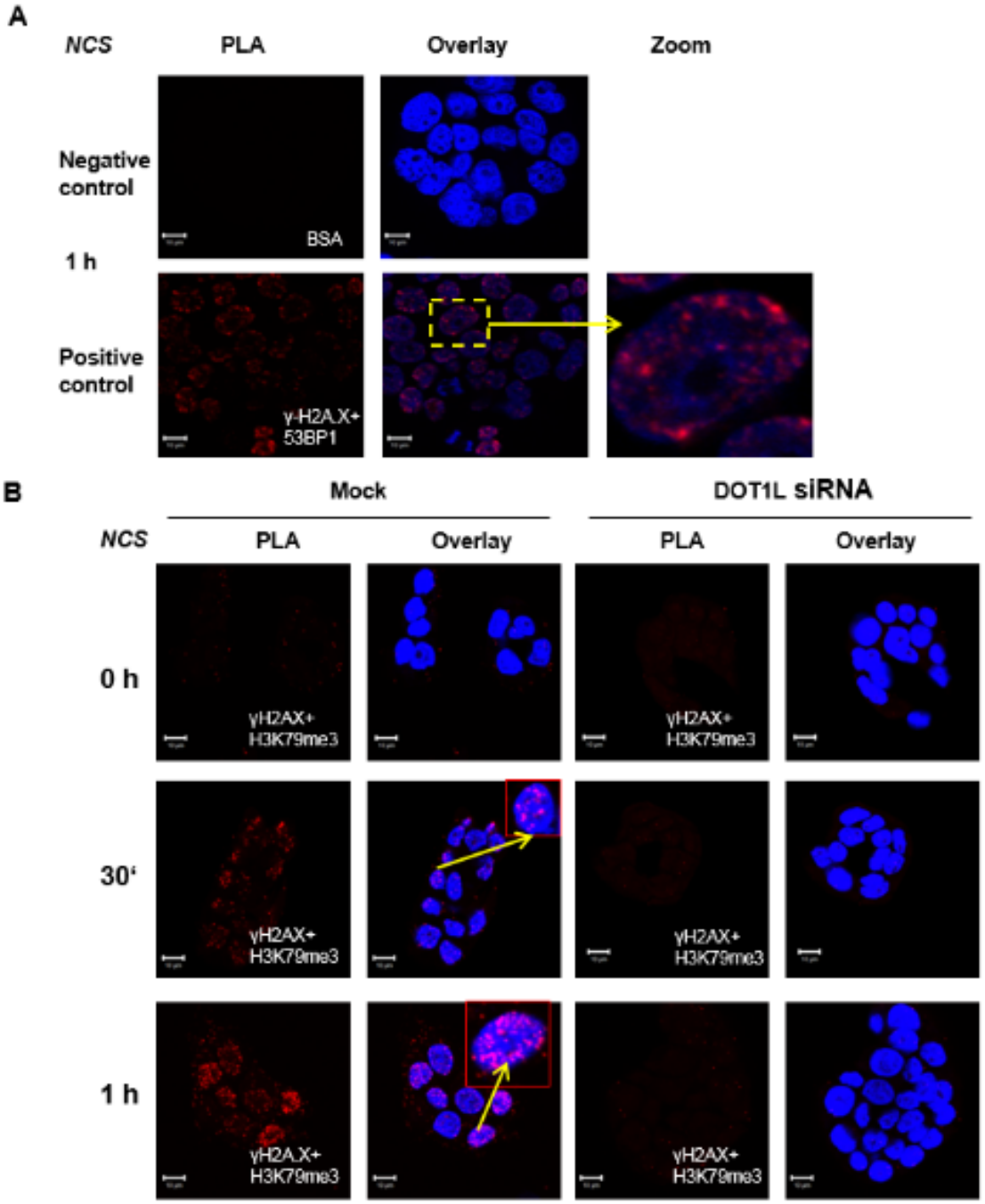

Figure 11: γH2AX and H3K79me co-localize at DSB sites. (A) SW837 cells were treated with NCS (100 ng/ml) for 1 h. The specificity of the proximity ligation assay (PLA) signal was confirmed by the interaction between γH2AX and 53BP1 antibodies. (B) SW837 mock and DOT1L siRNA transfected cells after indicated time points of NCS (100 ng/ml) treatment were processed for PLA assay with γH2AX and H3K79me3. The images were obtained using an Axioinverted microscope. Red dots represent the proximity between γH2AX and H3K79me3 and nuclei are stained with DAPI. Scale bar 20 µm.

4.6 DOT1L is crucial for homologous recombination (HR) DNA repair pathway

Dot1 was previously shown to play a role in repairing UV-induced DNA damage in yeast (Giannattasio et al., 2005). H3K79 methylation and Rad9 recruitment also play important roles in regulating resection of ssDNA (Lazzaro et al., 2008). Interestingly DOT1L was shown to be important for meiotic checkpoint control and also involved in double-strand break repair via sister chromatid recombination in *Saccharomyces cerevisiae* (Conde et al., 2009b).

To further investigate the importance and understand the role of DOT1L in DSB repair pathway, we examined which repair pathway is affected by DOT1L depletion. For this purpose, we have used homologous recombination (HR) and non-homologous end joining (NHEJ) cell reporter systems. We performed HR and NHEJ repair I-SceI-induced DSB assay, using GFP-based reporter systems using HeLa pDR-GFP cells, a cell line with the chromosomally integrated HR and NHEJ plasmid substrate DR-GFP. In this system, a DSB is generated by expressing the I-SceI endonuclease. The repair efficiency was calculated by flow cytometry based on the fraction of GFP-positive (GFP^+ cells) cells 48 h after transfection with an I-SceI expression vector.

We found that different individual siRNAs targeting DOT1L led to a significantly decreased HR efficiency as compared to siRNA controls (Figure 12 A). Interestingly, DOT1L depletion led to slightly elevated NHEJ efficiency. These results provide evidence that DOT1L promotes HR-mediated DSB repair.

To further test whether DOT1L is crucial for HR-mediated DNA repair, we performed chromatin fractionation analyses in DOT1L-depleted cells treated with NCS for different time periods. We checked the chromatin fractions obtained from SW837 cells by immunoblotting and examined the recruitment of repair proteins involved in

the HR pathway. Immediately after DNA damage, proteins involved in the DNA damage response and key HR repair mediators are recruited to the chromatin site. We show that the recruitment of the single stranded binding proteins RPA1 and RAD51 to chromatin in response to DNA DSB induction is increased in cells with DOT1L wildtype levels. Moreover, the C-terminal binding protein (CtBP)-interacting protein (CtIP) is recruited to chromatin and its levels increased over time in control cells. This protein plays a central role in DNA end resection DSB repair (Sartori et al., 2007). CtIP is decreased in DOT1L-depleted cells. Increased recruitment of the single stranded binding protein RPA1 and Rad51 were observed from 2-6 hours of NCS treatment. This is significantly decreased by RNA interference-mediated DOT1L knockdown (Figure 12 B). Taken together, our findings demonstrate that DOT1L regulates the recruitment of damage signaling machinery and promotes the homologous recombination pathway.

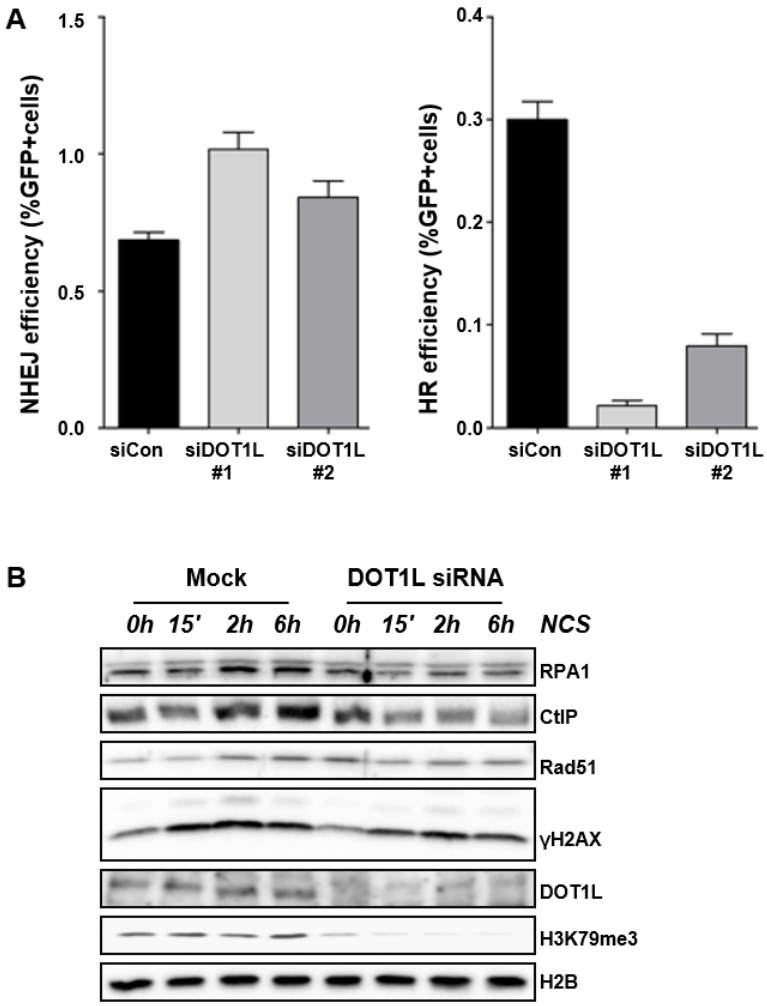

Figure 12: DOT1L is important for the homologous recombination-mediated repair pathway. (A) HeLa cells harboring of HR repair construct (pGC) or NHEJ repair construct (pEJ) were transfected either mock or DOT1L siRNA #1 or siRNA #2. After 24 hours of siRNA transfection, DSB was induced by transfecting cells with I-SceI-expressing vector (pCMV-I-SceI-3xNLS). 48 hours after transfection cells were assessed for green fluorescence-positive cells by flow cytometry (FACScan, BD Bioscience) for HR and NHEJ efficiency. HR repair efficiency is decreased in DOT1L depleted cells. (B) After 72 hours of post-siRNA transfection and following NCS treatment the insoluble chromatin fractions were harvested and subjected to Western blot analysis revealing an enrichment of Rad51 and CtIP in control cells.

4.7 Loss of DOT1L leads to increased sensitivity to ionizing radiation (IR)

We have observed that DOT1L functions in the homologous repair (HR)-mediated DNA double-strand break repair pathway. Based on the recruitment of repair factors to chromatin in response to DSBs, we next tested whether DOT1L is involved in cell survival after DNA damage. To test this, we irradiated cells with 6 Gy and harvested total cell lysates from 15 minutes to 6 hours of IR. Western blotting analysis

confirmed that γH2AX is accumulated in the control cells within 15 minutes of IR, as expected, it is less in DOT1L-depleted cells confirmed again its role in DSB repair process (Figure 13 A). We further performed a clonogenic assay to test cell survival after siRNA-mediated depletion of DOT1L and irradiation in SW837 cells for a period of 21 days. Both control and DOT1L-depleted cells were irradiated using 0, 1, 2, 4, 6 and 8 Gy and cell proliferation was measured. We observed that depletion of DOT1L leads to increased sensitivity to ionizing radiation as compared to control cells. DOT1L-deficient SW837 cells are moderately sensitive to low IR (Figure 13 B & C) suggesting that these cells are sensitive in the repair of IR-induced DNA lesions. This is in agreement with results shown in Figures 12 in which DOT1L is involved only in HR pathway.

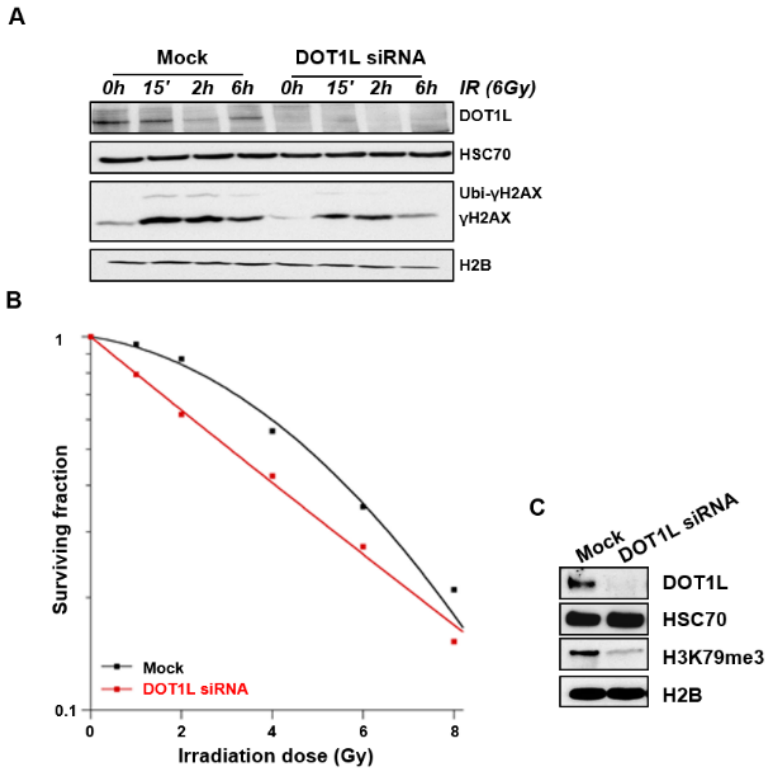

Figure 13: Depletion of DOT1L leads to increased sensitivity to ionization radiation (A) SW837 cells were transfected with DOT1L siRNA for 48 hours. Cells were treated with ionizing radiation (6Gy) and total protein lysates were harvested after indicated time points and immunoblotted with indicated antibodies. H2B and HSC70 used as a loading control. (B) Colony formation assay performed with SW837 cells which were transfected with either mock or DOT1L siRNA. After 48 hours of transfection cells were treated with indicated doses of irradiation (Gy) leading to an increase in γH2AX. (C) Whole cell lysates from DOT1L siRNA transfected SW837 cells after 48-hour knock down and its efficacy of knockdown checked with DOT1L and H3K79me3 antibodies.

4.8 Additive effect of DOT1L and PARP inhibition on cell proliferation

MLL-fusion protein-induced transformed cells exhibit local hyper-methylation of H3K79 and undergo apoptosis in the absence of DOT1L (Nguyen et al., 2011). Small molecule DOT1L inhibitors, such as SGC0946, EPZ004777 and EPZ5676 induce apoptosis in leukemia cells induced by MLL-fusion proteins (Chen et al., 2013).

While trying to clarify the cell death and proliferation defect, we employed the potential PARPi (veliparib) which will block the DNA repair of DSBs for better treatment cancer treatment options (Srivastava and Raghavan, 2015). We monitored the proliferation rate of cells, using an optical automated microscope Celigo® which measures the cell growth upon desired treatment of the cells. Initially, SW837 cells were treated either with the DOT1L inhibitor EPZ-5676 or the PARP inhibitor veliparib (ABT-888). The SW837 cells were treated alternatively every 48 h and the confluence was measured daily before media exchange. Finally, cell confluence was plotted against time (in days).

From the plotted graph it was clear that individual treatment with the DOT1L inhibitor using the highest concentration (1,000 nM) resulted in no changes in the proliferation. When treating cells with the PARP inhibitor veliparib (ABT-888), we observed a significant effect of proliferation which we also confirmed in another cell line, U2OS (Figure 14 A-C). Veliparib significantly reduced survival in cells at all tested treatment concentrations and durations and the inhibition increased with increasing dose and time.

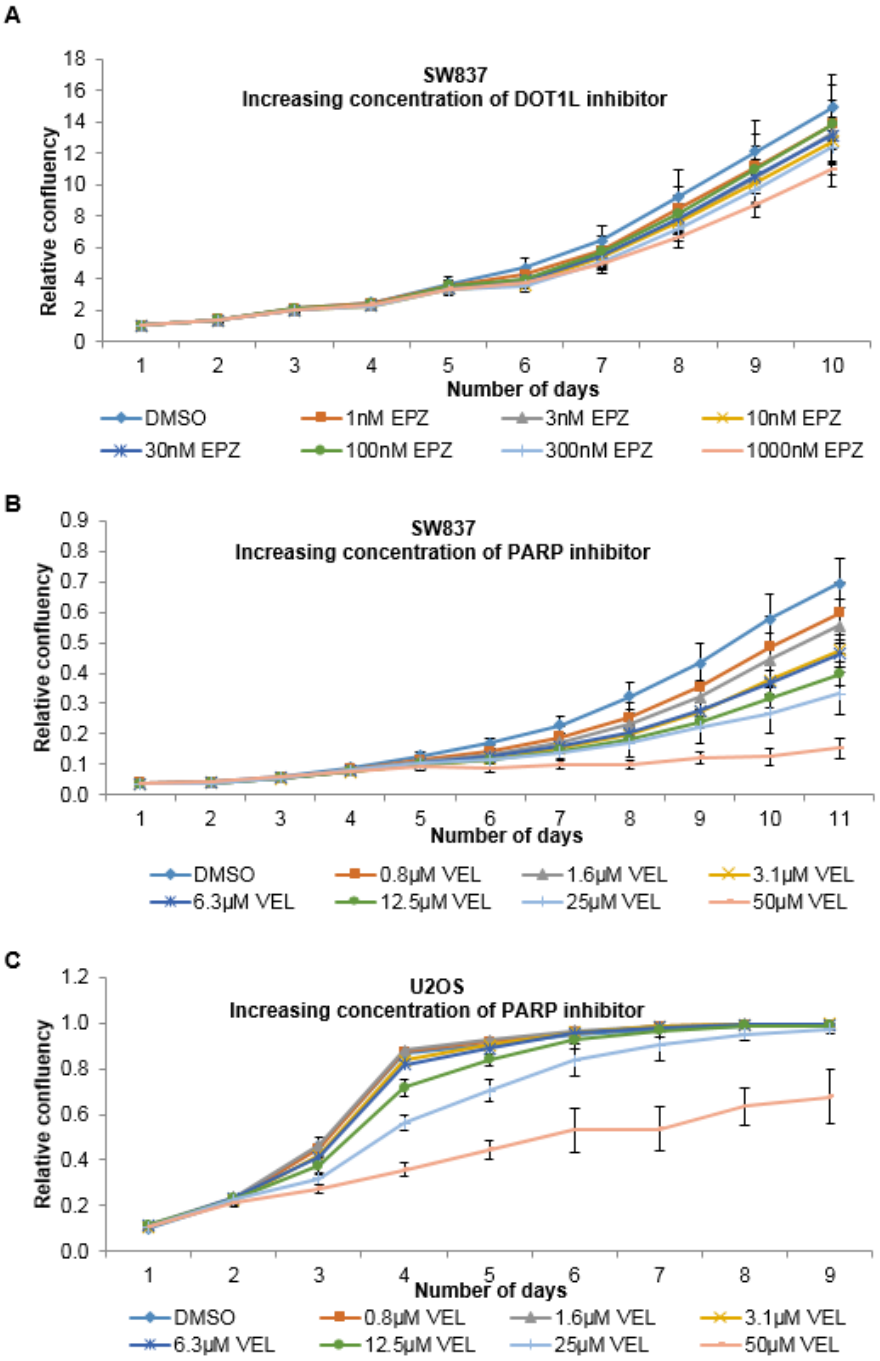

Figure 14: Cell proliferation assay with DOT1L and PARP inhibitors. (A) SW837 cells were treated with increasing concentrations of EPZ-5676 (1-1000 nM) every 48 hours. Cell confluence was measured at regular intervals of 24 hours using the Celigo® cytometer. (B) Treatment with PARP inhibitor (ABT-888) in SW837 cells as and in U2OS cells (C).

Treatment with a PARP inhibitor as a therapeutic anti-cancer drug is an alternative strategy in the context of a defective BRCA1 or BRCA2 gene (Farmer et al., 2005). The combination of PARP inhibitor with cytotoxic DNA damaging agents such as irinotecan hydrochloride is now being tried and reached phase 3 clinical trials in

locally advanced or metastatic colorectal cancer (NCT00535353). We further aimed at combination treatment strategy and compared the effects of different DNA-damaging agents when combined with a DOT1L inhibitor. Cellular proliferation was examined by while increasing the inhibitor dose. We observed cell proliferation defects with increasing concentrations of EPZ-5676 and in a combination of veliparib (Figure 15 A-C). The combined inhibition of DOT1L and veliparib inhibits cell proliferation in a continuous pattern where combining both compounds induced a greater effect on cell proliferation, compared to the DOT1L inhibitor alone. We show that the additive antiproliferative effect of DOT1L inhibitor when combined with PARP inhibitor was significantly more effective than either treatment alone in colorectal cells and loss of DOT1L function leads to increased sensitivity to PARP inhibition. Taken together, both inhibiting DOT1L and treatment with veliparib increased anti-proliferative effects.

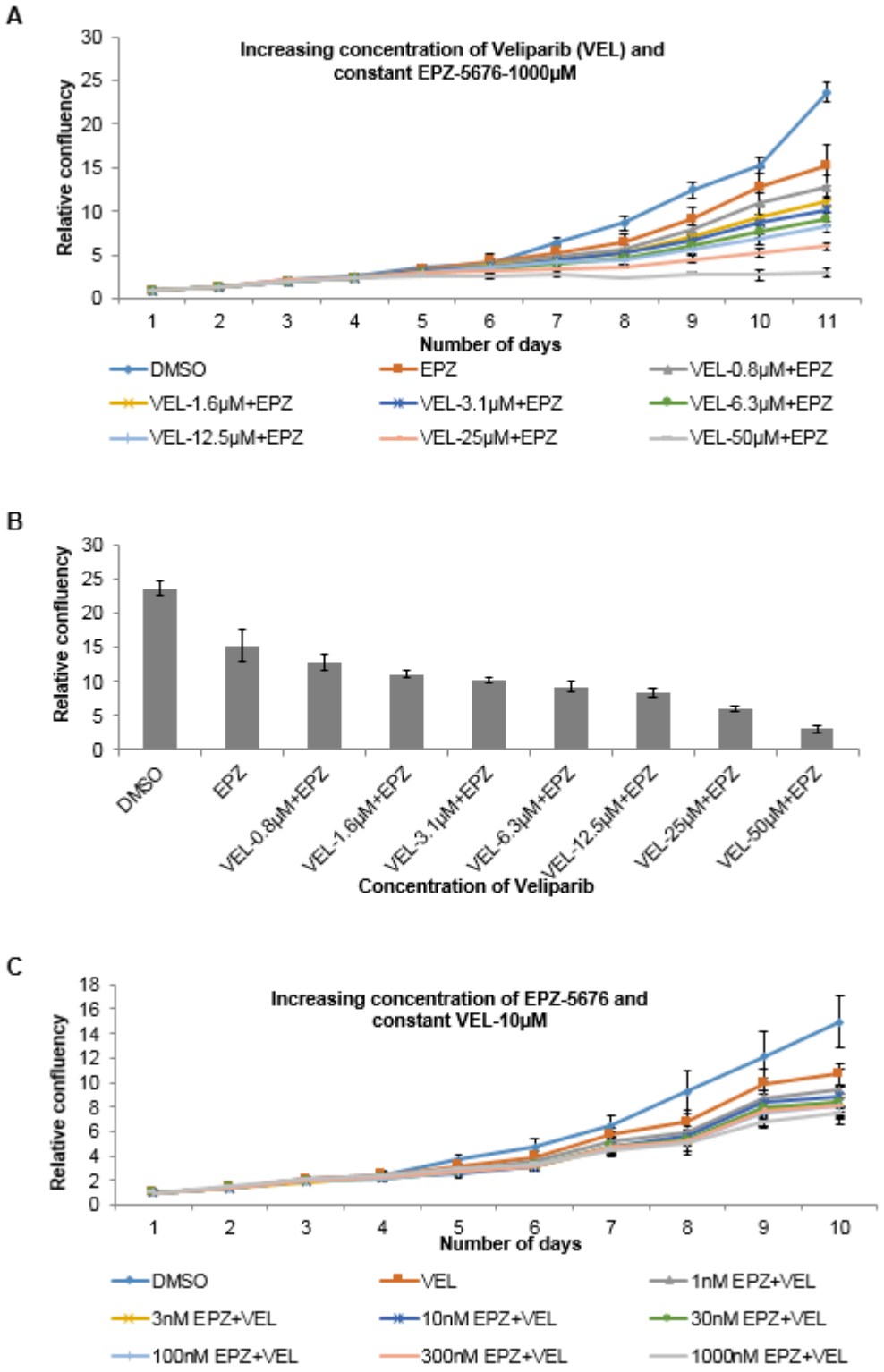

Figure 15: Additive effect on cell proliferation with dual DOT1L and PARP inhibition. (A) Dose-dependent treatment every 48 hours with vehicle (DMSO) or with EPZ alone and increasing concentration of veliparib (VEL) on SW837 cells. Each figure represents the mean ± s.d. of biological triplicates. Cells were pre-treated with EPZ for 3 hrs followed by 48 hrs of incubation time. (B) Data from A represented in the graph from the 11th day of treatment. (C) Dose-dependent treatment every 48 hours with vehicle (DMSO) or with VEL alone and increasing concentration of EPZ on SW837 cells. Each figure represents the mean ± s.d. of biological triplicates.

4.9 Additive effect of DOT1L inhibition and DNA-damaging agent irinotecan on cell proliferation

The study using PARP inhibitors suggests that co-treatment with DOT1L inhibitor with other DNA damaging agents, specifically single strand break (SSB)-inducing agents, could increase the sensitivity of cells to DNA damage. To test this, we used the topoisomerase I inhibitor irinotecan (IRI), which typically induces SSBs which further develop to DSBs in S-phase, which are mainly repaired via the HR pathway (Xu and Her, 2015). Initially, we treated SW837 cells with IRI for different time points from 2 hours to 48 hours. Upon treatment, phosphorylated H2AX rapidly accumulated from 2-6 hours and at later time points decreased due to the repair of damaged DNA. The cells treated with irinotecan which induced lower levels of γH2AX after 24 hours are seems to be repaired as observed with western blotting analysis (Figure 16).

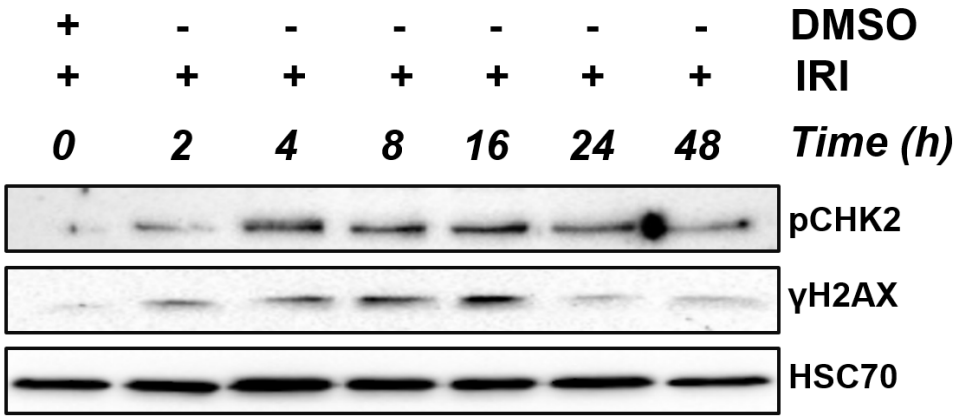

Figure 16: Irinotecan affects phosphorylation of histone variant H2AX. SW837 cells treated with irinotecan (300 nM) (IRI) at indicated time points and analyzed with Western blot revealing the effect of damage response.

To further check the combined effects of DOT1L inhibition and irinotecan on the proliferation rate of CRC cells, we investigated effects of the combination of the DOT1L inhibitor EPZ-5676 and irinotecan by performing Celigo®

measurements. Celigo image cytometer is a cell-based image cytometry assays which determined cell viability.

Interestingly, cells treated with DOT1L inhibitor combined with irinotecan showed a significant decrease in cell proliferation compared to either DOT1L inhibitor or irinotecan alone (Figure 17 A-B). The combined effects are more visible only at lower concentrations of irinotecan. These findings clearly showed that the addition of a DOT1L inhibitor further increased the effects of irinotecan on cell proliferation.

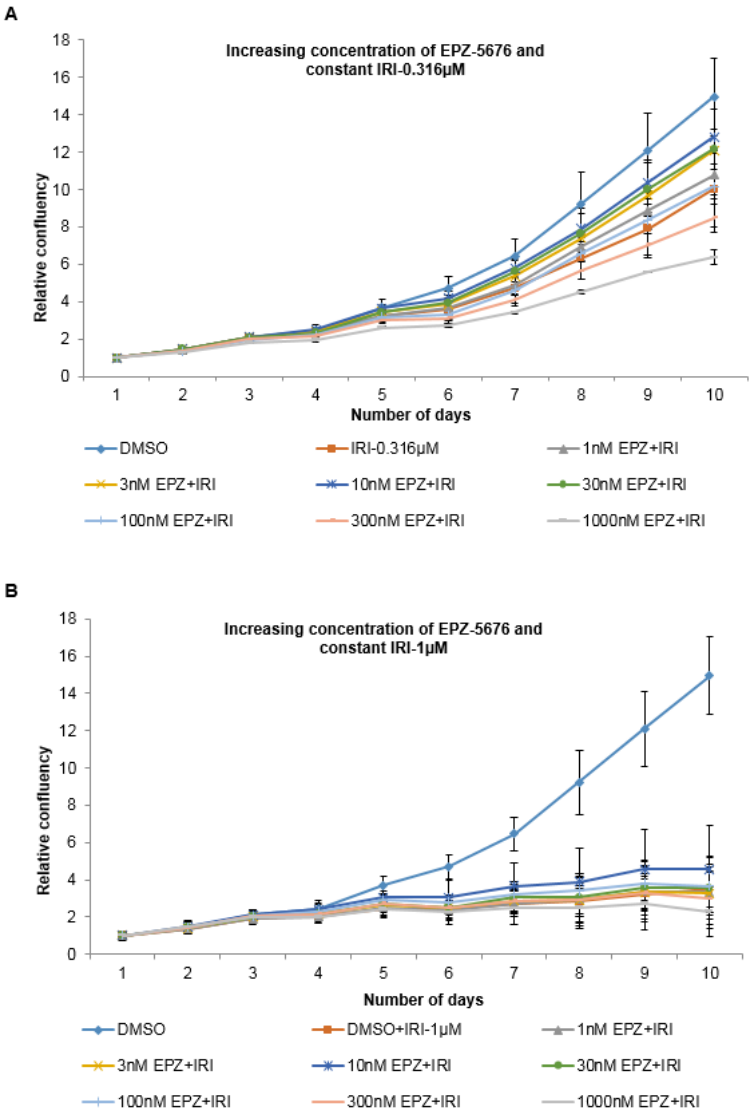

Figure 17: Increased sensitivity of CRC cells after combining irinotecan with a DOT1L inhibitor. (A) Dose-dependent treatment every 48 hours with vehicle (DMSO) or with irinotecan alone (0.316 µM) and increasing the concentration of EPZ on SW837 cells. Each figure represents the mean ± s.d. of biological triplicates. (B) Similar to A with constant concentration of irinotecan 1µM and increasing concentration of EPZ.

4.10 PARP inhibitor in combination with other DNA-damaging therapeutic agents

Several studies reported that PARP plays a key role in DNA-damage signaling and repair. Defective homologous recombination repair pathways (BRCA-associated mutations) are sensitive to PARP inhibition (Javle and Curtin, 2011). In recent years olaparib is FDA-approved PARP inhibitor, appear promising against cancers with BRCA1 or BRCA2 mutations, including breast and ovarian cancers (Fong et al., 2009). Since in our case, loss of DOT1L resulted in defective HR repair of DNA damage, we hypothesized that low DOT1L in the cancer cells can sensitize to PARP inhibition as well. We treated SW837 and SW480 cells with veliparib (ABT-888). We observed that increasing concentrations of veliparib markedly decreased cell proliferation in two different cell lines (Figure 14 B and C). The effect between inhibition of PARP and DOT1L was further enhanced when combined with irinotecan. Interestingly, we observed inhibition of PARP alone did not mediate significant anti-proliferative activity relative to irinotecan and PARP inhibition together, however, in combination with irinotecan, decreased proliferation (Figure 18 A-B). These findings clearly demonstrate that the addition of PARP inhibitors to irinotecan further increased anti-proliferative effects. This shows DOT1L-activating DSB repair in combining with PARP and chemotherapeutic agents.

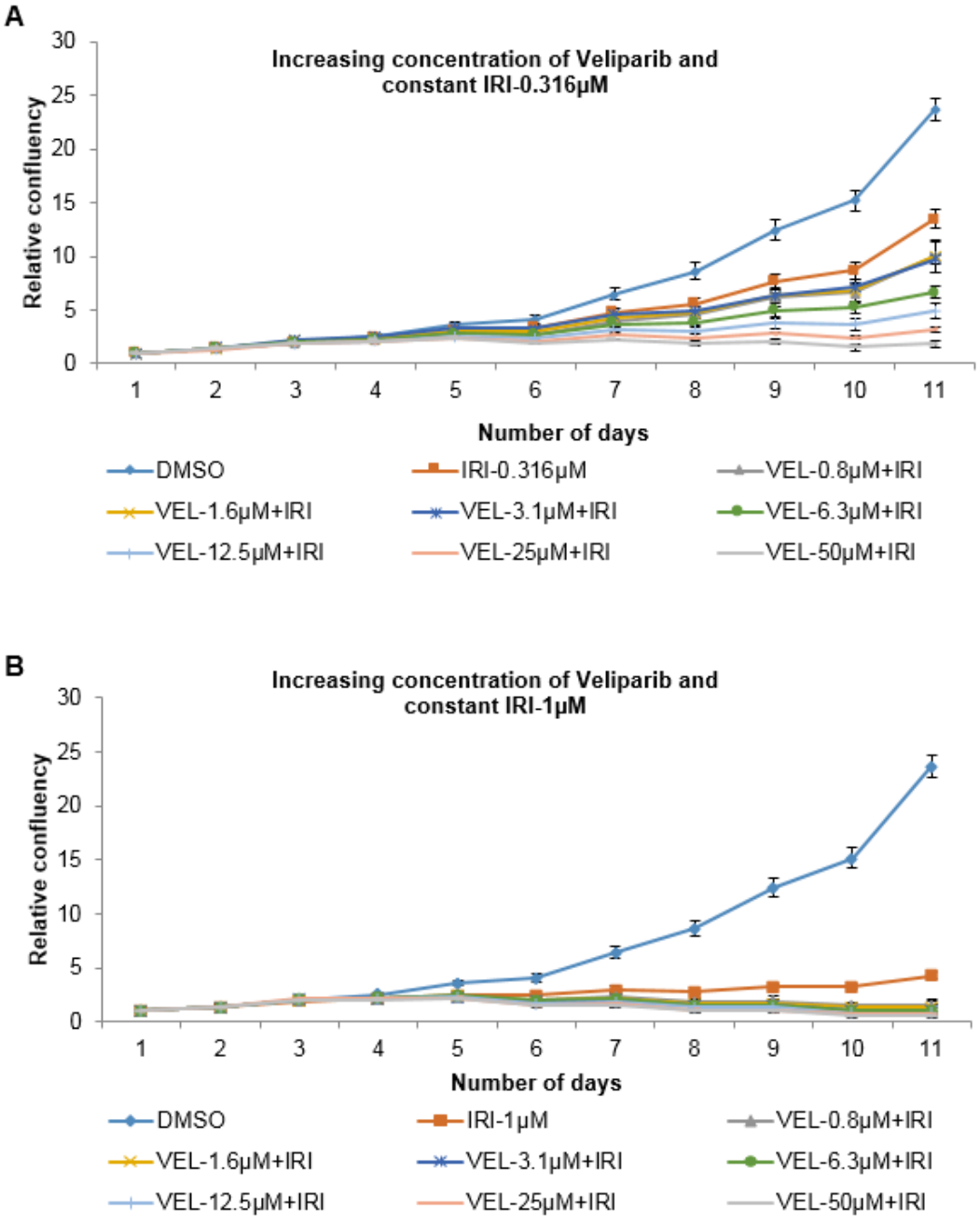

Figure 18: Increased sensitivity to veliparib combined with DOT1L and irinotecan. (A) Dose-dependent treatment every 48 hours with vehicle (DMSO) or irinotecan alone 0.316 µM and with increasing concentration of VEL on SW837 cells. Each figure represents the mean ± s.d. of biological triplicates. (B) With the constant concentration of irinotecan 1µM.

4.11 Combination treatment with 5-FU is more effective at reducing cell viability and repairs DSBs

Generally, the treatment of colorectal cancer includes the nucleoside analog 5-fluorouracil (5-FU) in combination with radiation. 5-FU leads to the generation of secondary DSBs in S phase, which is repaired by the HR pathway (Srinivas et al., 2015). Irinotecan plus 5-fluorouracil and folinic acid combined clinically and emerges as frontline chemotherapy for colorectal cancer (Glimelius et al., 2002).Therefore, we combine the DNA-damaging chemotherapeutic agents such as irinotecan with 5-FU in CRC cells for clinical utilization.

After seeding cells, we pretreated the CRC cells SW837 and SW480 with 5-FU for 24 hours in combination with EPZ and IRI or alternatively 48 hours treatment only with IRI and EPZ for a period of 7 days (Figure 19).

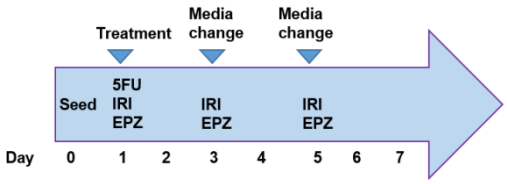

Figure 19: Schematic presentation of treating CRC cells with 5-FU, IRI, and EPZ. 24 hours after seeding SW480 and SW837 cells they were incubated with 5 µM 5-FU in combination with 1 µM IRI and 1 µM EPZ for 24 h followed by treatment with only IRI and EPZ against the indicated time points. The cell proliferation was measured daily before treatment.

With immunoblot analysis, we found after 5-FU and IRI combination, there is an increased accumulation of γH2AX as compared to 5-FU alone (Figure 20 A-B). Simultaneously we have performed a cell proliferation assay using the Celigo® cytometer for 7 days. We showed that the combination of DOT1L inhibitor, 5-FU and IRI led to a severe proliferation defect in both cell lines. This suggests that decreased cell proliferation occurs in the presence of both IRI and 5-FU inhibitor. 5-FU alone is less effective regarding reducing cell proliferation (Figure 20 C-D). While comparing the relative confluence after 7 days of treatment, it was observed that the decrease in cell proliferation after combining 5-FU and IRI is highly significant (*** P

≤ 0.001) (Figure 20 E-F). Therefore, these findings suggest that combinatorial treatment is more effective at reducing cell proliferation than treatments with a single agent.

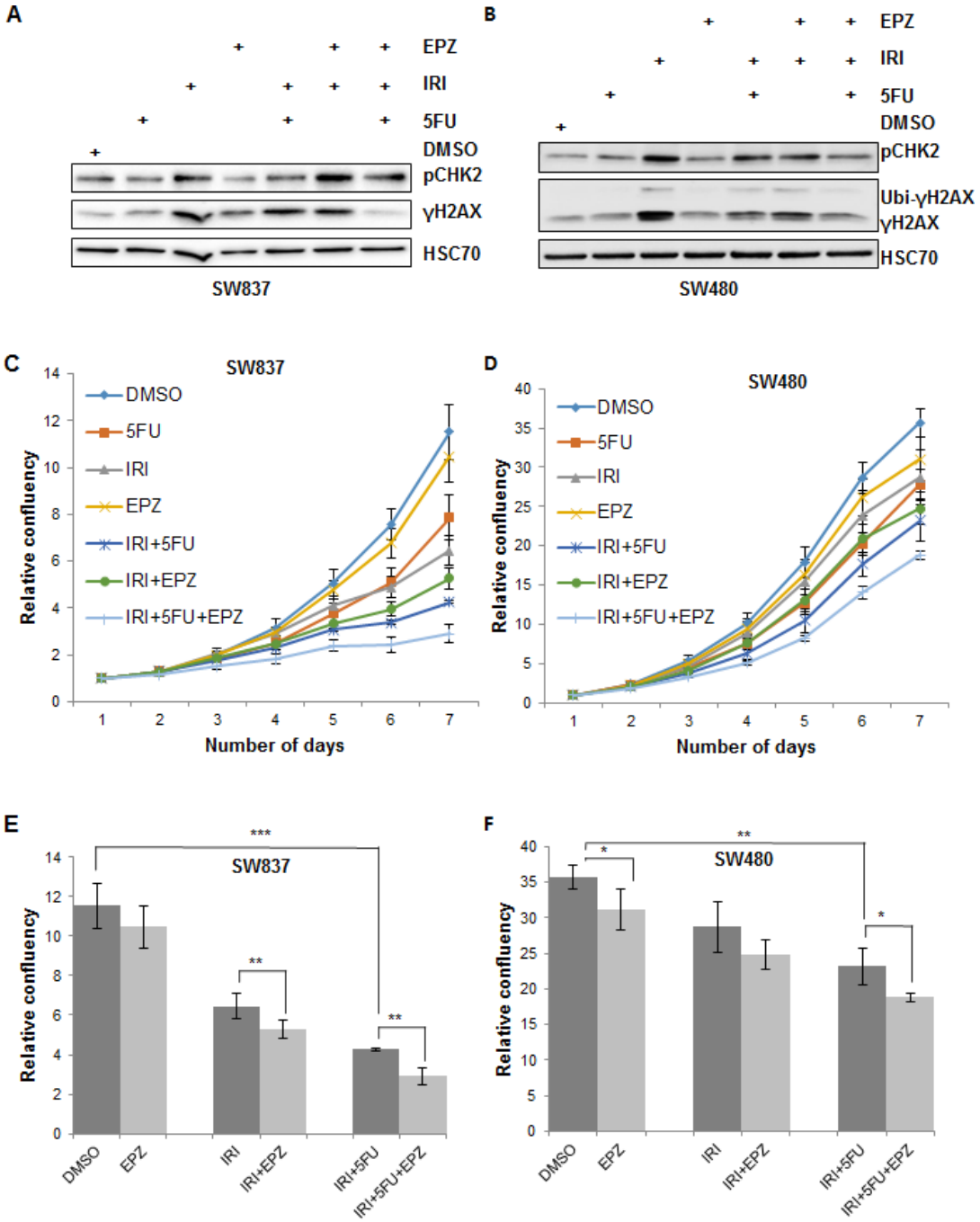

Figure 20: Combinational treatment of the DOT1L inhibitor EPZ-5676, irinotecan and 5-FU is highly effective at reducing cell viability. (A) SW837 (B) SW480 cell lysates were harvested after 48 hours of treatment as indicated, and Western blotting was carried out revealing that increasing breaks (C) SW837 and (D) SW480 cells were treated initially with 5-FU (5 µM), IRI (1 µM) or EPZ (1 µM) alone or in combination as indicated for 24 hours and later followed by media change every 48 hours. Cell confluence was measured at regular intervals of 24 hours using the Celigo® cytometer. (E), (F) Quantitative analysis of Celigo measurement from C and D from the 7th day of treatment. The error bars represent standard deviations (* P ≤ 0.05, ** P ≤ 0.01, and *** P ≤ 0.001).

4.12 Combinational treatment with veliparib is more effective at reducing cell viability and repairs DSBs

Mutations in either the BRCA1 or BRCA2 genes lead to defective homologous recombination (HR) and affected cells are sensitive to PARP inhibition. It has been shown with several studies that PARP inhibitors increase the efficacy of topoisomerase inhibitors (Kummar et al., 2011; Smith et al., 2005). It has also been suggested that niraparib, a PARP inhibitor, also showed additive to synergistic inhibition of cell proliferation despite MSI/MSS status of colorectal cancer cell (Genther Williams et al., 2015). We hypothesized that combined treatment of veliparib may enhance the sensitivity to irinotecan and the DOT1L inhibitor. As expected, we observed high accumulation of phosphorylated H2AX at ser139 in SW837 and SW480 cells after combined treatment with IRI+VEL and EPZ+IRI (Figure 21 A and B). Proliferation assays showed that continuous treatment with EPZ alone resulted in a very mild effect, while the combination of EPZ with veliparib resulted in a strong decrease in cell proliferation (Figure 21 C &D). We observed less γH2AX level with a combination of all three treatment options using Western blot analysis. Moreover, at day 10 of treatment, there is a significantly decreased cell proliferation (Figure 21 E-F), which is statistically very significant (****P ≤ 0.0001). Taken together, inhibiting DOT1L and PARP simultaneously results in less γH2AX accumulation and increased growth arrest. These results indicate that DOT1L loss affects HR-dependent DSB repair and results in a dependency on PARP as critical determinants of DSB repair. Consequently, the combination of veliparib, irinotecan and DOT1L inhibition seems a promising approach for targeting the DNA double-strand break repair pathway.

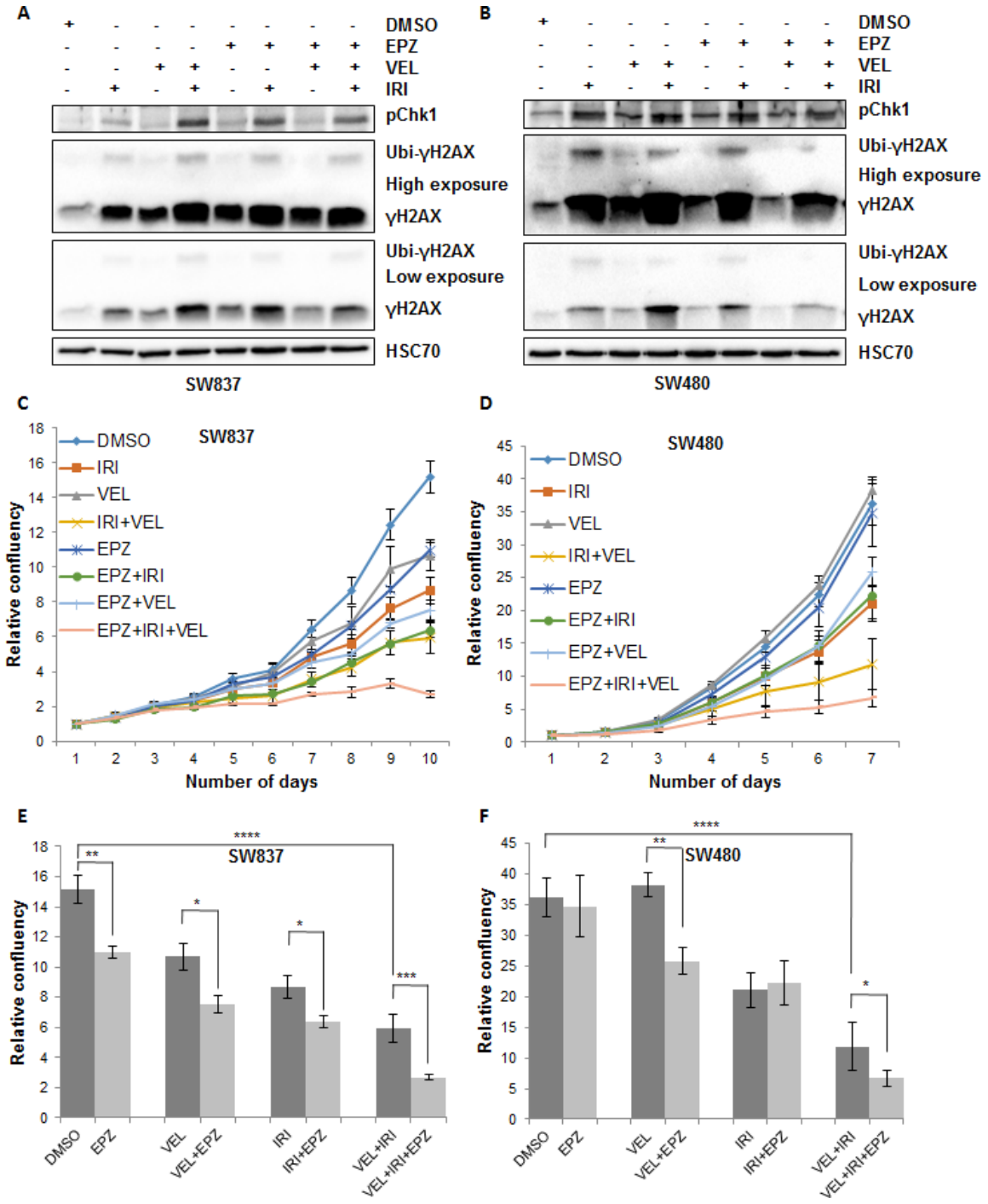

Figure 21: **Combined treatment of irinotecan, veliparib and EPZ-5676 reduces cell viability.** (A) SW837 (B) and SW480 cells were treated with the indicated drugs for 48 hours. Total lysates were immunoblotted showing less γH2AX after the combination of all three drugs. (C) SW837 and (D) SW480 cells were treated with the individual drugs or in combination of veliparib (10 µM), irinotecan (0.316 µM) and EPZ-5676 (1 µM) every 48 hours. Cell confluence was measured at regular intervals of 24 hours using the Celigo® cytometer. (E), (F) Effect of the chronic drug treatment as described in A and B in SW837 and SW480 cells and relative confluency was measured at day 10 using Celigo®.

4.13 H3K79me3 is a marker for molecular stratification of CRC patients

For improving patient treatments and outcomes, the identification of molecular biomarkers is essential. Mechanistically, DOT1L plays a role in HR-repair pathway. Studies in rectal cancer patient samples revealed that the DOT1L gene is differentially methylated and associated with an overall better survival (Gaedcke et al., 2014). In this study, we examined whether H3K79me3 levels may correlate with the survival rates of rectal cancer patients. To investigate H3K79me3 levels, we performed immunohistochemistry with H3K79me3 on tissue microarrays (TMAs) from rectal cancer patients treated in the Department of General, Visceral, and Pediatric Surgery. Interestingly, we observed very different levels of H3K79me3 among the patients tested (Figure 22 A). The patients were classified based on the H3K79me3 staining intensity either as no staining, low (5% staining), medium/heterogeneous (50%) or high (100%). Interestingly, the Kaplan-Meier plot showed that patients who had relatively strong H3K79me3 staining (p=0.051) displayed better overall survival rates (red line) compared to patients with medium or low H3K79me3 levels (blue line) (Figure 22 B). Together our result suggests that DOT1L is mainly required for repair of DSB via the HR pathway. These data suggest that combined targeting of PARP along with other standard available chemotherapeutics agents like irinotecan might be a promising approach for treating DNA-repair defects (HR) in H3K79me3-stratified colorectal cancers. Altogether, this study provides strong evidence for a central role of DOT1L in DNA DSB repair and may serve as a basis for further exploration of DOT1L as an anti-cancer therapeutic target in combination with other chemotherapeutic approaches. Therefore, we hypothesize that DOT1L activity (i.e. H3K79me3) may serve as a marker for molecular stratification of colorectal cancer.

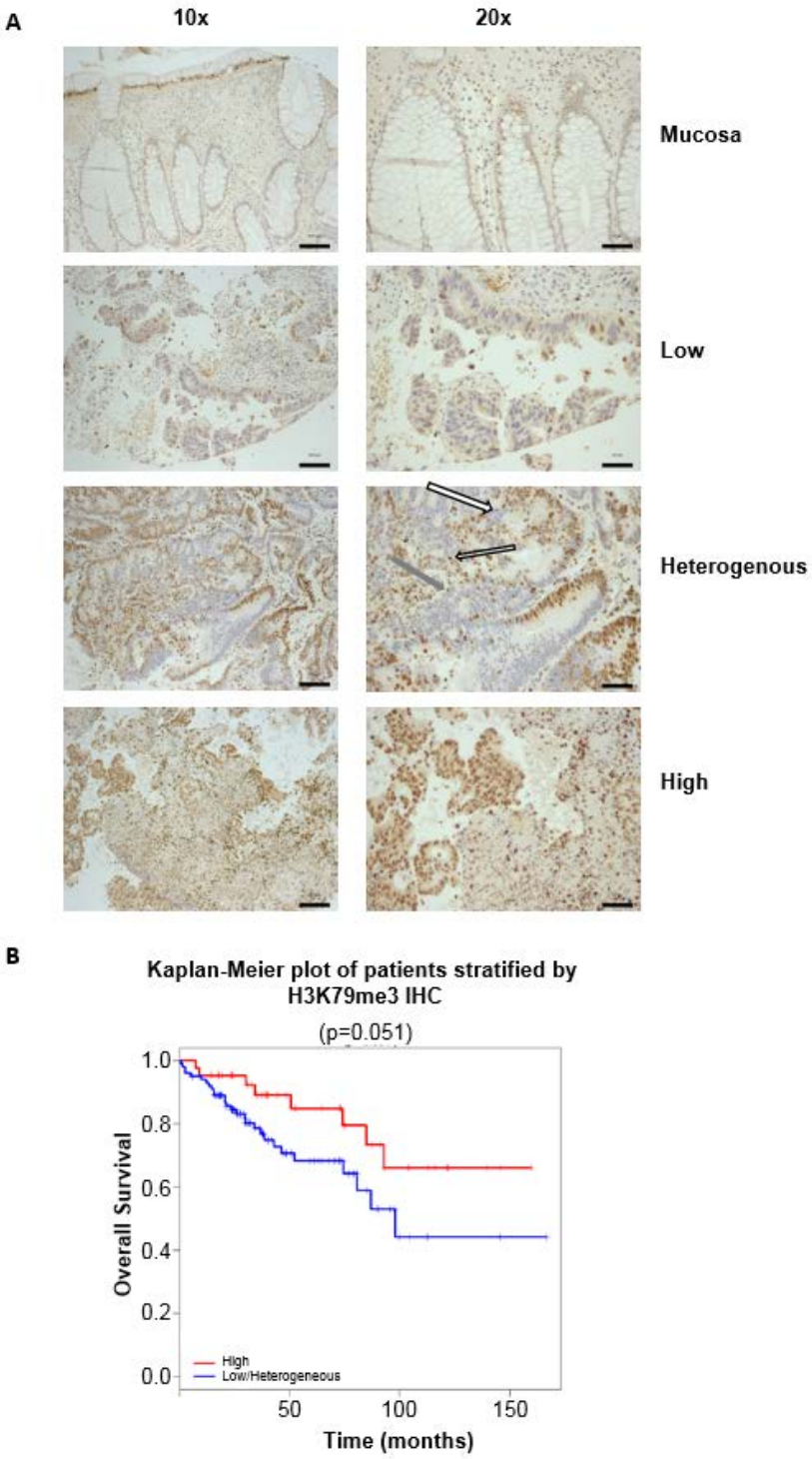

Figure 22: Low H3K79me3 levels result in poor overall survival in CRC patients. In total, samples from 156 patients were used for immunohistochemical analyses of H3K79me3 levels. Based on the staining intensity, the nuclei were given the relative score of 0 to 3, with 3 corresponding to highest staining intensity. Moreover, the overall percentage of the stained nuclei corresponding to each score were estimated for each analyzed sample. **A**. The patients' tissue samples were then classified based on the staining intensity and overall percentage of the stained nuclei as no staining, or low (5% of the nuclei with low score), medium/heterogeneous (50% of the nuclei stained heterogeneously), or high (100% of the nuclei with high score) staining. Solid arrows indicate positive, gray arrows weak and white arrows negative staining. **B**. The Kaplan-Meier survival rate was estimated for groups of patients with tissue samples classified as "High" (red line) and "Low or Heterogeneous" (blue line; comprising patients with no, low or heterogeneous staining).

5 Discussion

Maintaining genome integrity is essential for all living organisms. Damaged DNA which is not repaired properly may lead to different disease states like cancer. Several studies reported that the DOT1L methyltransferase is implicated in several biological processes such as cell cycle regulation, transcription, reprogramming, development, differentiation, and proliferation (Nguyen and Zhang, 2011b) where it mediates mono-, di-, and tri-methylation of H3K79. Moreover, DOT1L has been highlighted in the development of many diseases including leukemia, cardiac dysfunction and kidney injury (Kim et al., 2014). DOT1L and histone methylation (H3K79) are involved in the double-stranded DNA break repair during different cell cycle phases (Wakeman et al., 2012). Recent study reports that small molecule inhibition of DOT1L is effective in treating leukemia and aggressive breast cancer and DOT1L is a promising future drug target (Lee et al., 2015). Therefore, we have mechanistically dissected the role of DOT1L particularly in DNA DSBs repair in colorectal cancer and studied the applicability in regarding therapeutic aspects.

5.1 DOT1L affects γH2AX and DNA damage recognition

We showed that DOT1L expression is decreased upon siRNA-mediated knockdown resulting in the nearly complete absence or decreased of H3K79me3. We have demonstrated that upon DSB, the DNA damage-response-activated ATM had an increased phosphorylation level. Phosphorylation of H2AX by ATM has been shown to be crucial in DNA damage and response pathway and to activate checkpoints (Fernandez-Capetillo et al., 2002). Importantly we have found that there are drastically reduced levels of γH2AX in DOT1L-depleted cells as seen by Western blotting analysis which is further confirmed by Immunofluorescence study after 15 minutes of DNA DSB induction. This suggests the role of DOT1L in DNA repair. The

decreased γH2AX levels in DOT1L-depleted cells can be either because the breaks are not recognized properly which cause less DNA damage response or the breaks are repaired faster which leads to decreased γH2AX signal.

5.2 DOT1L is required for proper DNA-damage response

In contrast to less γH2AX after DOT1L depletion, we have also observe increased levels of phosphorylated NBS1 and CHK2 which are involved in the repair of DNA DSBs. Previous studies have indicated that KAP1 plays an important role during the DNA-damage response in heterochromatin regions (Cann and Dellaire, 2011; Pfeifer, 2012). Interestingly, we have shown that depletion of DOT1L leads to an increase of KAP1 phosphorylation and similar results were reported previously (Li et al., 2007). The possible explanation is that the loss of H3K79me3 leads to a heterochromatin-dependent increase of KAP1 phosphorylation, following DOT1L loss/inhibition. Our finding is supported by the previous report in mouse ES cells, Dot1L play role in the heterochromatin structure (Jones et al., 2008b). DOT1L-mediated H3K79 methylation is enriched in actively transcribed genes (Nguyen and Zhang, 2011b). These data indicate that DOT1L involvement extends from euchromatic to heterochromatic regions in DSB repair process.

Several reports suggested that DOT1L is a potential target for anti-cancer therapy and inhibitors are in the pre-clinical studies. The present study using DOT1L inhibitors further confirms the role of DOT1L in DNA-damage-response process. Consistent with our siRNA-mediated/depletion data, we observed increased levels of NBS1, ATM, CHK2, and KAP1 by using DOT1L inhibitor. This indicates that the methyltransferase activity of DOT1L responsible for H3K79 methylation and is essential for proper DNA-damage response. Importantly, the effectiveness of DOT1L inhibition with acute treatment of 3 hours observed to be the direct role of DOT1L,

which may block new the methylation (H3K79me3) with DOT1L short inhibition treatment. Indirectly, previous studies reported that cyclin-dependent kinase 12 (CDK12) which is a tumor suppressor protein and is important for regulation of several homologous recombination genes specifically BRCA1 expression (Blazek, 2012). The cdk12 loss led to increased PARPi sensitivity. Further experiments using irradiation shows that DOT1L-depleted cells are sensitive to DSBs which confirms, that DOT1L engaged in DNA-repair process. During DNA damage response either with NCS or IR, DOT1L expression promotes proper DNA repair. Thus, we placed our focus on the role of DOT1L-mediated H3K79me3 levels in DNA-damage repair and which has also been implicated as a mediator of DNA repair activity.

5.3 DOT1L is required for homologous recombination repair pathway

DSBs are generally repaired by two major pathways, NHEJ and HR. Knockdown of DOT1L in stably integrated plasmid-based HR and NHEJ reporter assays showed that HR efficiency has decreased but not NHEJ. This demonstrates that the histone methyltransferase DOT1L is involved in HR-mediated DSB repair.

We have discussed the role of chromatin recruitment factors in the efficient repair of DNA DSBs and the intermediate proteins which help during this repair process and finally summarized our findings in the mechanism of the HR pathway. During HR repair, DNA end-resection process is an important step. It is well known that during the end resection-process CtIP binds to the damaged site. After performing a chromatin fractionation assay we observed that CtIP is significantly decreased in DOT1L-depleted cells in response to DSB induction, hence that it is required for end resection. It is reported that the end processing of DNA generally determine whether it is repaired by HR or NHEJ. Previous studies (Sartori et al., 2007) demonstrated that CtIP is recruited to DSBs in S and G2 phases suggesting that its recruitment

favors the repair of DNA DSBs via the HR pathway. Besides, single-stranded DNA repair protein RPA1 recruited to the sites of DNA damage (Ng et al., 2002). The HR pathway is controlled by repair proteins such as RAD51 (Mansour et al., 2008). Previously, it was reported that the presence of ssDNA tails resulted in a RAD51-mediated initiation of HR (Loizou et al., 2006; Tsukuda et al., 2005). The proteins involved in the chromatin alterations and repair via HR are highly relevant. It appears that there is less γH2AX induction, which might be due to a quick repair of DSBs. We conclude that DOT1L regulated by HR is playing a crucial role in repairing DSB breaks and protecting the genome integrity while the loss of DOT1L leads to HR defects. Therefore, methylation at H3K79 may be considered as an essential mark for DNA damage signaling, allowing recruitment of repair factors. Our finding suggests that DOT1L critically contributes to DSB repair in CRC cell lines while we have also seen that it is involved primarily in DNA repair by homologous recombination.

5.4 H3K79me3 and γH2AX co-localize at the DSB sites

To further understand the DOT1L involvement in H2AX phosphorylation at the sites of DSBs, we performed co-localization studies using PLA assay. Few studies have described the background behind the mechanism of DOT1L involvement in DNA repair, the binding of 53BP1 to H3K79me3 (Wakeman et al., 2012) or the interaction with histone modifications such as H2B monoubiquitination (Giannattasio et al., 2005). Our finding is consistent with the previous reports in yeast and mammalian cells in which Dot1/DOT1L was described to be associated with H3K79 methylation and to play a role in DNA repair (Nguyen and Zhang, 2011b). Since there is co-localization or interaction of H3K79me3 and γH2AX, we proposed the explanation that DNA end-resection by CtIP recruitment and recruitment of other DNA repair proteins such as BRACA1/2 decreased recruitment with PARP-inhibitor sensitivity

may be involved in the repair of DSB (Benafif and Hall, 2015). We also provide the role of DOT1L in DNA damage function by showing that knockdown and inhibition of DOT1L is correlated with increased levels of pCHK2, pATM, and pKAP1.

We found that in control cells, histone H2AX phosphorylation (γH2AX) co-localizes with H3K79me3. γH2AX is upregulated in response to DSBs and therefore we assume that this domain may extend up to some kb from the site of damage. Our data propose that global H3K79me3 is not affected by DNA damage, i.e. H3K79me3 levels do not increase or decrease due to the induction of DSBs. Indeed, H3K79me3 is co-localized with γH2AX at the break site.

5.5 DOT1L and PARP inhibition decrease cell proliferation and cell viability

Our findings provide evidence of a role of DOT1L in DNA-damage response and repair via the HR pathway. Moreover, published data suggest that DOT1L is an important oncogene and a novel target in aggressive breast cancer therapy (Cho et al., 2015). Studies have described DOT1L to have a role in cell proliferation of prostate and lung cancers (Kim et al., 2012b). Many other studies have proposed DOT1L as a potential therapeutic target in human leukemia. These studies highlighted the importance of DOT1L enzymatic activities and H3K79 methylation levels as a target for therapy. In our study, we have focused on understanding the therapeutic aspects with the DSB repair defects.

Over the last years, many reports have investigated PARP and its involvement in DNA repair. Thus, we aimed to determine whether PARPi alone or in combination with DNA-damaging agents such irinotecan and oxaliplatin have anti-proliferative effects in CRC cell lines. We studied proliferation effects up to 7 days during continuous treatment with constant doses and different concentrations alone and in a combination of PARPi, irinotecan, and EPZ-5676. We have demonstrated that

increasing concentrations of PARPi and a constant dose of irinotecan and EPZ sensitizes both tested CRC cell lines. In this study, we demonstrate the optimal doses of all the compounds in our cell line-model system. To determine the effectiveness of combined therapy, we have treated cells always with fixed amounts of the PARP inhibitor together with increasing concentrations of irinotecan, vice versa. Irinotecan in combination with PARPi or EPZ results in the inhibition of cell proliferation. On the basis of our findings in cancer cell lines, the output of using PARP inhibitor and irinotecan is very promising and similar reports have been reported in mammalian tumor cells with preexisting DNA repair deficiencies (Zhang et al., 2011). Similar reports described less cell proliferation in yeast, mouse embryonic stem cells, and human cancer cells after depletion of DOT1L (Kim et al., 2014).

γH2AX is a marker for DNA damage (Bonner et al., 2008). We demonstrated that DNA damage caused by veliparib is minimal, however, after the addition of irinotecan the γH2AX levels increased. Moreover, after treatment with all three compounds VEL, IRI and EPZ-5676 we observed less γH2AX when compared to single treatment. This supports our findings obtained by Celigo® assay indicating increased drug sensitivity after drug combination.

Studies indicate that prostate cancer patients with HR defects respond better to PARP inhibitor treatment (Mateo et al., 2015). They showed that the prostate cancer patients who had defects with DNA repair showed a high response to the PARP inhibitor olaparib. We did a similar assay in our model system and demonstrated comparable effect when combining PARPi with DOT1L inhibitors. We also confirmed the effectiveness of PARPi with other DNA damaging agents in multiple cell lines.

The data demonstrate that PARPi alone sensitizes cells but it exerts stronger effects after the addition of DNA-damaging substances. These findings provide further insight into the increased sensitivity of PARP to DNA-damaging agents such as irinotecan. Therefore, our data suggest that PARPi has promising therapeutic effects in combination with irinotecan which will be beneficial in treating CRC patients.

Furthermore, our findings also demonstrate that the combination of chemotherapeutics such as 5-FU and irinotecan decreases cell proliferation, and combination with EPZ-5676 additionally decreases cell viability. Our results are supported by Srinivas et al. (2015) suggesting 5-FU and ionizing irradiation sensitize colorectal cancer cells towards double-stranded DNA breaks (DSBs) through homologous recombination repair (HRR).

5.6 H3K79me3 may serve as a marker for molecular stratification of colorectal cancer patients

The data using colorectal cancer patient samples provide preliminary evidence that H3K79me3 staining may serve as a marker for molecular stratification of CRC patients. This implicates defects in DNA repair and proliferation of cancer cells can be exploited by PARP inhibition. The data suggest that patients with low H3K79me3 level show poor survival. Importantly, our findings suggest that less H3K79me3 would increase the sensitivity to PARPi. We hypothesize that patients with low H3K79me3 levels, and therefore poor prognosis, will respond better to PARPi and irinotecan than patients with high H3K79me3 levels. The study of Mateo et al. (2015) observed olaparib sensitivity in patients with metastatic, castration-resistant prostate cancer. Several recent studies observing PARP-inhibitor sensitivity were correlated with defects in homologous recombination-DNA repair (Birkelbach et al., 2013; Weaver et al., 2015). Therefore, we assume that drug combinations

including PARPi can become important in the context of DNA-repair defects. Moreover, our finding suggests a model, where H3K79me3, in addition to its well characterized and explained important role in DNA repair, also possibly would be a molecular marker for colorectal cancer. We hypothesize that the DNA-DSB repair defects-mediated through HR pathway that we are studying can be treated with combinational therapy.

Indeed, the DOT1L inhibitor EPZ-5676 is in phase 1 clinical trials in leukemia patients. Based on these reports, a possible future approach to increase our understanding of combination treatment of PARP inhibitor with DNA-damaging agents such as irinotecan would be the generation of a stable cell line with DOT1L knockout using the CRISPR/Cas9 approach. In a xenograft animal model with and without PARP treatment the sensitivity can be examined. Therefore additional studies are needed to assess the therapeutic aspects of DNA double-strand break repair defects in colorectal patients using FOLFORI. A notable finding of this study was that a combination treatment is highly effective after the addition of DNA-damaging agents. Furthermore, personalized therapy with a combination of PARP inhibition may be used in combination with other DNA damaging agents such as irinotecan to better treat patients with HR defects in DNA repair. It is likely that the future therapeutic strategies in CRC involve DNA repair defects of HR pathway together with PARPi and radiotherapy. Our finding is novel and a promising approach for CRC patient’s treatment.

6 Bibliography

Abdullah, M., Sudoyo, A.W., Utomo, A.R., Fauzi, A., and Rani, A.A. (2012). Molecular profile of colorectal cancer in Indonesia: is there another pathway? Gastroenterol. Hepatol. Bed Bench *5*, 71–78.

Akhtar, R., Chandel, S., Sarotra, P., and Medhi, B. (2014). Current status of pharmacological treatment of colorectal cancer. World J. Gastrointest. Oncol. *6*, 177–183.

Anglin, J.L., Deng, L., Yao, Y., Cai, G., Liu, Z., Jiang, H., Cheng, G., Chen, P., Dong, S., and Song, Y. (2012). Synthesis and structure-activity relationship investigation of adenosine-containing inhibitors of histone methyltransferase DOT1L. J. Med. Chem. *55*, 8066–8074.

Bardhan, K., and Liu, K. (2013). Epigenetics and colorectal cancer pathogenesis. Cancers *5*, 676–713.

Barry, E.R., Corry, G.N., and Rasmussen, T.P. (2010). Targeting DOT1L action and interactions in leukemia: the role of DOT1L in transformation and development. Expert Opin. Ther. Targets *14*, 405–418.

Benafif, S., and Hall, M. (2015). An update on PARP inhibitors for the treatment of cancer. OncoTargets Ther. *8*, 519–528.

Bernt, K.M., Zhu, N., Sinha, A.U., Vempati, S., Faber, J., Krivtsov, A.V., Feng, Z., Punt, N., Daigle, A., Bullinger, L., et al. (2011). MLL-rearranged leukemia is dependent on aberrant H3K79 methylation by DOT1L. Cancer Cell *20*, 66–78.

Birkelbach, M., Ferraiolo, N., Gheorghiu, L., Pfäffle, H.N., Daly, B., Ebright, M.I., Spencer, C., O'Hara, C., Whetstine, J.R., Benes, C.H., et al. (2013). Detection of impaired homologous recombination repair in NSCLC cells and tissues. J. Thorac. Oncol. *8*, 279–286.

Black, J.C., Van Rechem, C., and Whetstine, J.R. (2012). Histone lysine methylation dynamics: establishment, regulation, and biological impact. Mol. Cell *48*, 491–507.

Blazek, D. (2012). The cyclin K/Cdk12 complex. Cell Cycle *11*, 1049–1050.

Bonner, W.M., Redon, C.E., Dickey, J.S., Nakamura, A.J., Sedelnikova, O.A., Solier, S., and Pommier, Y. (2008). γH2AX and cancer. Nat. Rev. Cancer *8*, 957–967.

Bostelman, L.J., Keller, A.M., Albrecht, A.M., Arat, A., and Thompson, J.S. (2007). Methylation of histone H3 lysine-79 by Dot1p plays multiple roles in the response to UV damage in Saccharomyces cerevisiae. DNA Repair *6*, 383–395.

Braun, M.S., and Seymour, M.T. (2011). Balancing the efficacy and toxicity of chemotherapy in colorectal cancer. Ther. Adv. Med. Oncol. *3*, 43–52.

Cann, K.L., and Dellaire, G. (2011). Heterochromatin and the DNA damage response: the need to relax. Biochem. Cell Biol. Biochim. Biol. Cell. *89*, 45–60.

Castaño Betancourt, M.C., Cailotto, F., Kerkhof, H.J., Cornelis, F.M.F., Doherty, S.A., Hart, D.J., Hofman, A., Luyten, F.P., Maciewicz, R.A., Mangino, M., et al. (2012). Genome-wide association and functional studies identify the DOT1L gene to be involved in cartilage thickness and hip osteoarthritis. Proc. Natl. Acad. Sci. U. S. A. *109*, 8218–8223.

Chapman, J.R., Taylor, M.R.G., and Boulton, S.J. (2012). Playing the end game: DNA double-strand break repair pathway choice. Mol. Cell *47*, 497–510.

Chen, E.X., Jonker, D.J., Siu, L.L., McKeever, K., Keller, D., Wells, J., Hagerman, L., and Seymour, L. (2016). A Phase I study of olaparib and irinotecan in patients with colorectal cancer: Canadian Cancer Trials Group IND 187. Invest. New Drugs *34*, 450–457.

Chen, L., Deshpande, A., Banka, D., Bernt, K.M., Dias, S., Buske, C., Olhava, E.J., Daigle, S.R., Richon, V.M., Pollock, R.M., et al. (2013). Abrogation of MLL-AF10 and CALM-AF10 mediated transformation through genetic inactivation or pharmacological inhibition of the H3K79 methyltransferase Dot1l. Leukemia *27*, 813–822.

Chen, S., Yang, Z., Wilkinson, A.W., Deshpande, A.J., Sidoli, S., Krajewski, K., Strahl, B.D., Garcia, B.A., Armstrong, S.A., Patel, D.J., et al. (2015). The PZP domain of AF10 senses unmodified H3K27 to regulate DOT1L-mediated methylation of H3K79. Mol. Cell *60*, 319–327.

Chernikova, S.B., Razorenova, O.V., Higgins, J.P., Sishc, B.J., Nicolau, M., Dorth, J.A., Chernikova, D.A., Kwok, S., Brooks, J.D., Bailey, S.M., et al. (2012). Deficiency in mammalian histone H2B ubiquitin ligase Bre1 (Rnf20/Rnf40) leads to replication stress and chromosomal instability. Cancer Res. *72*, 2111–2119.

Chiruvella, K.K., Liang, Z., and Wilson, T.E. (2013). Repair of double-strand breaks by end joining. Cold Spring Harb. Perspect. Biol. *5*, a012757.

Cho, M.-H., Park, J.-H., Choi, H.-J., Park, M.-K., Won, H.-Y., Park, Y.-J., Lee, C.H., Oh, S.-H., Song, Y.-S., Kim, H.S., et al. (2015). DOT1L cooperates with the c-Myc-p300 complex to epigenetically derepress CDH1 transcription factors in breast cancer progression. Nat. Commun. *6*, 7821.

Conde, F., Refolio, E., Cordón-Preciado, V., Cortés-Ledesma, F., Aragón, L., Aguilera, A., and San-Segundo, P. a (2009). The Dot1 histone methyltransferase and the Rad9 checkpoint adaptor contribute to cohesin-dependent double-strand break repair by sister chromatid recombination in Saccharomyces cerevisiae. Genetics *182*, 437–446.

Copeland, R.A., Solomon, M.E., and Richon, V.M. (2009). Protein methyltransferases as a target class for drug discovery. Nat. Rev. Drug Discov. *8*, 724–732.

Cunningham, D., Atkin, W., Lenz, H.-J., Lynch, H.T., Minsky, B., Nordlinger, B., and Starling, N. (2010). Colorectal cancer. The Lancet *375*, 1030–1047.

Daigle, S.R., Olhava, E.J., Therkelsen, C. a, Majer, C.R., Sneeringer, C.J., Song, J., Johnston, L.D., Scott, M.P., Smith, J.J., Xiao, Y., et al. (2011). Selective killing of mixed lineage leukemia cells by a potent small-molecule DOT1L inhibitor. Cancer Cell *20*, 53–65.

Daigle, S.R., Olhava, E.J., Therkelsen, C.A., Basavapathruni, A., Jin, L., Boriack-Sjodin, P.A., Allain, C.J., Klaus, C.R., Raimondi, A., Scott, M.P., et al. (2013). Potent inhibition of DOT1L as treatment of MLL-fusion leukemia. Blood *122*, 1017–1025.

Daley, J.M., and Sung, P. (2014). 53BP1, BRCA1, and the choice between recombination and end joining at DNA double-strand breaks. Mol. Cell. Biol. *34*, 1380–1388.

Davie, J.R. (2003). Inhibition of histone deacetylase activity by butyrate. J. Nutr. *133*, 2485S–2493S.

Davies, J.M., and Goldberg, R.M. (2011). Treatment of metastatic colorectal cancer. Semin. Oncol. *38*, 552–560.

Deshpande, A.J., Chen, L., Fazio, M., Sinha, A.U., Bernt, K.M., Banka, D., Dias, S., Chang, J., Olhava, E.J., Daigle, S.R., et al. (2013). Leukemic transformation by the MLL-AF6 fusion oncogene requires the H3K79 methyltransferase Dot1l. Blood *121*, 2533–2541.

Dobbelstein, M., and Sørensen, C.S. (2015). Exploiting replicative stress to treat cancer. Nat. Rev. Drug Discov. *14*, 405–423.

Downs, J.A., Lowndes, N.F., and Jackson, S.P. (2000). A role for Saccharomyces cerevisiae histone H2A in DNA repair. Nature *408*, 1001–1004.

Fackenthal, J.D., and Olopade, O.I. (2007). Breast cancer risk associated with BRCA1 and BRCA2 in diverse populations. Nat. Rev. Cancer *7*, 937–948.

Farmer, H., McCabe, N., Lord, C.J., Tutt, A.N.J., Johnson, D.A., Richardson, T.B., Santarosa, M., Dillon, K.J., Hickson, I., Knights, C., et al. (2005). Targeting the DNA repair defect in BRCA mutant cells as a therapeutic strategy. Nature *434*, 917–921.

Favoriti, P., Carbone, G., Greco, M., Pirozzi, F., Pirozzi, R.E.M., and Corcione, F. (2016). Worldwide burden of colorectal cancer: a review. Updat. Surg. *68*, 7–11.

Ferguson, L.R., Chen, H., Collins, A.R., Connell, M., Damia, G., Dasgupta, S., Malhotra, M., Meeker, A.K., Amedei, A., Amin, A., et al. (2015). Genomic instability in human cancer: Molecular insights and opportunities for therapeutic attack and prevention through diet and nutrition. Semin. Cancer Biol. *35*, S5–S24.

Fernandez-Capetillo, O., Chen, H.-T., Celeste, A., Ward, I., Romanienko, P.J., Morales, J.C., Naka, K., Xia, Z., Camerini-Otero, R.D., Motoyama, N., et al. (2002). DNA damage-induced G2–M checkpoint activation by histone H2AX and 53BP1. Nat. Cell Biol. *4*, 993–997.

Fong, P.C., Boss, D.S., Yap, T.A., Tutt, A., Wu, P., Mergui-Roelvink, M., Mortimer, P., Swaisland, H., Lau, A., O'Connor, M.J., et al. (2009). Inhibition of Poly(ADP-Ribose) Polymerase in tumors from BRCA mutation carriers. N. Engl. J. Med. *361*, 123–134.

Gaedcke, J., Leha, A., Claus, R., Weichenhan, D., Jung, K., Kitz, J., Grade, M., Wolff, H.A., Jo, P., Doyen, J., et al. (2014). Identification of a DNA methylation signature to predict disease-free survival in locally advanced rectal cancer. Oncotarget *5*, 8123–8135.

Genther Williams, S.M., Kuznicki, A.M., Andrade, P., Dolinski, B.M., Elbi, C., O'Hagan, R.C., and Toniatti, C. (2015). Treatment with the PARP inhibitor, niraparib, sensitizes colorectal cancer cell lines to irinotecan regardless of MSI/MSS status. Cancer Cell Int. *15*, 14.

Giannattasio, M., Lazzaro, F., Plevani, P., and Muzi-Falconi, M. (2005). The DNA damage checkpoint response requires histone H2B ubiquitination by Rad6-Bre1 and H3 methylation by Dot1. J. Biol. Chem. *280*, 9879–9886.

Glimelius, B., Ristamäki, R., Kjaer, M., Pfeiffer, P., Skovsgaard, T., Tveit, K.M., Linné, T., Frödin, J.E., Boussard, B., Oulid-Aïssa, D., et al. (2002). Irinotecan combined with bolus 5-fluorouracil and folinic acid Nordic schedule as first-line therapy in advanced colorectal cancer. Ann. Oncol. *13*, 1868–1873.

Greer, E.L., and Shi, Y. (2012). Histone methylation: a dynamic mark in health, disease and inheritance. Nat. Rev. Genet. *13*, 343–357.

Guppy, B.J., and McManus, K.J. (2015). Mitotic accumulation of dimethylated lysine 79 of histone H3 is important for maintaining genome integrity during mitosis in human cells. Genetics *199*, 423–433.

Haber, J.E. (2000). Partners and pathways: repairing a double-strand break. Trends Genet. *16*, 259–264.

Haggar, F.A., and Boushey, R.P. (2009). Colorectal cancer epidemiology: Incidence, mortality, survival, and risk factors. Clin. Colon Rectal Surg. *22*, 191–197.

Hall, M.J., Reid, J.E., Burbidge, L.A., Pruss, D., Deffenbaugh, A.M., Frye, C., Wenstrup, R.J., Ward, B.E., Scholl, T.A., and Noll, W.W. (2009). BRCA1 and BRCA2 mutations in women of different ethnicities undergoing testing for hereditary breast-ovarian cancer. Cancer *115*, 2222–2233.

Harper, J.W., and Elledge, S.J. (2007). The DNA damage response: Ten years after. Mol. Cell *28*, 739–745.

Hassa, P.O., and Hottiger, M.O. (2005). An epigenetic code for DNA damage repair pathways? Biochem. Cell Biol. *83*, 270–285.

Ho, L.-L., Sinha, A., Verzi, M., Bernt, K.M., Armstrong, S., and Shivdasani, R. (2013). DOT1L-mediated H3K79 methylation in chromatin is dispensable for Wnt pathway-specific and other intestinal epithelial functions. Mol. Cell. Biol. *33*, 1735–1745.

Huen, M.S.Y., Grant, R., Manke, I., Minn, K., Yu, X., Yaffe, M.B., and Chen, J. (2007). RNF8 transduces the DNA-damage signal via histone ubiquitylation and checkpoint protein assembly. Cell *131*, 901–914.

Humpal, S.E., Robinson, D.A., and Krebs, J.E. (2009). Marks to stop the clock: histone modifications and checkpoint regulation in the DNA damage response. Biochem. Cell Biol. *87*, 243–253.

Hunt, C.R., Ramnarain, D., Horikoshi, N., Iyengar, P., Pandita, R.K., Shay, J.W., and Pandita, T.K. (2013). Histone modifications and DNA double-strand break repair after exposure to ionizing radiations. Radiat. Res. *179*, 383–392.

Huyen, Y., Zgheib, O., Ditullio, R.A., Gorgoulis, V.G., Zacharatos, P., Petty, T.J., Sheston, E.A., Mellert, H.S., Stavridi, E.S., and Halazonetis, T.D. (2004). Methylated lysine 79 of histone H3 targets 53BP1 to DNA double-strand breaks. Nature *432*, 406–411.

Ikura, T., Ogryzko, V.V., Grigoriev, M., Groisman, R., Wang, J., Horikoshi, M., Scully, R., Qin, J., and Nakatani, Y. (2000). Involvement of the TIP60 histone acetylase complex in DNA repair and apoptosis. Cell *102*, 463–473.

Issa, J.-P. (2000). The epigenetics of colorectal cancer. Ann. N. Y. Acad. Sci. *910*, 140–155.

Iyer, B.V., Kenward, M., and Arya, G. (2011). Hierarchies in eukaryotic genome organization: Insights from polymer theory and simulations. BMC Biophys. *4*, 8.

Jackson, S.P., and Bartek, J. (2009). The DNA-damage response in human biology and disease. Nature *461*, 1071–1078.

Jackson, S.P., and Helleday, T. (2016). Drugging DNA repair. Science *352*, 1178–1179.

Janzen, C.J., Hake, S.B., Lowell, J.E., and Cross, G.A.M. (2006). Selective di- or trimethylation of histone H3 lysine 76 by two DOT1 homologs is important for cell cycle regulation in Trypanosoma brucei. Mol. Cell *23*, 497–507.

Javle, M., and Curtin, N.J. (2011). The role of PARP in DNA repair and its therapeutic exploitation. Br. J. Cancer *105*, 1114–1122.

Jones, B., Su, H., Bhat, A., Lei, H., Bajko, J., Hevi, S., Baltus, G.A., Kadam, S., Zhai, H., Valdez, R., et al. (2008). The histone H3K79 methyltransferase DOT1L is essential for mammalian development and heterochromatin structure. PLOS Genet *4*, e1000190.

Kari, V., Mansour, W.Y., Raul, S.K., Baumgart, S.J., Mund, A., Grade, M., Sirma, H., Simon, R., Will, H., Dobbelstein, M., et al. (2016). Loss of CHD1 causes DNA repair defects and enhances prostate cancer therapeutic responsiveness. EMBO Rep. *17*, 1609–1623.

Karpiuk, O., Najafova, Z., Kramer, F., Hennion, M., Galonska, C., König, A., Snaidero, N., Vogel, T., Shchebet, A., Begus-Nahrmann, Y., et al. (2012). The histone H2B monoubiquitination regulatory pathway is required for differentiation of multipotent stem cells. Mol. Cell *46*, 705–713.

Kim, S.-K., Jung, I., Lee, H., Kang, K., Kim, M., Jeong, K., Kwon, C.S., Han, Y.-M., Kim, Y.S., Kim, D., et al. (2012). Human histone H3K79 methyltransferase DOT1L protein binds actively transcribing RNA Polymerase II to regulate gene expression. J. Biol. Chem. *287*, 39698–39709.

Kim, W., Kim, R., Park, G., Park, J.-W., and Kim, J.-E. (2012). Deficiency of H3K79 histone methyltransferase Dot1-like protein (DOT1L) inhibits cell proliferation. J. Biol. Chem. *287*, 5588–5599.

Kim, W., Choi, M., and Kim, J.-E. (2014). The histone methyltransferase Dot1/DOT1L as a critical regulator of the cell cycle. Cell Cycle *13*, 726–738.

Kocarnik, J.M., Shiovitz, S., and Phipps, A.I. (2015). Molecular phenotypes of colorectal cancer and potential clinical applications. Gastroenterol. Rep. *3*, 269–276.

Krajewska, M., Fehrmann, R.S.N., de Vries, E.G.E., and van Vugt, M.A.T.M. (2015). Regulators of homologous recombination repair as novel targets for cancer treatment. Front. Genet. *6*.

Kummar, S., Chen, A., Ji, J., Zhang, Y., Reid, J.M., Ames, M., Jia, L., Weil, M., Speranza, G., Murgo, A.J., et al. (2011). Phase I study of PARP inhibitor ABT-888 in combination with topotecan in adults with refractory solid tumors and lymphomas. Cancer Res. *71*, 5626–5634.

Lacoste, N., Utley, R.T., Hunter, J.M., Poirier, G.G., and Côte, J. (2002). Disruptor of telomeric silencing-1 is a chromatin-specific histone H3 methyltransferase. J. Biol. Chem. *277*, 30421–30424.

Lazzaro, F., Sapountzi, V., Granata, M., Pellicioli, A., Vaze, M., Haber, J.E., Plevani, P., Lydall, D., and Muzi-Falconi, M. (2008). Histone methyltransferase Dot1 and Rad9 inhibit single-stranded DNA accumulation at DSBs and uncapped telomeres. EMBO J. *27*, 1502–1512.

Ledermann, J., Harter, P., Gourley, C., Friedlander, M., Vergote, I., Rustin, G., Scott, C.L., Meier, W., Shapira-Frommer, R., Safra, T., et al. (2014). Olaparib maintenance therapy in patients with platinum-sensitive relapsed serous ovarian cancer: a preplanned retrospective analysis of outcomes by BRCA status in a randomised phase 2 trial. Lancet Oncol. *15*, 852–861.

Lee, J.-Y., Kong, G., Lee, J.-Y., and Kong, G. (2015). DOT1L: a new therapeutic target for aggressive breast cancer. Oncotarget *6*, 30451–30452.

van Leeuwen, F., Gafken, P.R., and Gottschling, D.E. (2002). Dot1p modulates silencing in yeast by methylation of the nucleosome core. Cell *109*, 745–756.

Leung, M., Rosen, D., Fields, S., Cesano, A., and Budman, D.R. (2011). Poly(ADP-ribose) polymerase-1 inhibition: preclinical and clinical development of synthetic lethality. Mol. Med. Camb. Mass *17*, 854–862.

Li, X., Lee, Y.-K., Jeng, J.-C., Yen, Y., Schultz, D.C., Shih, H.-M., and Ann, D.K. (2007). Role for KAP1 serine 824 phosphorylation and sumoylation/desumoylation switch in regulating KAP1-mediated transcriptional repression. J. Biol. Chem. *282*, 36177–36189.

Lin, Y.-H., Yuan, J., Pei, H., Liu, T., Ann, D.K., and Lou, Z. (2015). KAP1 deacetylation by SIRT1 promotes non-homologous end-joining repair. PLOS ONE *10*, e0123935.

List, O., Togawa, T., Tsuda, M., Matsuo, T., Elard, L., and Aigaki, T. (2009). Overexpression of grappa encoding a histone methyltransferase enhances stress resistance in Drosophila. Hereditas *146*, 19–28.

Loizou, J.I., Murr, R., Finkbeiner, M.G., Sawan, C., Wang, Z.-Q., and Herceg, Z. (2006). Epigenetic information in chromatin: the code of entry for DNA repair. Cell Cycle *5*, 696–701.

Lowndes, N.F., and Toh, G.W.-L. (2005). DNA Repair: The importance of phosphorylating histone H2AX. Curr. Biol. *15*, R99–R102.

Mailand, N., Bekker-Jensen, S., Faustrup, H., Melander, F., Bartek, J., Lukas, C., and Lukas, J. (2007). RNF8 ubiquitylates histones at DNA double-strand breaks and promotes assembly of repair proteins. Cell *131*, 887–900.

Mansour, W.Y., Schumacher, S., Rosskopf, R., Rhein, T., Schmidt-Petersen, F., Gatzemeier, F., Haag, F., Borgmann, K., Willers, H., and Dahm-Daphi, J. (2008). Hierarchy of nonhomologous end-joining, single-strand annealing and gene conversion at site-directed DNA double-strand breaks. Nucleic Acids Res. *36*, 4088–4098.

Mateo, J., Carreira, S., Sandhu, S., Miranda, S., Mossop, H., Perez-Lopez, R., Nava Rodrigues, D., Robinson, D., Omlin, A., Tunariu, N., et al. (2015). DNA-repair defects and olaparib in metastatic prostate cancer. N. Engl. J. Med. *373*, 1697–1708.

Maze, I., Noh, K.-M., Soshnev, A.A., and Allis, C.D. (2014). Every amino acid matters: essential contributions of histone variants to mammalian development and disease. Nat. Rev. Genet. *15*, 259–271.

McCabe, N., Turner, N.C., Lord, C.J., Kluzek, K., Bialkowska, A., Swift, S., Giavara, S., O'Connor, M.J., Tutt, A.N., Zdzienicka, M.Z., et al. (2006). Deficiency in the repair of DNA damage by homologous recombination and sensitivity to poly(ADP-ribose) polymerase inhibition. Cancer Res. *66*, 8109–8115.

McGinty, R.K., Kim, J., Chatterjee, C., Roeder, R.G., and Muir, T.W. (2008). Chemically ubiquitylated histone H2B stimulates hDot1L-mediated intranucleosomal methylation. Nature *453*, 812–816.

Meehan, R.S., and Chen, A.P. (2016). New treatment option for ovarian cancer: PARP inhibitors. Gynecol. Oncol. Res. Pract. *3*, 3.

Michels, J., Vitale, I., Saparbaev, M., Castedo, M., and Kroemer, G. (2014). Predictive biomarkers for cancer therapy with PARP inhibitors. Oncogene *33*, 3894–3907.

Mohan, R.D., Dialynas, G., Weake, V.M., Liu, J., Martin-Brown, S., Florens, L., Washburn, M.P., Workman, J.L., and Abmayr, S.M. (2014). Loss of Drosophila Ataxin-7, a SAGA subunit, reduces H2B ubiquitination and leads to neural and retinal degeneration. Genes Dev. *28*, 259–272.

Moyal, L., Lerenthal, Y., Gana-Weisz, M., Mass, G., So, S., Wang, S.-Y., Eppink, B., Chung, Y.M., Shalev, G., Shema, E., et al. (2011). Requirement of ATM-dependent monoubiquitylation of histone H2B for timely repair of DNA double-strand breaks. Mol. Cell *41*, 529–542.

Murr, R., Loizou, J.I., Yang, Y.-G., Cuenin, C., Li, H., Wang, Z.-Q., and Herceg, Z. (2006). Histone acetylation by Trrap–Tip60 modulates loading of repair proteins and repair of DNA double-strand breaks. Nat. Cell Biol. *8*, 91–99.

Nagarajan, S., Benito, E., Fischer, A., and Johnsen, S.A. (2015). H4K12ac is regulated by estrogen receptor-alpha and is associated with BRD4 function and inducible transcription. Oncotarget *6*, 7305–7317.

Nakamura, K., Kato, A., Kobayashi, J., Yanagihara, H., Sakamoto, S., Oliveira, D.V.N.P., Shimada, M., Tauchi, H., Suzuki, H., Tashiro, S., et al. (2011). Regulation of homologous recombination by RNF20-dependent H2B ubiquitination. Mol. Cell *41*, 515–528.

Nambiar, M., and Raghavan, S.C. (2011). How does DNA break during chromosomal translocations? Nucleic Acids Res. *39*, 5813–5825.

Nebbioso, A., Carafa, V., Benedetti, R., and Altucci, L. (2012). Trials with “epigenetic” drugs: An update. Mol. Oncol. *6*, 657–682.

Ng, H.H., Xu, R.-M., Zhang, Y., and Struhl, K. (2002). Ubiquitination of histone H2B by Rad6 is required for efficient Dot1-mediated methylation of histone H3 lysine 79. J. Biol. Chem. *277*, 34655–34657.

Nguyen, A.T., and Zhang, Y. (2011). The diverse functions of Dot1 and H3K79 methylation. *3*, 1345–1358.

Nguyen, A.T., Taranova, O., He, J., and Zhang, Y. (2011). DOT1L, the H3K79 methyltransferase, is required for MLL-AF9–mediated leukemogenesis. Blood *117*, 6912–6922.

O’Connor, M.J. (2015). Targeting the DNA damage response in cancer. Mol. Cell *60*, 547–560.

Oh, S., Jeong, K., Kim, H., Kwon, C.S., and Lee, D. (2010). A lysine-rich region in Dot1p is crucial for direct interaction with H2B ubiquitylation and high level methylation of H3K79. Biochem. Biophys. Res. Commun. *399*, 512–517.

Okada, Y., Feng, Q., Lin, Y., Jiang, Q., Li, Y., Coffield, V.M., Su, L., Xu, G., and Zhang, Y. (2005). hDOT1L links histone methylation to leukemogenesis. Cell *121*, 167–178.

Okugawa, Y., Grady, W.M., and Goel, A. (2015). Epigenetic alterations in colorectal cancer: Emerging biomarkers. Gastroenterology *149*, 1204–1225.e12.

Panier, S., and Durocher, D. (2009). Regulatory ubiquitylation in response to DNA double-strand breaks. DNA Repair *8*, 436–443.

Peterson, C.L., and Almouzni, G. (2013). Nucleosome dynamics as modular systems that integrate DNA damage and repair. Cold Spring Harb. Perspect. Biol. *5*.

Pfeifer, G.P. (2012). Protein phosphatase PP4: Role in dephosphorylation of KAP1 and DNA strand break repair. Cell Cycle *11*, 2590–2590.

Polo, S.E., and Jackson, S.P. (2011). Dynamics of DNA damage response proteins at DNA breaks: a focus on protein modifications. Genes Dev. *25*, 409–433.

Price, B.D., and D'Andrea, A.D. (2013). Chromatin remodeling at DNA double strand breaks. Cell *152*, 1344–1354.

Rau, R.E., Rodriguez, B.A., Luo, M., Jeong, M., Rosen, A., Rogers, J.H., Campbell, C.T., Daigle, S.R., Deng, L., Song, Y., et al. (2016). DOT1L as a therapeutic target for the treatment of DNMT3A-mutant acute myeloid leukemia. Blood *128*, 971–981.

Rodgers, K., and McVey, M. (2016). Error-prone repair of DNA double-strand breaks. J. Cell. Physiol. *231*, 15–24.

Rogakou, E.P., Pilch, D.R., Orr, A.H., Ivanova, V.S., and Bonner, W.M. (1998). DNA double-stranded breaks induce histone H2AX phosphorylation on serine 139. J. Biol. Chem. *273*, 5858–5868.

Rogakou, E.P., Boon, C., Redon, C., and Bonner, W.M. (1999). Megabase chromatin domains involved in DNA double-strand breaks in vivo. J. Cell Biol. *146*, 905–916.

Rossetto, D., Truman, A.W., Kron, S.J., and Côté, J. (2010). Epigenetic modifications in double strand break DNA damage signaling and repair. Clin. Cancer Res. Off. J. Am. Assoc. Cancer Res. *16*, 4543–4552.

Rossetto, D., Avvakumov, N., and Côté, J. (2012). Histone phosphorylation. Epigenetics *7*, 1098–1108.

Samol, J., Ranson, M., Scott, E., Macpherson, E., Carmichael, J., Thomas, A., and Cassidy, J. (2012). Safety and tolerability of the poly(ADP-ribose) polymerase (PARP) inhibitor, olaparib (AZD2281) in combination with topotecan for the treatment of patients with advanced solid tumors: a phase I study. Invest. New Drugs *30*, 1493–1500.

Sanders, S.L., Portoso, M., Mata, J., Bähler, J., Allshire, R.C., and Kouzarides, T. (2004). Methylation of histone H4 lysine 20 controls recruitment of Crb2 to sites of DNA damage. Cell *119*, 603–614.

Sartori, A.A., Lukas, C., Coates, J., Mistrik, M., Fu, S., Bartek, J., Baer, R., Lukas, J., and Jackson, S.P. (2007). Human CtIP promotes DNA end resection. Nature *450*, 509–514.

Schreiber, V., Dantzer, F., Ame, J.-C., and de Murcia, G. (2006). Poly(ADP-ribose): novel functions for an old molecule. Nat. Rev. Mol. Cell Biol. *7*, 517–528.

Shanower, G.A., Muller, M., Blanton, J.L., Honti, V., Gyurkovics, H., and Schedl, P. (2005). Characterization of the grappa Gene, the Drosophila histone H3 lysine 79 methyltransferase. Genetics *169*, 173–184.

Shrivastav, M., De Haro, L.P., and Nickoloff, J.A. (2008). Regulation of DNA double-strand break repair pathway choice. Cell Res. *18*, 134–147.

Singer, M.S., Kahana, a, Wolf, a J., Meisinger, L.L., Peterson, S.E., Goggin, C., Mahowald, M., and Gottschling, D.E. (1998). Identification of high-copy disruptors of telomeric silencing in Saccharomyces cerevisiae. Genetics *150*, 613–632.

Smith, L.M., Willmore, E., Austin, C.A., and Curtin, N.J. (2005). The novel poly(ADP-Ribose) polymerase inhibitor, AG14361, sensitizes cells to topoisomerase I poisons by increasing the persistence of DNA strand breaks. Clin. Cancer Res. Off. J. Am. Assoc. Cancer Res. *11*, 8449–8457.

Souglakos, J., Androulakis, N., Syrigos, K., Polyzos, A., Ziras, N., Athanasiadis, A., Kakolyris, S., Tsousis, S., Kouroussis, C., Vamvakas, L., et al. (2006). FOLFOXIRI (folinic acid, 5-fluorouracil, oxaliplatin and irinotecan) vs FOLFIRI (folinic acid, 5-fluorouracil and irinotecan) as first-line treatment in metastatic colorectal cancer (MCC): a multicentre randomised phase III trial from the Hellenic Oncology Research Group (HORG). Br. J. Cancer *94*, 798–805.

Srinivas, U.S., Dyczkowski, J., Beißbarth, T., Gaedcke, J., Mansour, W.Y., Borgmann, K., Dobbelstein, M., Srinivas, U.S., Dyczkowski, J., Beißbarth, T., et al. (2015). 5-Fluorouracil sensitizes colorectal tumor cells towards double stranded DNA breaks by interfering with homologous recombination repair. Oncotarget *6*, 12574–12586.

Srivastava, M., and Raghavan, S.C. (2015). DNA double-strand break repair inhibitors as cancer therapeutics. Chem. Biol. *22*, 17–29.

Steger, D.J., Lefterova, M.I., Ying, L., Stonestrom, A.J., Schupp, M., Zhuo, D., Vakoc, A.L., Kim, J.-E., Chen, J., Lazar, M. a, et al. (2008). DOT1L/KMT4 recruitment and H3K79 methylation are ubiquitously coupled with gene transcription in mammalian cells. Mol. Cell. Biol. *28*, 2825–2839.

Strahl, B.D., and Allis, C.D. (2000). The language of covalent histone modifications. Nature *403*, 41–45.

Swift, L.H., and Golsteyn, R.M. (2014). Genotoxic anti-cancer agents and their relationship to DNA damage, mitosis, and checkpoint adaptation in proliferating cancer cells. Int. J. Mol. Sci. *15*, 3403–3431.

Toyota, M., Ahuja, N., Ohe-Toyota, M., Herman, J.G., Baylin, S.B., and Issa, J.P. (1999). CpG island methylator phenotype in colorectal cancer. Proc. Natl. Acad. Sci. U. S. A. *96*, 8681–8686.

Tsukuda, T., Fleming, A.B., Nickoloff, J.A., and Osley, M.A. (2005). Chromatin remodelling at a DNA double-strand break site in Saccharomyces cerevisiae. Nature *438*, 379–383.

Vakoc, C.R., Sachdeva, M.M., Wang, H., and Blobel, G.A. (2006). Profile of histone lysine methylation across transcribed mammalian chromatin. Mol. Cell. Biol. *26*, 9185–9195.

Vardabasso, C., Hasson, D., Ratnakumar, K., Chung, C.-Y., Duarte, L.F., and Bernstein, E. (2014). Histone variants: emerging players in cancer biology. Cell. Mol. Life Sci. CMLS *71*, 379–404.

Vissers, J.H., Nicassio, F., van Lohuizen, M., Di Fiore, P.P., and Citterio, E. (2008). The many faces of ubiquitinated histone H2A: insights from the DUBs. Cell Div. *3*, 8.

Wakeman, T.P., Wang, Q., Feng, J., and Wang, X.-F. (2012). Bat3 facilitates H3K79 dimethylation by DOT1L and promotes DNA damage-induced 53BP1 foci at G1/G2 cell-cycle phases. EMBO J. *31*, 2169–2181.

Weaver, A.N., Cooper, T.S., Rodriguez, M., Trummell, H.Q., Bonner, J.A., Rosenthal, E.L., Yang, E.S., Weaver, A.N., Cooper, T.S., Rodriguez, M., et al. (2015). DNA double strand break repair defect and sensitivity to poly ADP-ribose polymerase (PARP) inhibition in human papillomavirus 16-positive head and neck squamous cell carcinoma. Oncotarget *6*, 26995–27007.

Wong, M., Polly, P., and Liu, T. (2015). The histone methyltransferase DOT1L: regulatory functions and a cancer therapy target. Am. J. Cancer Res. *5*, 2823–2837.

Woodcock, C.L., and Ghosh, R.P. (2010). Chromatin higher-order structure and dynamics. Cold Spring Harb. Perspect. Biol. *2*.

Wu, H., and Sun, Y.E. (2006). Epigenetic regulation of stem cell differentiation. Pediatr. Res. *59*, 21R–25R.

Xu, Y., and Her, C. (2015). Inhibition of Topoisomerase (DNA) I (TOP1): DNA damage repair and anticancer therapy. Biomolecules *5*, 1652–1670.

Yu, W., Chory, E.J., Wernimont, A.K., Tempel, W., Scopton, A., Federation, A., Marineau, J.J., Qi, J., Barsyte-Lovejoy, D., Yi, J., et al. (2012). Catalytic site remodelling of the DOT1L methyltransferase by selective inhibitors. Nat. Commun. *3*, 1288.

Zhang, L., Deng, L., Chen, F., Yao, Y., Wu, B., Wei, L., Mo, Q., and Song, Y. (2014). Inhibition of histone H3K79 methylation selectively inhibits proliferation, self-renewal and metastatic potential of breast cancer. Oncotarget *5*, 10665–10677.

Zhang, Y.-W., Regairaz, M., Seiler, J.A., Agama, K.K., Doroshow, J.H., and Pommier, Y. (2011). Poly(ADP-ribose) polymerase and XPF-ERCC1 participate in distinct pathways for the repair of topoisomerase I-induced DNA damage in mammalian cells. Nucleic Acids Res. *39*, 3607–3620.

7 Curriculum Vitae

Sanjay Kumar Raul
Albrecht-Thaer-Weg 8, 37075 Göttingen
Email: sraul@uni-goettingen.de, rausanjay@gmail.com
Mobile: +49 176 82442052

Education

2012-Present	Ph.D. ‘‘Molecular Medicine’’
	Georg-August-Universität Göttingen, Germany
	April 2014 – present
	Laboratory of Tumor Epigenetics, Department for General, Visceral and Pediatric Surgery, *University Medical Center* Göttingen*, Germany*
	November 2012-March2014
	Institute for Tumor Biology, *University Medical Center Hamburg-Eppendorf*, Germany
	Ph.D. thesis title: ‘‘Epigenetic regulation of DNA repair”
	Supervisor: Prof. Dr. Steven A. Johnsen
2002 – 2005	M.Sc. ‘‘Microbiology’’
	Orissa University of Agriculture and Technology, Bhubaneswar, India
	March 2004 – December 2004
	Master dissertation: Department of Aquatic Animal Health, *Central Institute of Freshwater Aquaculture* (CIFA), Bhubaneswar, India
	M.Sc. research work project title “Analysis of *Staphylococcus aureus* strains using RAPD and RFLP-PCR fingerprinting”
1999 – 2002	B.Sc. Chemistry, Zoology and Botany (Honours)
	Fakir Mohan University, India

Work History

2/2006-9/2012	Biotechnology Industry
	Research Scientist: *IMGENEX India private limited*, Bhubaneswar, India
	Job area: 'Development and production of antibodies and mammalian cell culture"
3/2005-2/2006	CSIR Laboratory
	Project Assistant: *Regional Research Laboratory*, Bhubaneswar, India
	Projecttitle: "Isolation and molecular characterization of microbial Isolates of marine sponges*"*

Publications

Kari, V., Mansour, W.Y., Raul, S.K., Baumgart, S.J., Mund, A., Grade, M., Sirma, H., Simon, R., Will, H., Dobbelstein, M., Dikomey, E., and Johnsen, S.A. (2016). Loss of CHD1 causes DNA repair defects and enhances prostate cancer therapeutic responsiveness. EMBO Rep. *17*, 1609–1623.

Contributed equally as a **1st co-author** to this paper.

National and International Conference/Workshop

• **07/09/2015-08/09/2015** Oral presentation and Organizing member

Sanjay Kumar Raul, Vijaya Lakshmi Kari, Wael Yassin Mansour, Melanie Spitzner, Marian Grade, Jochen Gaedcke, Steven A. Johnsen (2015). The histone methyltransferase DOT1L required for DNA damage recognition and repair. 6th Molecular Medicine Retreat*, Wernigerode, Germany,* P-20

• **04/06/2015-07/06/2015** Poster presentation

Sanjay Kumar Raul, Vijayalakshmi Kari, Melanie Spitzner, Wael Yassin Mansour, Steven A. Johnsen (2015). The histone methyltransferase DOT1L required for the DNA damage recognition and repair. The 2015 IMB Conference, DNA Repair & Genome Stability in a Chromatin Environment*, Institute of Molecular Biology (IMB), Mainz, Germany,* P98

• **21/09/2014-23/09/2014** Poster presentation

Sanjay Kumar Raul, Vijaya Lakshmi Kari, Steven A. Johnsen (2014). The histone methyltransferase DOT1L required for DNA damage recognition and repair. 30th Ernst Klenk Symposium in Molecular Medicine, DNA Damage Response and Repair Mechanisms in Aging and Disease, Center for Molecular Medicine Cologne (CMMC)*, University of Cologne, Germany,* D-15

• **15/06/2009-24/06/2009** Workshop

10-day wet workshop: Application of Flow Cytometry, Real Time PCR and Stem cell culturing for characterization of Human Embryonic & Mesenchymal Stem cells, *Manipal Institute of Regenerative Medicine, Manipal University, Bangalore, India*

• **17/01/2007-19/01/2007** Poster presentation

Sanjay Raul, AVV Vidyanand, Javed Akhtar, Krupa S Panda, Sanjay Panda, Prasanta K Maiti and Sujay Singh "Immunoexpression of Caspase-1 in regressive human colon cancer". 26th Annual convention of Indian association for cancer research and International symposium on translational research in cancer, *Imgenex India Pvt. Ltd, Bhubaneswar, India*

• **08/12/2005-10/12/2005** Poster presentation

M. Rath, **S. K. Raul** and A. Sree "Studies on Biodiversity and Biotechnological Potential of Bacterial Isolates of Selected Marine Sponges of Orissa coast". 46th National annual conference: Association of Microbiologists of India", *Osmania University, Hyderabad, India*

Book

Lisa Stein, Debashree Sahu, Javed Akhtar, Kody Andrew, Hyun-ku Lee, Satya Mishra, Payton Quintel, **Sanjay Raul**, Jonathan Rosenberg, M. Simple, Gita Singh, Sujay Singh, Jason Stampfl, Lauren Wardle. TOLL-LIKE RECEPTORS IMGENEX & Innate Immunity: The Story Toll'd OVERVIEW & HANDBOOK. FIRST EDITION• 2010 *IMGENEX* (www.imgenex.com) 11175 Flintkote Avenue, Suite E, San Diego, CA 92121.

Volunteer Activity

2000	Elected General Secretary from the whole college and serve as Union body leader during final year of bachelor study
1999	Elected as class representative to represent 1st year students at College Union wing during bachelor study

Awards and Honors

2011	*Government of India* awarded "National Overseas Scholarship" for higher studies in abroad for Ph.D. or equivalent degree

Laboratory Techniques Known

Molecular Biology: CRISPR/Cas9 system, chromatin fractionation**,** chromatin immunoprecipitation (ChIP), plasmid/DNA isolation, cloning techniques, RNA isolation from cells, cDNA preparation, quantitative real-time PCR, restriction fragment length polymorphism

Protein chemistry: Co-immunoprecipitation, SDS-PAGE, 2D gel electrophoresis, protein isolation from cells, protein quantification, Western blotting

Cell culture: Mammalian cells S1 and S2 work, siRNA and plasmid transfections, MTT assay, cell proliferation assay, colony formation assay, Celigo® cytometer assay, small molecular inhibitors, and drugs does kinetic study

Staining/Microscopy and Image analysis: Immunofluorescence, immunohistochemistry, ELISA, confocal microscopy, Image J software, LSM image browser

Microbiology: Culture, isolation and maintenance of bacterial cells, biochemical tests and antimicrobial sensitivity test

References

Prof. Dr. Steven A. Johnsen

Professor for Translational Cancer Research
Clinic for General, Visceral and Pediatric Surgery
University Medical Center Goettingen,
37075 Goettingen, Germany
Email: steven.johnsen@med.uni-goettingen.de

Prof. Dr. Hans Will

Senior Professor, Department of Tumor Biology
University Medical Center Hamburg-Eppendorf,
20246 Hamburg, Germany
Email: hanskilianwill@gmail